4-15-2010

On the Catalytic Roles of HIS351, ASN510, and HIS466 in Choline Oxidase and the Kinetic Mechanism of Pyranose 2-Oxidase

Kunchala Rungsrisuriyachai
Georgia State University

ON THE CATALYTIC ROLES OF HIS351, ASN510, AND HIS466 IN CHOLINE OXIDASE AND THE KINETIC MECHANISM OF PYRANOSE 2-OXIDASE

by

KUNCHALA RUNGSRISURIYACHAI

Under the Direction of Giovanni Gadda

ABSTRACT

Choline oxidase (E.C. 1.1.3.17) from *Arthrobacter globiformis* catalyzes the four-electron oxidation of choline to glycine betaine (*N,N,N*-trimethylglycine) via two sequential, FAD-dependent reactions in which betaine aldehyde is formed as an enzyme-bound intermediate. In each oxidative half-reaction, molecular oxygen acts as electron acceptor and is converted into hydrogen peroxide. Biochemical, structural, and mechanistic studies on the wild-type and a number of mutant variants of choline oxidase have recently been carried out, allowing for the depiction of the mechanism of alcohol oxidation catalyzed by the enzyme.

Catalysis by choline oxidase is initiated by the removal of the hydroxyl proton of alcohol substrate by a catalytic base in the enzyme-substrate complex, yielding the formation of the alkoxide species. In this dissertation, the roles of His351 and conserved His466 were investigated. The results presented demonstrate that His351 is involved in the stabilization of the transition state for the hydride transfer reaction and contributes to substrate binding. His466 is likely to be a catalytic base in choline oxidase due to its dramatic effect on enzymatic activity.

Comparison of choline oxidase and other enzymes within its superfamily reveals the presence of a conserved His-Asn pair within the active site of enzymes. Therefore, the role of the conserved Asn510 in choline oxidase was examined in this study. The results presented here establish the importance of Asn510 in both the reductive and oxidative half-reactions. The lost of ability to form a hydrogen bond interaction between the side chain at position 510 with neighboring residues such as His466 resulted in a change from stepwise to concerted mechanism for the cleavages of OH and CH bonds of choline, as seen in the Asn510Ala mutant. Finally, the steady-state kinetic mechanism of pyranose 2-oxidase in the pH range from 5.5 to 8.5 was investigated. It was found that pH exerts significant effects on enzyme mechanism. This study has established the involvement of the residues in the initiation of enzyme catalysis and the stabilization of the alkoxide intermediate in choline oxidase. In addition, this work demonstrates the first instance in which the kinetic mechanism of a flavin-dependent oxidase is governed by pH.

INDEX WORDS: Choline Oxidase, Pyranose 2-oxidase, Flavin, Catalytic base, Hydride ion transfer, Chemical mechanism, Flavoprotein.

ON THE CATALYTIC ROLES OF HIS351, ASN510, AND HIS466 IN CHOLINE OXIDASE AND THE KINETIC MECHANISM OF PYRANOSE 2-OXIDASE

by

KUNCHALA RUNGSRISURIYACHAI

A Dissertation Submitted in Partial Fulfillment of the Requirements for the Degree of

Doctor of Philosophy

in the College of Arts and Sciences

Georgia State University

2010

ON THE CATALYTIC ROLES OF HIS351, ASN510, AND HIS466 IN CHOLINE OXIDASE AND THE KINETIC MECHANISM OF PYRANOSE 2-OXIDASE

by

KUNCHALA RUNGSRISURIYACHAI

Committee Chair: Dr. Giovanni Gadda

Committee: Dr. Al Baumstark

Dr. Dabney White Dixon

Electronic Version Approved by:

Office of Graduate Studies

College of Arts and Sciences

Georgia State University

May 2010

ACKNOWLEDGEMENTS

This dissertation arose out of the years of research undertaken since I joined Dr. Gadda's group. During that time, I have worked with a great number of people whose assorted contributions to the research and completion of this dissertation deserve special mention. It makes me happy to communicate my gratitude here to all of these people.

First, I would like to express my deepest appreciation to my advisor, Dr. Giovanni Gadda, for his advice, supervision, and guidance from earliest stages of this dissertation. He taught me different ways to approach research problems and the need to be persistent to accomplish any goal. Without him this dissertation would not have been possible.

I would like to acknowledge my committee members, Dr. Baumstark and Dr. Dixon, for your great suggestions for my project and your constant support during these years. In a variety of ways, all of you have inspired me to be a great scientist. Dr. Dixon, who always asked me good questions and rescued me from various red tape crises, I would like you to know especially that your advice on career goals is not only going to be used right after my program but for my whole life. You are not only a committee member whose scientific expertise I respect, but you are also a caring professor with whom I can share my joys and tribulations and always find thoughtful opinions and suggestions.

It is a pleasure to pay tribute also to the past and present members of Dr. Giovanni Gadda's laboratory. Fan, Mahmoud, Kevin, Trang, Tran Bao, Osbourne, Merid, Steffan, Slavica, Anthony, Andrea, Hongling, Sharonda, Lydia, Philip, Nicole, Stephen, Swathi and Danila: you all made the lab such an exciting place. As the one who had been with me the longest time, Osbourne, I am really glad to have worked with you and will always think about all the obstacles we have been through together. To Slavica, thank for your encouragement and for being a model

of a strong woman. Andrea and Hongling, I owe both of you big thanks. Like you always said "don't worry, Andrea is here" and "Kunchala, tell me what is the problem." You were always there for me like a family with whom I can share my cheers and tears. I know that I can always count on you. Again, you have been my "brother" and "sister" during this time in the United States, and will be for the rest of my life.

Collective and individual acknowledgements are also owed to the following people at Georgia State University. Edna, Sina Stephanie, Diane, Robert, Dan, Chris, etc. your willingness and smiles to always provide the needed help were so soothing they will never be forgotten. Will Lovett, I would like to thank for helping me at any time, and solving any unsolvable problems concerning Ph.D. students. To Charles Bush, thank for your order supply assistances and for sharing various thoughts during my Ph.D. program. It is also a pleasure to mention Chadia, Elizabeth, and Ya-shu Huang for the lunch meeting and dry humor about the scientist's life. Elizabeth, without you my dissertation would be unintelligible to read at all due to my "poor" English. I was extraordinarily fortunate to have my best Thai friend, Patra. Thank for your kindness and for helping me to live in the United States much more easily. You have been a great friend who was always ready to lend a hand.

Where would I be without my family? My parents, my dad Swang, my mom Chula and my brother Setha deserve special mention for their inseparable support and unconditional love. No words can address my sincere feeling toward all of them. Without them, there would have been no me.

Words fail me to express my appreciation to my husband, Tawan Teopipithaporn for his dedication, love, and persistent confidence in me. It is an honor for me to thank my parents-and brother-in law for warmly accepting me as a new member of the family and for their thoughtful

support. For the new member of the family, Matthew Teopipithaporn, you are the sweetest person in my life and thinking about you and your future encourage me to be more successful and proceed constantly in my career; you are really the light of my life!

Finally, I would like to thank everybody who was important to the successful realization of this dissertation, as well as to express my apologies that I could not mention everyone personally one by one.

TABLE OF CONTENTS

LIST OF TABLES

LIST OF FIGURES

LIST OF SCHEMES

CHAPTER 1

Introduction

1.1 The versatility of flavoenzymes

Flavoenzymes play roles in a number of biochemical reactions (Figure 1.1), such as electron transfer reactions, oxidation and hydroxylation reactions (*1*), and dehydrogenation. Flavin is a derivative of riboflavin, which is known as vitamin B_2. The core chemical structure of flavin is the isoalloxazine ring (Figure 1.2). Flavoenyzmes normally contain either an FMN or an FAD as a cofactor non-covalently bound to an apoprotein (*2*). In some flavoproteins, however, the flavin is either attached to the 8α-methyl position via a histidine, tyrosine, or cysteine residue, or to the 6α-methyl position via a cysteine residue (*3-5*). There are five different types of covalent linkages as shown in Figure 1.3. Studies have found that the flavin can also be attached to the protein via a dual covalent linkage, as seen in glucooligosaccharide oxidase and berberine bridge enzymes (*6, 7*). This covalent bond plays a significant role in stabilizing the flavin by preventing the protein from being modified and/or inactivated. It also plays roles in oxygen reactivity, facilitating electron transfer and flavin redox potential (*4*).

Flavoenzymes catalyze redox reactions and can exist in different states, i.e., oxidized, semiquinone (one-electron reduced), and fully reduced (two-electron reduced) as shown in Figure 1.4. At least six states are found under physiological conditions. Based on p*K*a values, the flavin semiquinone can exist in a neutral (blue) or an anionic (red) form at the pK_a of ~ 8.5 (*8, 9*). This pK_a can change significantly depending on the protein environment. For example, some enzymes can stabilize the blue semiquinone over the pH range at which the enzymes are stable (pK_a >> 8.5) and other enzymes stabilize the anionic semiquinone form (pK_a << 8.5). In

glucose oxidase the pK_a is in the detectable pH range allowing the characterization of the spectral properties of both species (Figure 1.5) (*8*). At neutral pH, the pyrimidine moiety of the isolloxazine ring nucleus is an electron rich molecule in the reduced state with a negative charge at the N1-C2=(O) moiety, forming anionic hydroquinone, and a pK_a value of ~ 6.5 was determined for the ionization of the N(1) locus of the reduced flavin (*8*).

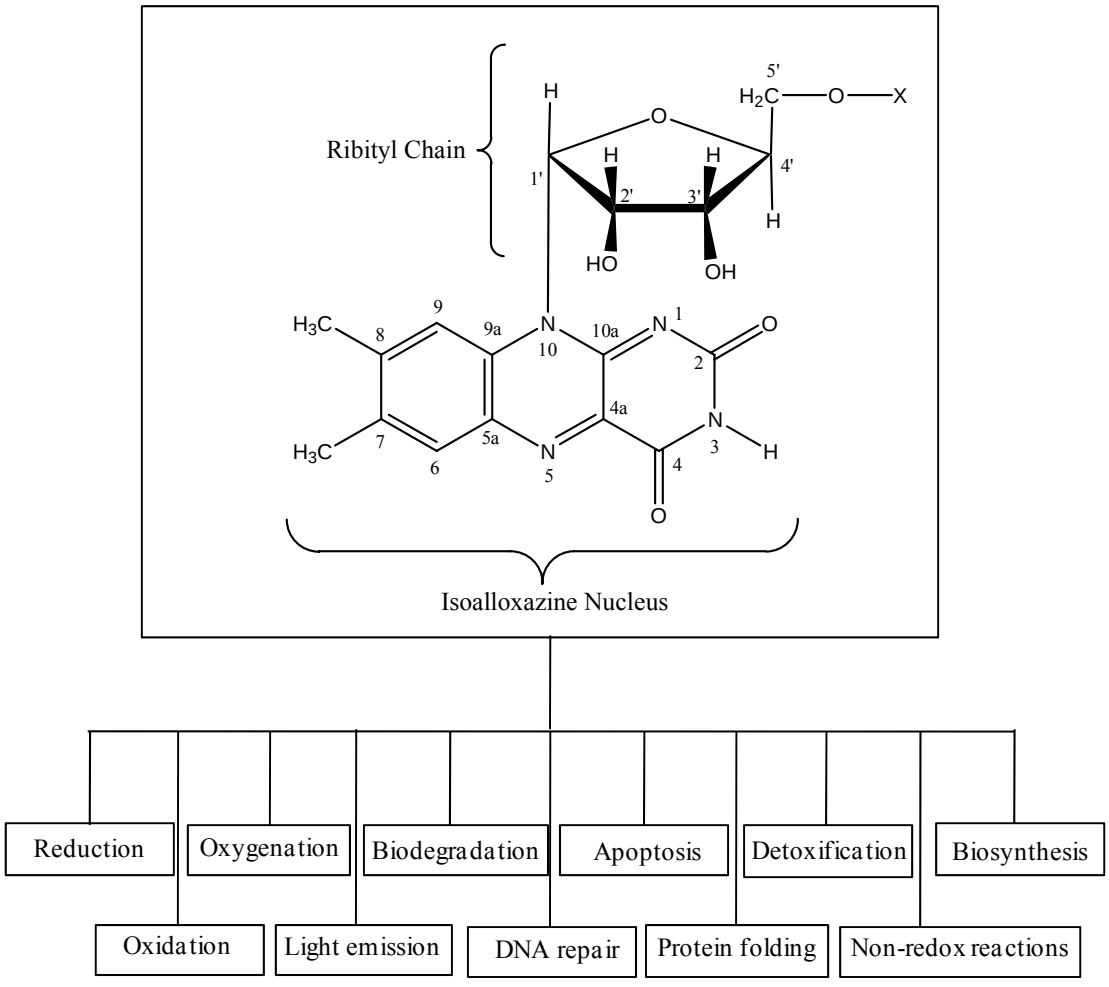

Figure 1.1. Biological functions of flavoenzymes.
Riboflavin, X=H; FMN, X= PO_3^{2-}; FAD, X=ADP.
Modified from ref. (*7*)

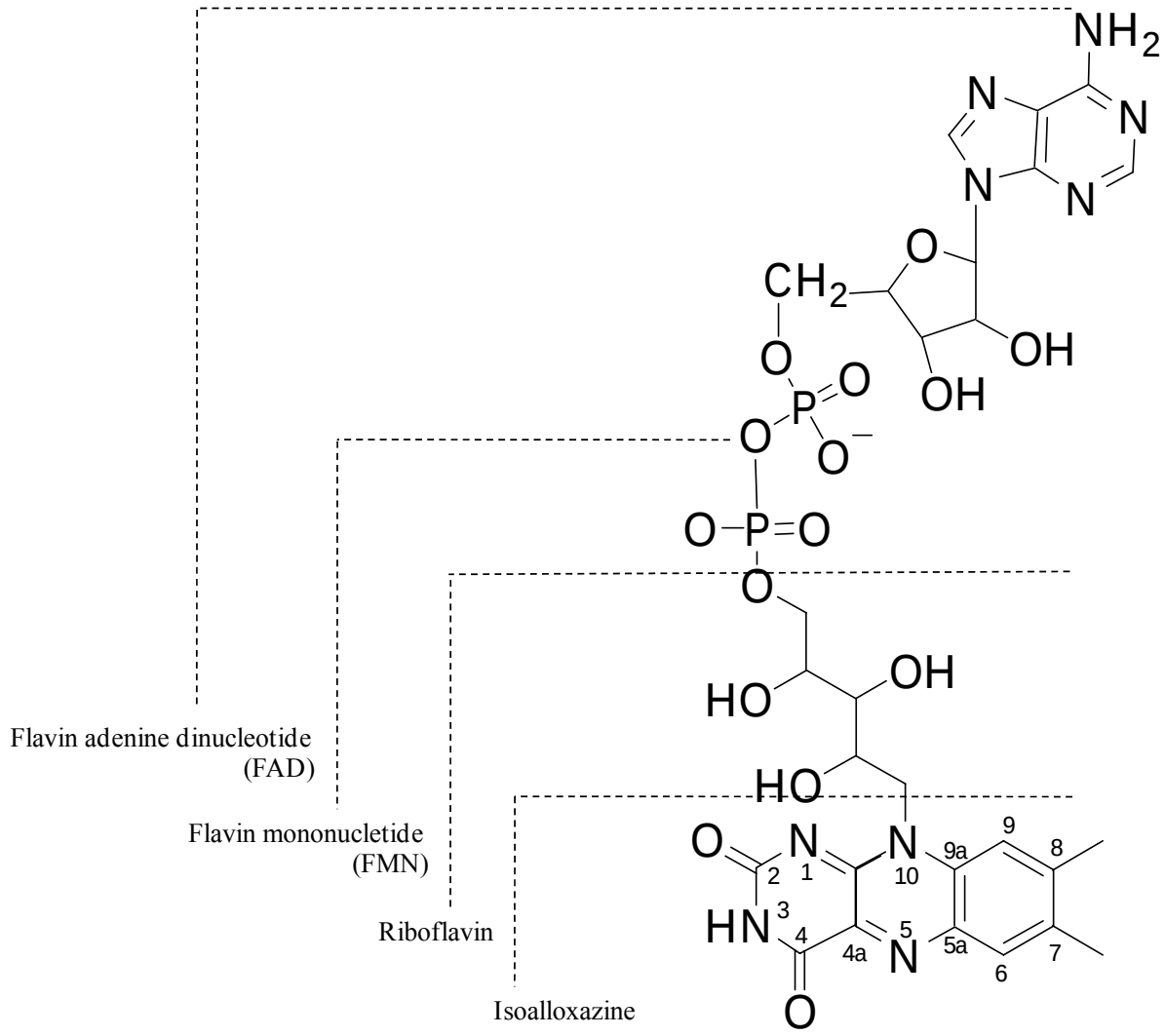

Figure 1.2. The structures of isoalloxazine, riboflavin, FMN, and FAD.
Modified from ref. (*9*)

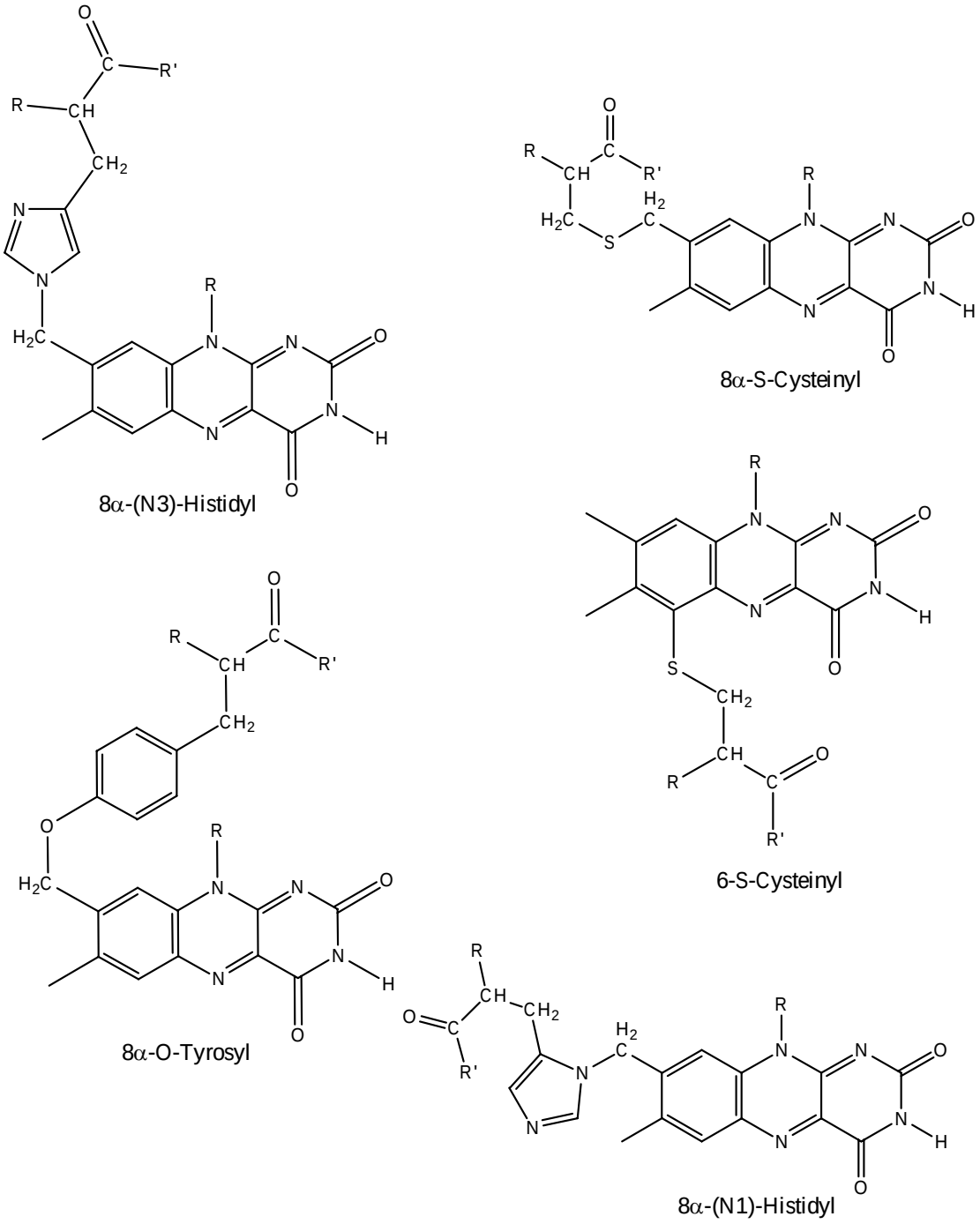

Figure 1.3. Mode of covalent attachment of flavin to the protein in flavoproteins.

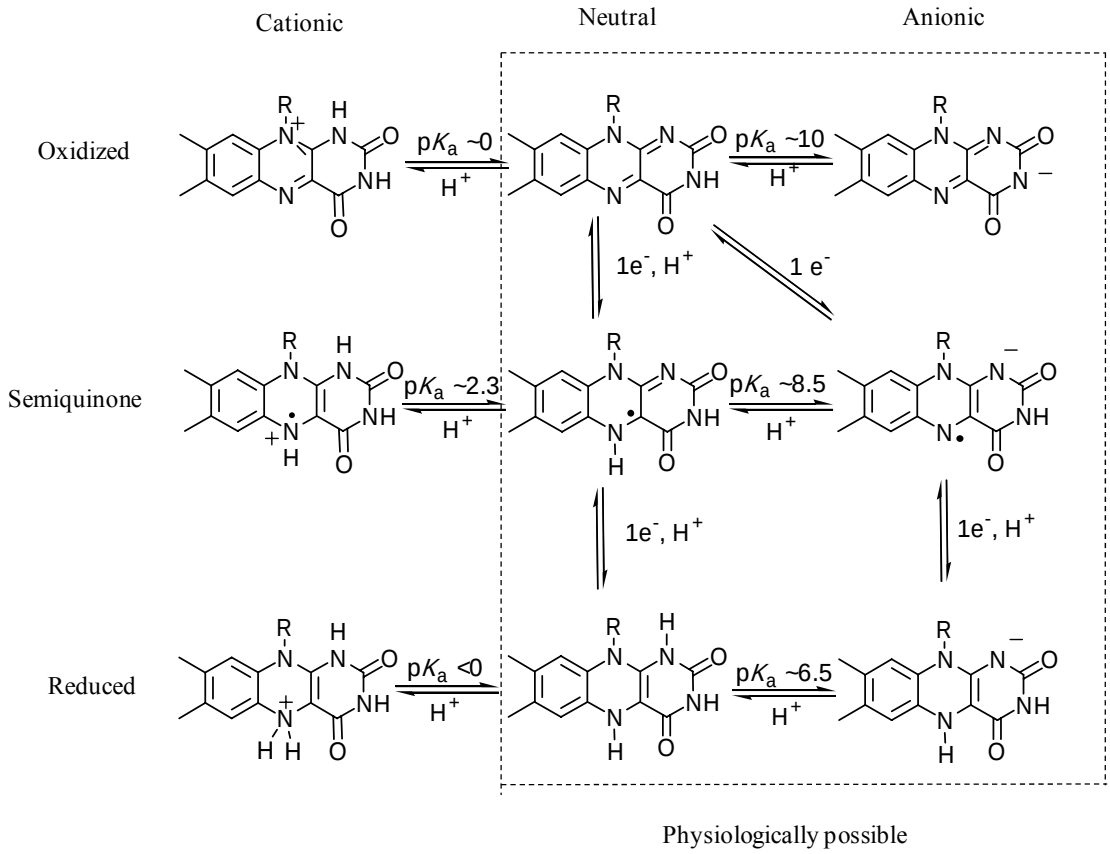

Figure 1.4. Redox and ionization states of flavins.
Modified from ref. (*9*).

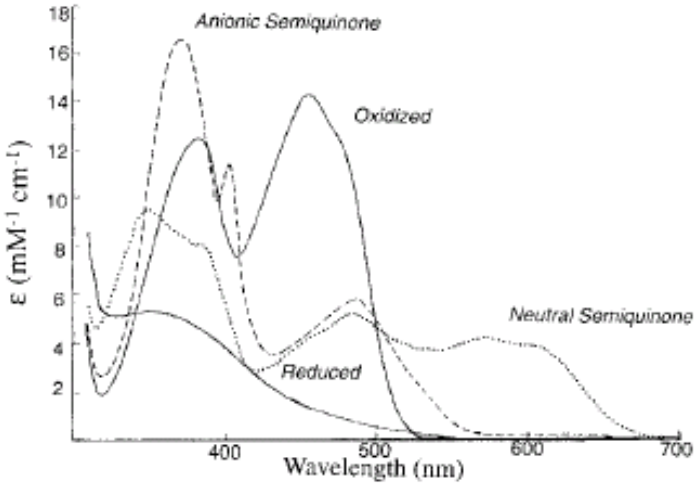

Figure 1.5. Spectra of glucose oxidase in the oxidized, semiquinone (neutral and anionic) and fully reduced forms. Taken from ref. (*10*).

1.1.1 Classification of flavoenzymes

Flavoenzymes are classified based on their types of chemical reactions, physicochemical properties, substrates, and crystal structures (*8*). Hemmerich *et al*. proposed four classes of flavoenzymes according to their redox state forms at the half-reaction without substrates. These are: blue, red semiquinone, no paramagnetic intermediate (i.e., flavoenzymes that contain a cysteine residue which participates in the catalytic reaction), and non-stoichiometric amounts of semiquinone (i.e., metalloflavoproteins) (*11*). Here we follow the classification of flavoenzymes as designated by Palfey and Massey based on the chemical reactions catalyzed by the enzyme (*12*) and provide a description of each class. These are oxidases, dehydrogenases/reductases, disulfide oxidoreductases, and monooxygenases.

Oxidases. Flavoprotein oxidases (such as choline oxidase, pyranose 2-oxidase, sarcosine oxidase, monoamine oxidase, or D-amino acid oxidase) convert their substrates by first catalyzing the oxidation reaction of the organic substrates and then, in a separate step called the oxidative half-reaction, they catalyze the oxidation of the reduced flavin by molecular oxygen, yielding hydrogen peroxide. The enzymes in this class have been observed to share many common properties. They all stabilize a flavin N(5)-sulfite adduct (*13-21*) and the benzoquinoid anion form of 6- and 8- substituted hydroxyl-and mercaptoflavins, where the negative charge of anionic flavin is localized in the N(1)-C(2)=O region (*13, 17, 22*). In addition, they stabilize the red anionic semiquinone flavin radical upon a one-electron reduction. Flavoprotein oxidases exhibit the negative charge of the anionic flavin localized at the N(1)-C(2)=O region of the isoalloxazine ring. The positively charged locus of proteins around this region interacts electrostatically with the pyrimidine ring to stabilize the negative charge of the flavins that readily react toward molecular oxygen (*13, 17-19, 23*). This positively charged locus of the

protein also serves to increase the midpoint potential of the bound flavin, making the reduction more thermodynamically favorable and facilitating the flavinylation process for those enzymes in which flavin is covalently linked to the protein moiety (*24*). Crystal structures of several flavoprotein oxidases have been solved, including glycolate oxidase (*25*), cholesterol oxidase (*26, 27*), and glucose oxidase (*28, 29*). Most of the crystal structures of oxidases indicate the presence of positively charged amino acids in the vicinity of the N(1)-C(2)=O locus of flavin.

Dehydrogenases/reductases. Enzymes in this class, such as acyl-coA dehydrogenase (*30*), D-lactate dehydrogenase (*32*), or NADPH-cytochrome P-450 reductase (*32*), are capable of transferring electrons from one substrate to another, but they do not react with molecular oxygen. *In vitro*, dehydrogenases catalyze the oxidation of organic substrates with the use of artificial electron acceptors such as phenazine and $NADP^+$, whereas reductases transfer electrons from electron donors such as NADH to the substrates. Acyl-CoA dehydrogenases have been well-studied (*30*). These enzymes share a similar catalytic mechanism with many oxidases which catalyze the oxidation of the acyl-CoA substrate through a proton abstraction and hydride transfer from the β-carbon to the N(5) of flavin (*31*). Two examples of flavin-containing reductases are ferredoxin-$NADP^+$ reductase (*115*) and NADPH-cytochrome P-450 reductase (*115*). These enzymes react sluggishly with O_2 to produce $O_2^{\bullet-}$ and stabilize the blue neutral form of the flavin semiquinone. In contrast to the oxidases, the reductases cannot form flavin N(5)-sulfite adducts or stabilize the benzoquinoid forms of the 6-and 8-substituted flavins (*22*).

Disulfide oxidoreductases. The enzymes in this class use both an FAD cofactor and cysteine residues as electron transfer mediators. In general, catalysis involves interactions between the flavin and pyridine nucleotide followed by a hydride transfer to the flavin. The reduced flavin then reacts rapidly with the active site disulfide/dithiol, such as glutathione in

glutathione reductase and thioredoxin in thioredoxin reductase. Next, the thiol is eliminated from the cysteinyl adduct. This reaction yields a thiolate and a newly oxidized flavin (*32*). The disulfide oxidoreductases play important roles in cellular metabolism. Studies have been conducted to develop thioredoxin reductase inhibitors that can be used to treat microbial infections and parasitic diseases (*33*).

Monooxygenases. In this class of flavoenzymes, the reduced enzyme reacts with molecular oxygen to form a flavin C4(a)-hydroperoxide intermediate (*1*). Another common feature of these enzymes is that they use NADH or NADPH to reduce the flavin (FAD). Monooxygenases can be divided into two subgroups: aromatic hydroxylases (such as *p*-hydroxybenzoate hydroxylase (*1*)), and nucleophilic monooxygenases (such as bacterial luciferase and cyclohexanone monooxygenase (*1*)). In aromatic hydroxylases, the enzyme-aromatic substrate complex is required for the flavin reduction by NAD(P)H. In the absence of the organic substrate, the flavin hydroperoxide is very unstable and can decay to H_2O_2. This process results in an oxidized flavin. A difference in the rate constant of as much as 100,000 fold has been observed experimentally between reactions that contain the substrate and those that do not (*8*). In contrast, in the nucleophilic monooxygenases, the C4(a)-hydroperoxide is stabilized by the protein and is reactive only in the presence of the substrate for the oxygen transfer (*1*).

1.1.2 The flavin binding site

The tricyclic isoalloxazine ring system is the reactive part of the flavin (Figure 1.6). The isoalloxazine moiety of the flavin is amphipathic. Its hydrophobic dimethylbenzene moiety can react with the hydrophobic part of the protein, and its hydrophilic pyrimidine ring is capable of interacting with the protein via hydrogen bonds and electrostatic interactions (Figure 1.6) (*22*). Based on the crystal structures of many flavoproteins, the N(1)-C(2)=O locus of the flavin is commonly found to be close to the positively charged amino acids, lysine or arginine, histidine side chains, the N terminus of an α-helix or a cluster of peptide nitrogens (*34*). A positive charge at this position can stabilize the anionic form of reduced flavin, increase the redox potential and favor flavin binding (*34*). Moreover, the positively charged residues could also be responsible for the formation of flavin-N(5)-sulfite adduct by facilitating the nucleophilic attachment of sulfite to the N(5) locus of the oxidized flavin (*34*).

The ability of sulfite ions to react with flavoproteins and to form a reversible flavin-N(5)-sulfite adduct has also been investigated in flavoenzymes (*18*) such as glucose oxidase (*35*), lactate oxidase (*13*), *D*- and *L*-amino acid oxidase (*18, 36*), glycolate oxidase (*37*), cholesterol oxidase (*15*), monomeric oxidase (*21*), and choline oxidase (*38*). Interestingly, it was found that the formation of the flavin sulfite adduct depends on the sulfite concentration, temperature, and pH (*18, 20*). However, the amount of light or the presence of oxygen do not seem to affect the adduct formation (*18, 20*). Studies have shown that the formation of the reversible flavin-N(5)-sulfite adduct only results from the flavoenzymes that react readily with molecular oxygen (*8, 18, 20, 22*), but not from flavoprotein dehydrogenases (*18, 20*). As a result, the formation of covalent N(5)-flavin adduct with sulfite has become a key feature to distinguish flavoprotein oxidases from dehydrogenases (*18, 20, 23*). Since the oxidized flavin is electron deficient and

the sulfite is a powerful nucleophile, flavin in its oxidized state can react with either SO_3^{2-} or HSO_3^- (*20*).

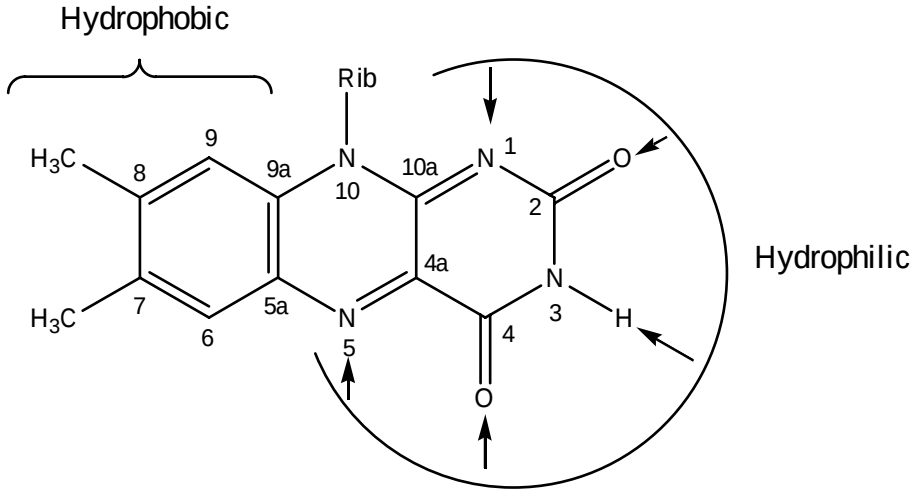

Figure 1.6. The tricyclic isoalloxazine ring with the possible flavin-protein interactions.
Rib = Riboflavin; FMN = Rib- PO_3^{2-}; FAD = Rib-ADP.
Modified from ref. (*22*).

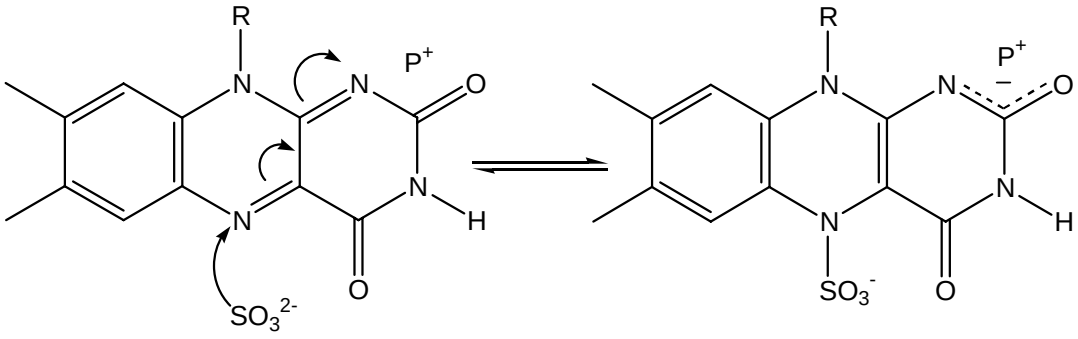

Figure 1.7. Mode of reaction of sulfite with oxidized flavin.
R= FMN or FAD.
P^+, protein positively charged amino acid residue or α-helix dipole.

1.2 Histidine residue in proximity of N(1)-C(2)=O of flavin

Based on the three-dimensional structures of flavoprotein oxidases that are available through the PDB (Protein Data Bank) and kinetic studies, there is a positively charged residue located close to the N(1)-C(2)=O locus of flavin (*34*). This positive charge is contained on side chains of lysine, arginine, and histidine. Alternatively, the N terminus of an α-helix and a cluster of peptide nitrogens may also be found in this region (*34*). The functional roles of this positive charge, the N terminus of an α-helix, and the cluster of peptide nitrogens have all been investigated. It was ascertained that these features help stabilize the negatively charged N(1)-C(2)=O region in the reduced-form flavin (*13, 17-19, 34*), facilitating flavin flavinylation process for those enzymes in which the flavin is covalently linked to the protein moiety (*24*) and making the flavin reduction thermodynamically favorable by elevating the midpoint reduction-oxidation potential of the bound flavin (*17, 19, 34, 39*). Examples of flavoenzymes with histidine residues in proximity of the N(1)-C(2) atom of flavin will be discussed and summarized here: choline oxidase on page 11, chorismate synthase on page 14, aryl-alcohol oxidase on page 15, and glucose oxidase on page 17.

Choline oxidase (E.C. 1.1.3.17), a flavin-dependent enzyme, catalyzes the oxidation of choline to glycine betaine (Figure 1.8). The enzyme is a homodimer with a molecular mass of 120 kDa and it contains covalently bound FAD in a 1:1 ratio (*40*). The structural, biophysical, and mechanistic properties of choline oxidase have been characterized (*38, 41-46*). The crystal structures and the amino acid sequence alignment of the GMC oxidoreductases reveal that His466 is highly conserved and is located ~ 3 Å from the N(1)-C(2)=O of flavin (Figure 1.9) (*46, 47*). The mechanistic role of this residue has been elucidated by using a combination of biochemical, spectroscopic, and mechanistic probes (*46, 99*).

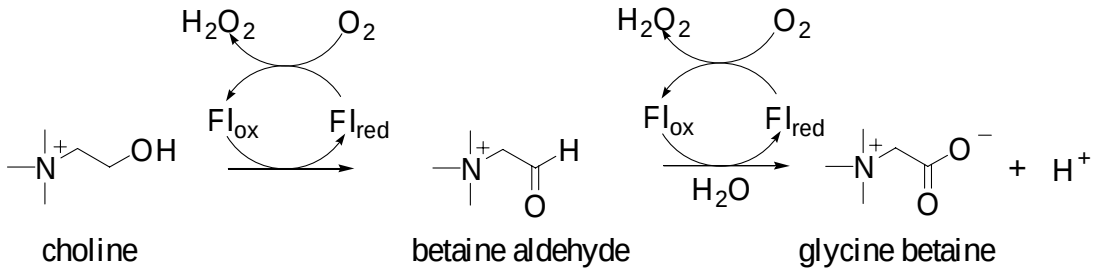

Figure 1.8. Reaction catalyzed by choline oxidase.

Replacement of histidine with an alanine residue at position 466 in choline oxidase resulted in destabilization of the anionic flavin semiquinone (as purified) and of the sulfite N(5)-flavin adduct (*46*). His466Ala lost its ability to form an N(5)-flavin adduct with the sulfite due to the absence of the positively charged side chain of His466. The proposed role of His466 in the stabilization of the negatively charged oxygen atom of the sulfite N(5)-flavin adduct is shown in Figure 1.10. A decrease of ~ 25 mV in the midpoint reduction potential of the enzyme-bound flavin in His466Ala, compared to that of the wild-type, also indicated a significant electrostatic contribution of the imidazole side chain His466 to the N(1)-C(2)=O locus of the flavin cofactor (*46*). His466 also stabilizes the transition state that is formed during the oxidation of choline to betaine aldehyde. This is supported by the change in the relative timing for bond cleavages in the His466Ala in which the OH and CH bond cleavages are in the same transition state. In contrast, wild-type choline oxidase, exhibits a kinetically fast proton abstraction step followed by a hydride transfer (*42*). In addition, when His466 is replaced by an aspartate, the mutant enzyme completely loses enzymatic activity (*46*). In His466Asp, ~75% of FAD is not covalently bound to the protein moiety, whereas both wild-type and His466Ala contain only covalently

bound FAD (*40, 46*). In addition, in both His466Ala and His466Asp variants the total FAD content was 3-4 fold lower than in the wild-type, for which a 1:1 stoichiometry of FAD to protein was observed. Finally, the His466Asp mutant showed a ~ 160 mV decrease in the midpoint reduction-oxidation potential of the enzyme-bound flavin for two-electron transfer. Taken all together, these data suggest that the presence of a positively charged protein near the N(1) position of the flavin is important for the flavin content and for the covalent linkage between FAD and the protein.

Figure 1.9. The active site of wild-type choline oxidase with selected amino acids at a resolution of 1.86 Å (PDB 2jbv) (*47*).

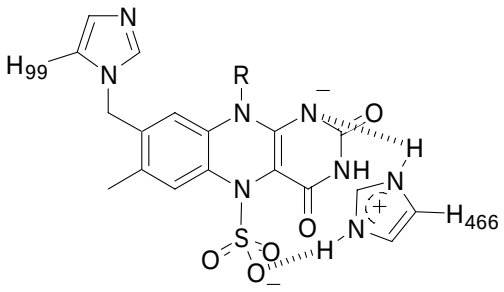

Figure 1.10. Proposed interaction of His466 with the flavin N(5)-sulfite adduct.
Modified from ref. (*46*).

Chorismate synthase catalyzes the conversion of 5-enolppyruvylshikimate-3-phosphate (EPSP) to chorismate by 1,4-*anti*-elimation of the 3-phosphate group and the C-(6*pro*R) hydrogen from EPSP (*48, 49*). Even though the reaction does not involve an overall change in redox state, the enzyme requires reduced FMN as a cofactor as shown in Scheme 1.1 (*50*).

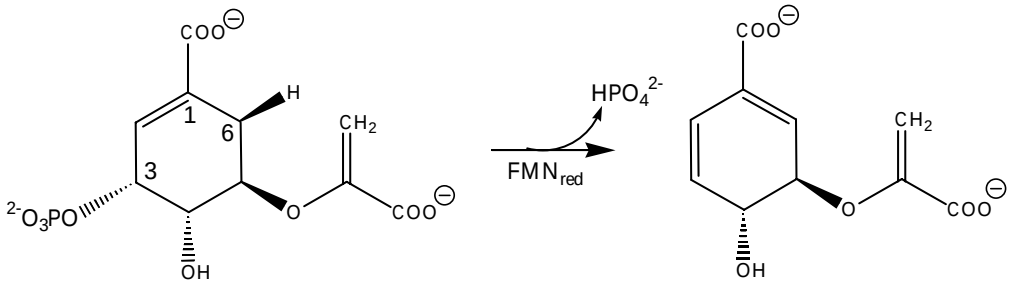

Scheme 1.1. Reaction catalyzed by chorismate synthase.
Modified from ref. (*51*).

The chorismate synthase crystal structure (*52*) reveals that there are two conserved histidines in the active site of the enzyme. In chorismate synthase of *Neurospora crassa*, His17 and His106 are located within 2.7 and 3 Å, respectively, of the C(2)=O of the flavin ring and the substrate phosphate group as shown in Scheme 1.2. Site-directed mutagenesis studies reveal the potential roles of these two histidines in more detail. Both of the single mutant proteins His17Ala and His106Ala showed 10- and 20- fold decreases in the elimination reaction, compared to the results obtained from the wild-type enzyme, suggesting important roles of both histidines in the

chorismate synthase reaction. From previous redox potential and kinetic studies (*51, 53*) it was shown that His106 stabilizes the neutral reduced flavin in the active site of chorismate synthase and functions as an acid that donates a proton to N(1) of flavin during formation of the enzyme-substrate complex (Scheme 1.2). At this stage, the negatively charged C(1)-carboxylate triggers the protonation of N(1) of the flavin by causing an increase of its pK_a; studies performed on FMN derivatives have shown that there is preferential binding of the protonated, reduced FMN species rather than the N(1)-deprotonated species (pK_a = 6.7) in free solution (*53*) .

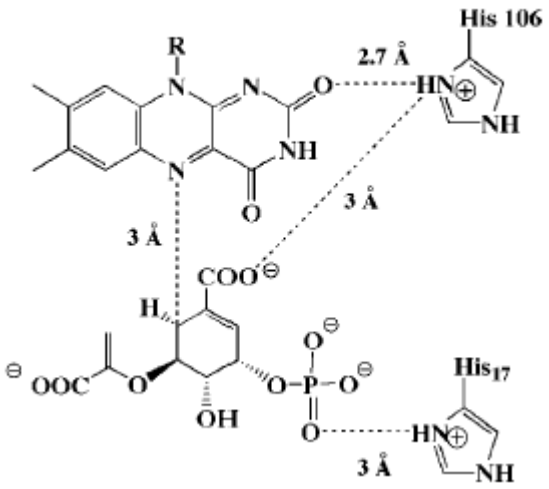

Scheme 1.2. The active site of chorismate synthase with two conserved histidine residues. Taken from ref. (*51*).

Aryl-alcohol oxidase (AAO, EC 1.1.3.7) catalyzes the oxidation of aromatic and aliphatic polyunsaturated alcohols to their corresponding aldehydes, and the molecular oxygen functions as an electron acceptor that produces hydrogen peroxide (Figure 1.11 and Figure 1.12) (*54*). The product, H_2O_2, is known to be involved in lignin biodegradation, which is a key process for carbon recycling in land ecosystems (*54*).

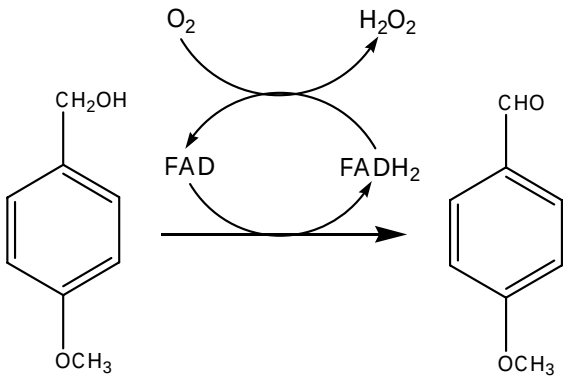

Figure 1.11. The reaction catalyzed by aryl-alcohol oxidase.
Modified from ref. (*54*).

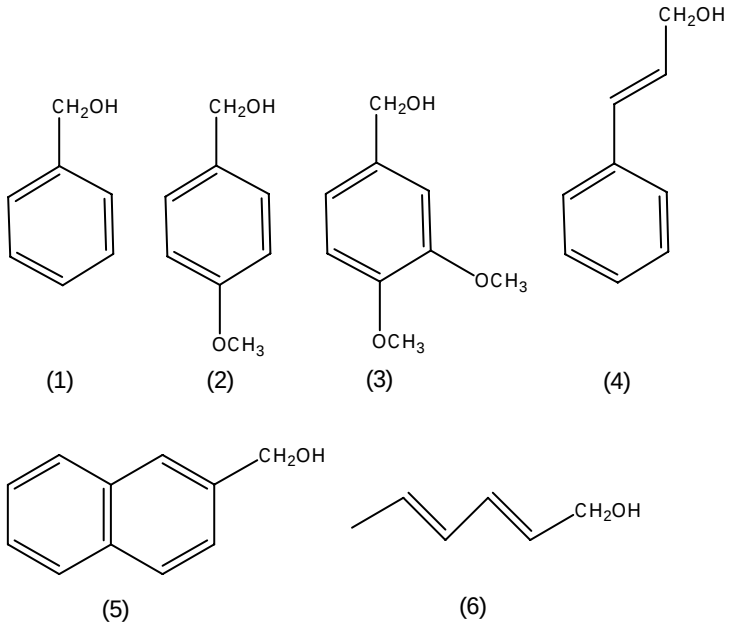

Figure 1.12. The variety of aromatic substrates of aryl-alcohol oxidase; (1) benzyl alcohol; (2) p-anisyl alcohol; (3) veratryl alcohol; (4) cinnamyl alcohol; (5) 2-naphthalenemethanol; and (6) 2,4- hexadien-1-ol.
Modified from ref. (*54*).

Aryl-alcohol oxidase belongs to the glucose-methanol-choline (GMC) oxidoreductase enzyme superfamily (*55*). A histidine residue is fully conserved in members of this superfamily, including glucose oxidase (*56, 57*), choline oxidase (*40, 47*), cholesterol oxidase (*58, 59*),

hydroxynitrile lyase (*60*), and the flavin domain of cellobiose dehydrogenase (*61*). When His502 and His546 of AAO were mutated to leucine and serine, respectively, the enzyme variants were completely inactive (*54*). In contrast, His502Arg and His546Arg mutants demonstrated enzymatic activity ~ 100-200 fold lower than that of the wild-type, indicating that these two histidine residues could contribute to the stabilization of the substrate alkoxide. Furthermore, the histidines are located at a similar distance from the hydroxyl group of the substrate, and His546 is located in proximity of the N(1)-C(2)=O locus of flavin. This suggests that the histidines could also play a role in facilitating the hydride transfer from the substrate to FAD (*54*).

Glucose oxidase (GO, E.C. 1.1.3.4) catalyzes the oxidation of β-D-glucose to glucono-δ-lactone, which subsequently hydrolyzes spontaneously to gluconic acid concomitant with the reduction of molecular oxygen to hydrogen peroxide (Figure 1.13) (*62*). The crystal structure of GO from *Aspergillus niger* was determined to a resolution of 2.3 Å (*28*). Figure 1.14 shows the active site of GO with selected amino acids. Kinetic and structural data indicate that His559 is hydrogen bonded to Glu412 and a water molecule (W110). The carboxylate group of the glutamate plays a role in substrate binding and specificity (*63*). The modeled enzyme-substrate complex of glucose oxidase revealed that the binding of the substrate to the enzyme involves protonation of Glu412. This disrupts the hydrogen bond of His559 and results in reorganization of the active site (*64*). His516, a conserved amino acid in the GMC family, is located 3.8 Å away from the negative charge N(1) of reduced flavin (Figure 1.14). It has been concluded that His516 can act as a base or an acid catalyst in the reductive (*62*) or in the oxidative half-reaction (*57*), respectively. Moreover, site-directed mutagenesis studies indicate that His516 catalyzes the reaction with O_2 by contributing a positive charge to the reaction (*65*). In general, the

catalytic rates of the O_2 activation by flavoprotein oxidases require the presence of a positively charged amino acid in the active site, especially in proximity of N(1)-C(2)=O (*18, 66*). In GO, for example, removal of the positively charged His516 near N(1)-C(2)=O of flavin by changing the pH or by mutating the His to Ala results in a decrease in the rate constants k_{cat}/K_m of O_2 from 1.5×10^6 $M^{-1}s^{-1}$ to 5.7×10^2 $M^{-1}s^{-1}$ (*65*). These results indicate that the positively charged His516 stabilizes the negative charge at the N(1)-C(2)=O locus of the flavin and is involved in the activation of O_2 in the oxidative half-reaction.

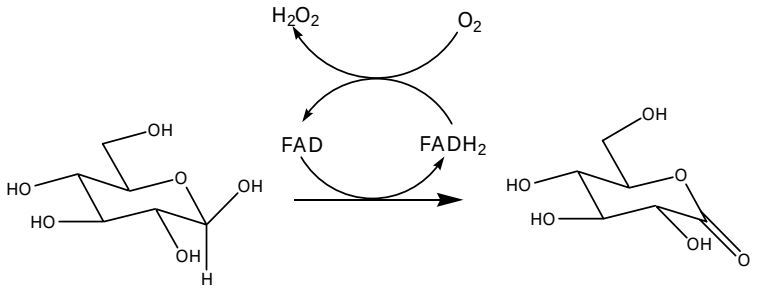

Figure 1.13. The reaction catalyzed by glucose oxidase.

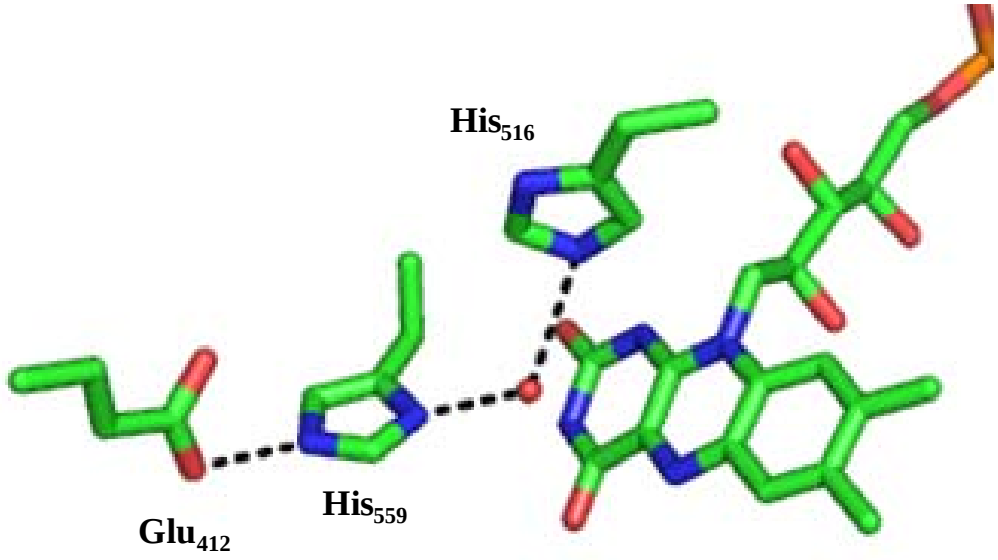

Figure 1.14. Active site of glucose oxidase (PDB 1CF3).
Modified from ref. (*62*).

1.3. His-Asn pair in flavoenzymes

Based on comparison of the crystal structures and gene sequences of many flavoenzymes it has been found that two enzyme families, the old yellow enzyme family and the glucose-methanol-choline (GMC) oxidoreductase enzyme superfamily, have two highly conserved residues, His and Asn or His, in their catalytic sites. These residues are in proximity of the isoalloxazine ring of the flavin. The conservation of these residues suggests that they could play important roles in the protein functions.

The crystal structures of old yellow enzyme (OYE) from brewer's bottom yeast (OYE1) (*67*) (Figure 1.15) reveal that the phenolic ligand is positioned parallel to the isoalloxazine ring in FMN. The phenolate oxygen was found to be within hydrogen-bonding distance to the conserved His191 and Asn194. The sequence around His191 and Asn194 of OYE1 was compared with OYE1-homologues (Figure 1.16) and the results showed that the residues are conserved in other enzymes. Mutation of His191 to Asn resulted in decreased binding affinities for substituted phenols. A decrease of 145-fold was observed for *p*-hydroxybenzaldehyde and a 2500 to 4000-fold decrease was observed for *p*-chlorophenol, pentafluorophenol and *p*-cyanophenol (*68*). From the crystal structure of OYE (*67*), the amide nitrogen of Asn194 is located 3.3 Å from N(1) and 3.5 Å from C(2)=O of the flavin. These distances are not affected greatly by the *p*-hydroxybenzaldehyde binding. Substitution of Asn194 to His resulted in expression of a protein that is difficult to isolate (*67*). The crystal structure of the mutant enzyme clearly showed that the FMN position has changed compared to the wild-type (*67*). In the mutant protein, more spaces are observed between the ribityl side chain and the FMN. This change caused the FMN to lose its ability to bind to the Asn194His variant. The conserved His186 and Asn189 of morphinone reductase (MR), a member of the old yellow enzyme family,

were also investigated for their functional roles (*69*). Figure 1.17 shows the location of these two conserved residues in the active site of the enzyme, close to the redox region of the FMN isoalloxazine ring (*70*). Site-directed mutagenesis studies showed that both conserved His186 and Asn189 in MR are involved in binding the oxidizing substrates 2-cyclohexen-1-one and 1-nitrocyclohexene as well as coenzyme NADH (*69*). Interestingly, the redox potential study showed that even though the Asn189 residue is in proximity to the N(1)-C(2)=O region of the FMN isoalloxazine ring, the Asn189Ala variant does not have a different redox potential when compared to the wild-type (*71*). Results from recent studies are consistent with these data which indicate that the positively charged side chain Arg23 near the N(1) locus is neither required for stabilization of the reduced form of FMN nor does it affect the reduction potential of the FMN (*71*).

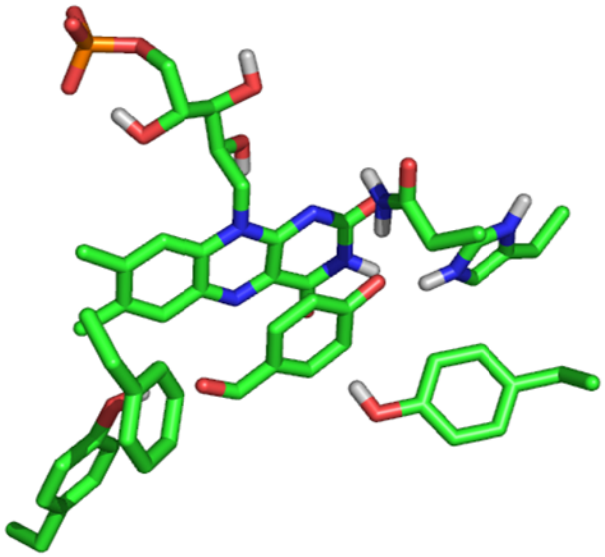

Figure 1.15. The active sites of OYE1 (PDB code 1OYB). PHB: *p*-hydroxybenzaldehyde (*67*).

		191 194			
OYE1	AKNSIA**A**GAD	GVEI**H**SA**N**GY	LL.NQ**F**LDPH	S**N**NRT**D**E**Y**G.	G**S**IEN**R**ARFT
OYE2	AKNSIA**A**GAD	GVEI**H**SA**N**GY	LL.NG**F**LDPH	S**N**TRT**D**E**Y**G.	G**S**IEN**R**ARFT
OYE3	AKNSIA**A**GAD	GVEI**H**SA**N**GY	LL.NG**F**LDPH	S**N**KRT**D**E**Y**G.	G**T**IEN**R**ARFT
KYEI	AKKCID**A**GAD	GVEI**H**SA**N**GY	LL.NQ**F**LDPI	S**N**KRT**D**E**Y**G.	G**S**IEN**R**ARFV
EBPI	AKHALE**A**GFD	YVEI**H**GA**H**GY	LL.DQ**F**LNLA	S**N**KRT**D**K**Y**GC	G**S**IEN**R**ARLL
NER A	ARAALW**A**GFD	GVEI**H**A**A**NGY	LI.EQ**F**LKSS	T**N**QRT**D**D**Y**G.	G**S**IEN**R**ARFL
NEM A	IANARE**A**GFD	LVEL**H**SA**H**GY	LL.HQ**F**LSPS	S**N**HRT**D**Q**Y**G.	G**S**VEN**R**ARLV
OPDA	ARNAME**A**GFD	GVEI**H**GA**N**GY	LI.DQ**F**MKDT	V**N**DRT**D**E**Y**G.	G**S**LQN**R**CKFP
PETN	VABARE**A**GFD	LVEL**H**SA**H**GY	LL.HQ**F**LSPS	S**N**QRT**D**Q**Y**G.	G**S**VEN**R**ARLV
MOR B	AQRAKR**A**GFD	MVEV**H**A**A**NAC	LP.NQ**F**LATG	T**N**RRT**D**Q**Y**G.	G**S**IEN**R**ARFP

Figure 1.16. The sequence of OYE and OYE homologues. The proteins showed here are OYE1 from brewer's bottom yeast (*72*), OYE2 from *S. cerevisiae* (*73*), OYE3 from *S. cerevisiae* (*74*), KYE1 from *Kluveromyces lactis* (*75*), estrogen-binding protein (*EBP I*) from *Candida albicans* (*76*), glycerol trinitrate reductase (*NER A*) from *Agrobacterium radiobacter* (*77*), N-ethylmaleimide reductase (*NEM A*) from *E. coli* (*78*), 12-oxophytodienoate reductase (*OPDA*) from *A. thaliana* (*79*), pentaerythritol tetranitrate reductase (*PETN*) from *Enterobacter cloacae* (*80*), MOR B (morphinone reducatse) (*MOR B*) from *P. putida* (*81*).
Taken from ref. (*68*).

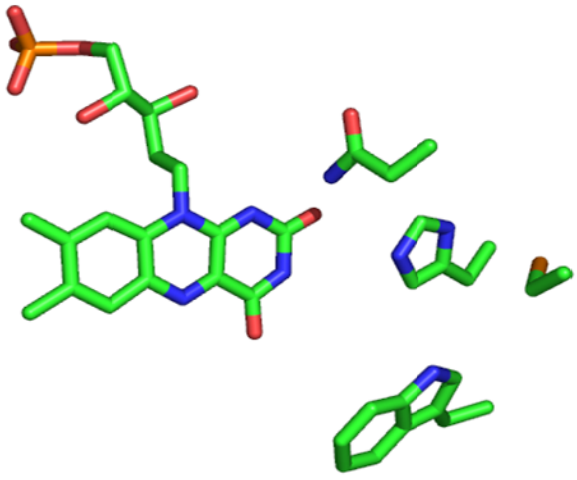

Figure 1.17. Active site structure of morphinone reductase.
Taken from ref. (*70*).

As mentioned on page 19, GMC enzymes have a highly conserved catalytic site that contains a His-Asn pair as shown in Figure 1.18. In glucose oxidase, however, the asparagine residue is replaced by a histidine. The two residues His689 and Asn732 in the active site of the flavin domain of cellobiose dehydrogenase (CDHdh) were investigated their functional roles. All His689 mutants (for examples, His689Ala, His689Val, and His689Asn) showed a decrease of more than 1000 fold in k_{cat} values, whereas the K_m values for cellobiose and lactose substrates appeared similar to that of the wild-type (*82*). The authors proposed that this histidine acts as a base in the oxidation of cellobiose. Absence of this residue resulted in a loss of the ability to deprotonate the *β*-hydroxyl of the substrate, as indicated by the lower observed k_{cat} values. Figure 1.19 shows that the position of the Asn732 is very close to *β*-hydroxyl of cellobiose; hence, it cannot act as a base in catalysis. All the asparagine variants exhibit not only a decrease in the rate of cellobiose oxidation, but also an increase in the K_m values, up to 60-fold compared to the wild-type (*82*). Furthermore, mutation of the Asn732 resulted in a weakening of the binding to lactose and cellobiose substrates. This supports the assertion that Asn732 is involved in substrate binding (*82*). In the case of cholesterol oxidase, the functions of the conserved His-Asn residues (His447 and Asn485) also were investigated (*83-85*). In brief, His447 increases the basicity of Wat541 by forming a hydrogen bond with Wat541 and Asn485 instead of abstracting the hydroxyl proton from the steroid during hydride transfer, and helps position the substrate with respect to the flavin and Glu361. It was found that the imidazole moiety is important, since site-directed mutagenesis studies showed that a neutral and positively charged residue is required at this position (only two mutants, His447Asn and His447Gln, were active and His447Glu and His447Asp were completely devoid of activity) (*83*). It was also concluded that the other

conserved residue, Asn485, is important for creating an electrostatic potential around the FAD to favor the oxidation of the alcohol substrate. Since Asn485 is located near N(1)-C(2)=O of the flavin, the Asn485Leu mutant resulted in 76 mV decrease in the reduction potential of the FAD (*85*).

In glucose oxidase, His516 and His559 residues were identified as a highly conserved catalytic pair (Figure 1.18). His516 has been proposed to act as a catalytic base that abstracts the proton from the substrate hydroxyl group and initiates the reductive half-reaction (*28, 57, 63, 64*). However, studies including site-directed mutagenesis, pH profiles, kinetic isotope effects, and crystal structure determination, all suggest that the protonated form of His516 is involved in the oxidative half-reaction. Removal of the positive charge contributed by histidine by changing pH or by mutagenesis makes the reduced flavin more likely to reduce O_2. At high pH, the His516Ala mutant showed a decrease of k_{cat}/K_m value for O_2 that was three orders of magnitude lower than the wild-type. In contrast, it was found that the enzyme reacts faster under acidic conditions, where His516 and His559 would be protonated (*57, 65*). Furthermore, results from NMR studies of the reduced glucose oxidase at pH 5.6 and the crystal structure suggest that the N(1)-C(2)=O locus of the bound flavin could be stabilized by the protonated form of His516, which is found ~3.8 Å away from the locus (*28, 86*). The other member of the proposed catalytic pair, His559, has been suggested to form hydrogen bonds with Glu412 and a water molecule (W110) and to be involved in substrate binding (*28*). The X-ray crystal structure of glucose oxidase revealed that binding of the substrate to the enzyme was prevented by the protonated form of Glu412. The protonated Glu412 interrupts the hydrogen bond with His559 and results in a reorganization of the active site (*64*).

Another member of GMC enzymes, pyranose 2-oxidase, also has a highly conserved active site containing His548 and Asn593 (Figure 1.20) (*87*). To date, there are no detailed studies of the roles of His548 and Asn593. However, based on the crystal structure of pyranose 2-oxidase compared to other GMC enzymes, it has been proposed that His548 could behave as a catalytic base that abstracts hydroxyl proton from the substrate, initiating the reaction (*87*). A recent docking model of β-D-glucose into the active site of pyranose 2-oxidase showed that the β-hydrogen atom of C2 or C3 of glucose is oriented directly toward the N5 atom of isoalloxazine locus of the bound FAD (Figure 1.21). This suggests that pyranose 2-oxidase could catalyze the glucose oxidation via a hydride transfer mechanism (*87*).

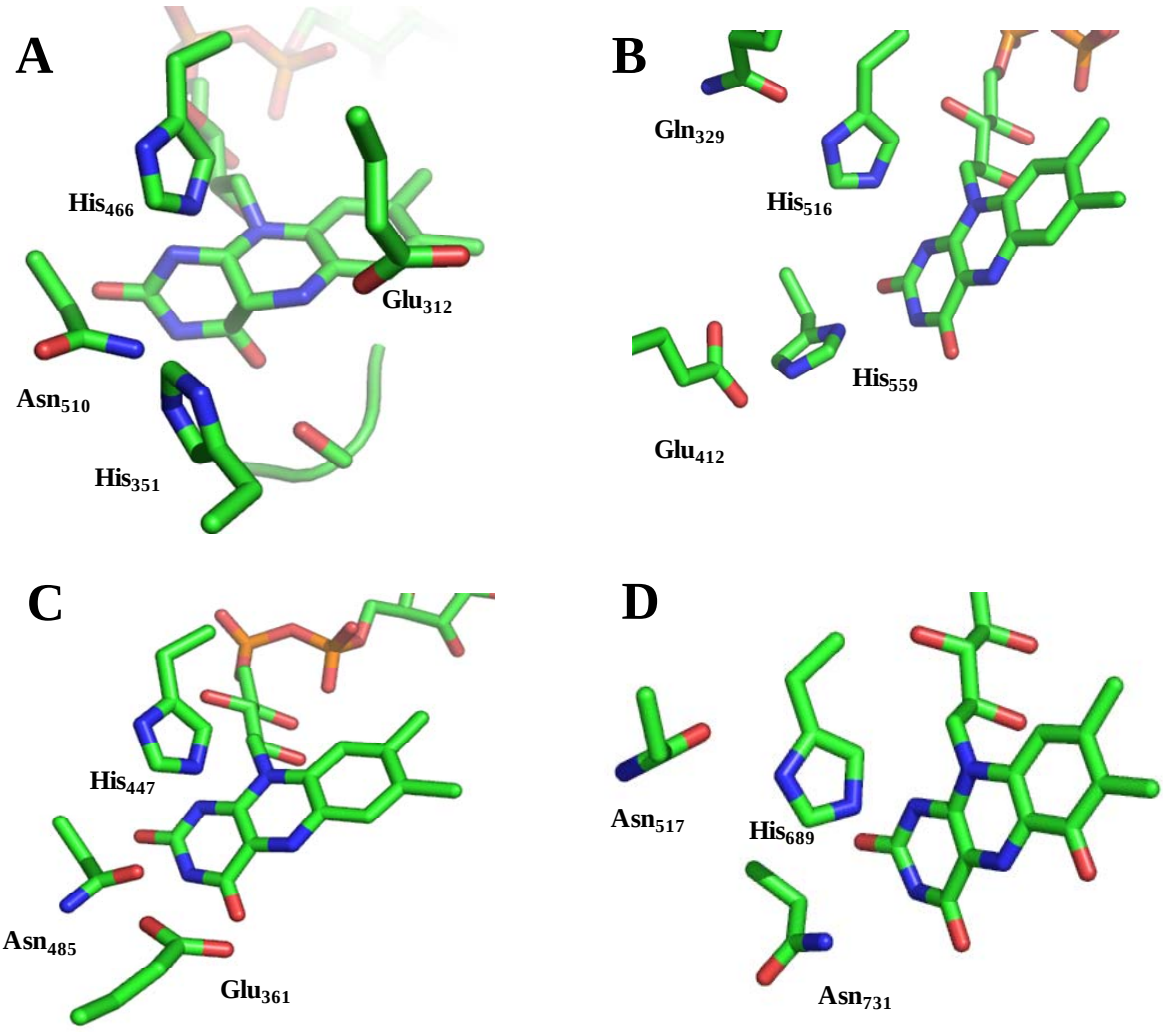

Figure 1.18. Active site residues of GMC oxidoreductase enzyme superfamily. (A) Choline oxidase from *Arthrobacter globiformis* (PDB 2jbv) (*47*); (B) glucose oxidase from *Aspergillus niger* (PDB 1CF3) (*64*); (C) cholesterol oxidase from *Brevibacterium sterolicum* (PDB 1COY) (*83*); (D) cellobiose dehydrogenase from *Phanerochaete chrysosporium* (PDB 1NAA) (*82*).

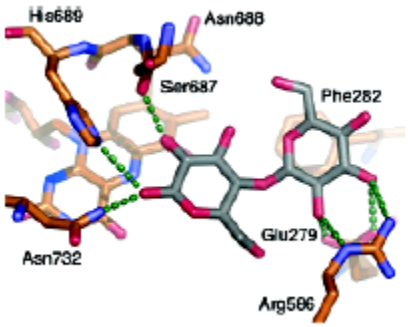

Figure 1.19. Active site of flavin domain cellobiose dehydrogenase complex with docked cellobiose.
Taken from Ref. (*82*)**.**

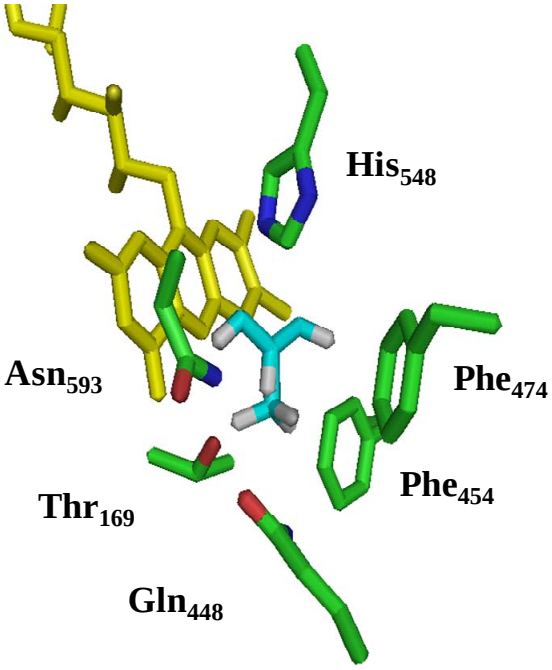

Figure 1.20. The active site of pyranose 2-oxidase (PDB 1TT0) (*87*).

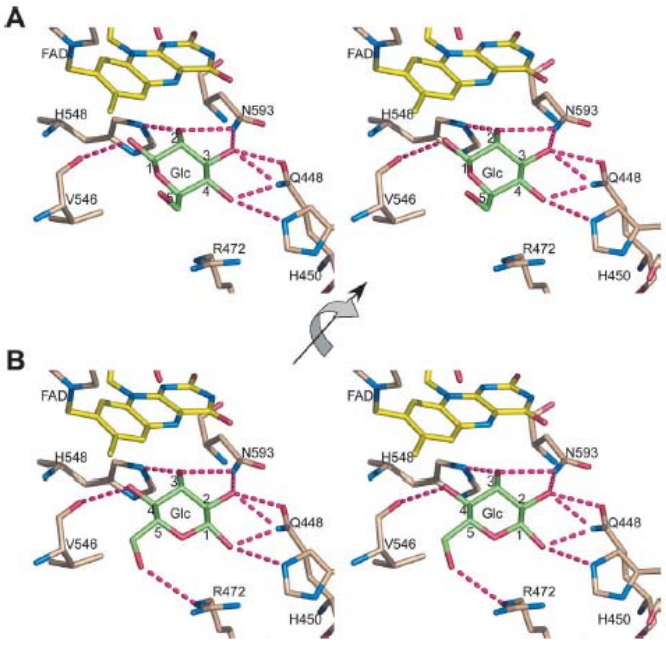

Figure 1.21. Docking of β-D-glucose to the pyranose 2-oxidase active site. (A) Glucose positioned for oxidation at C2; (B) Glucose positioned for oxidation at C3.
Taken from Ref. (*87*).

1.4. Histidine residue as a catalytic base

A number of flavoproteins catalyze the oxidation of primary alcohols to aldehydes (*109*). These are, for example, choline oxidase, cholesterol oxidase, the flavin domain of cellobiose dehydrogenase and glucose oxidase. As extensive studies on choline oxidase have been performed (*38, 41-46*), the enzyme serves as as a model for understanding the mechanism of the oxidation of the alcohol by flavoprotein oxidases. Mechanistic and crystallographic studies of choline oxidase suggest that catalysis is carried out by a hydride transfer mechanism (*42*). In this mechanism, catalysis is initiated by the active site base which abstracts the hydroxyl proton from the substrate and is followed by the hydride transfer to the N(5) atom of the flavin. Details of the mechanism of choline oxidase will be discussed in the following section. A histidine residue is proposed to be the catalytic base for the hydride transfer mechanism of most

of the enzymes. Examples of studies on enzymes in which the histidine residue is proposed to be the active site base are summarized below.

Flavocytochrome b_2 from *Saccharomyces cerevisae* catalyzes the transfer of a hydride equivalent from the hydroxyl acid substrate to the enzyme-bound flavin, as observed in the oxidation of lactate to pyruvate (*88*). The enzyme has two cofactors that are located in different domains of the protein (*89*). The heme binding domain is composed of residues 1-99 and its structure resembles cytochrome b_2. Residues 100-486 make up the flavin domain, FMN, which is homologous to other α-hydroxy acid-oxidizing flavoproteins (*90*). This flavin domain can catalyze lactate oxidation without the heme domain (*91*). His373 in flavocytochrome b_2 has been proposed to act as an active site base by removing the lactate hydroxyl proton during the oxidation of lactate to pyruvate (Figure 1.22) (*92*). A recent study of the wild-type enzyme and a Tyr254Phe mutant showed that the mechanism of the enzyme is likely to involve hydride transfer (Figure 1.23) (*92*). His373, which is proposed to be the base, abstracts the hydroxyl proton from substrate and initiates the reaction. A kinetic study of His373Gln demonstrated that the k_{cat} and $k_{cat}/K_{lactate}$ values are 3 to 4 orders of magnitude lower than those of the wild-type. If the His373 functions as an active-site base, the solvent isotope effect should be significant in the mutant protein, since removal of the hydroxyl proton becomes the rate-limiting step. However, the primary deuterium and solvent kinetic isotope effects results for the His373Gln mutant are significantly smaller than those of the wild-type. This suggests that the bond cleavage steps in the mutant are less rate-limiting than in the wild-type enzyme. The crystal structure of the mutant was analyzed to gain insights into the altered activity (*93*). The analysis revealed that the mutation affected the interaction between Asp282 and the glutamine at position 373. Positions of other amino acids in the active site, such as Arg289, Asp292, and Leu286, have also changed

(Figure 1.24). These alterations are due to a conformational change that causes the substrate lactate to bind unproductively.

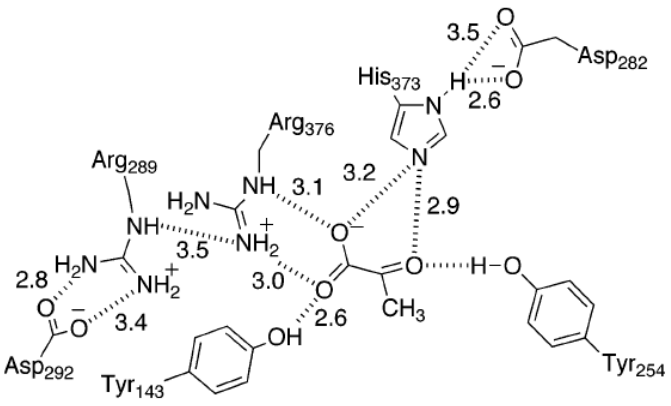

Figure 1.22. Active site of flavocytochrome b_2 with bound pyruvate product (PDB code 1KBI). Taken from Ref. (*93*).

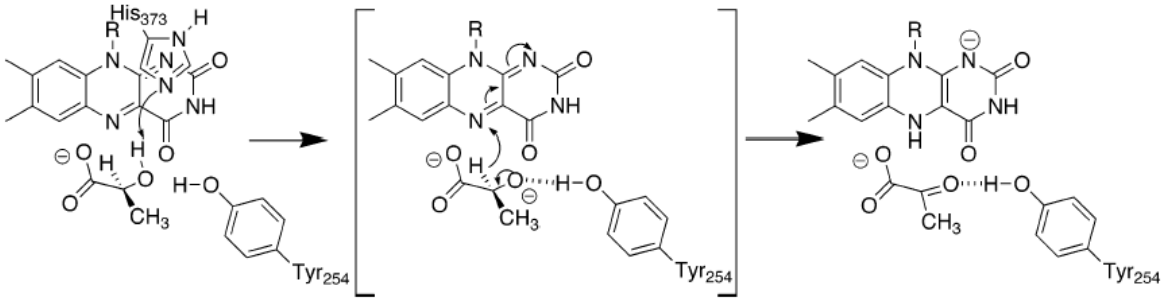

Figure 1.23. A proposed hydride transfer mechanism for oxidation of lactate by flavocytochrome b_2.
Taken from Ref. (*93*).

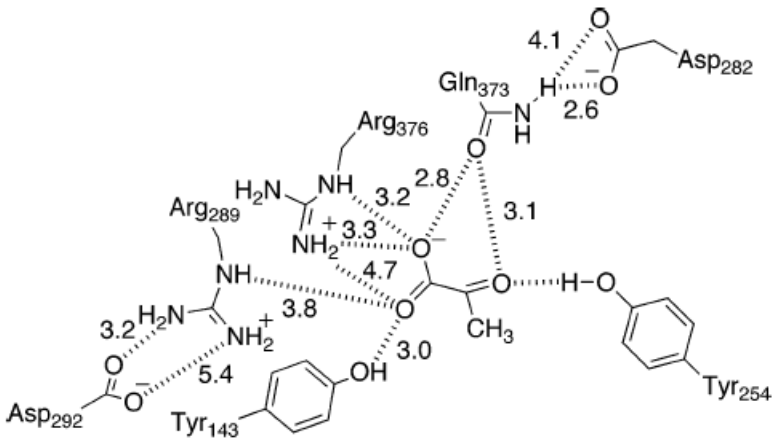

Figure 1.24. Interaction between active site residues His373Gln mutant flavocytochrome b_2 and pyruvate.
Taken from Ref. (*93*).

Cholesterol oxidase (E.C. 1.1.3.6) catalyzes the oxidation and isomerization of cholesterol to form cholest-4-en-3-one via cholest-5-en-3-one (Scheme 1.3) (*83*). The enzyme is a dimeric protein with one FAD molecule in each monomer and a total molecular mass of 110 kDa (*83*). The overall structure is composed of an FAD binding domain (the primary region of sequence similarity) and a substrate binding domain. Interestingly, the conserved active site residues in cholesterol oxidase are Glu361, His447, and Asn485 (Figure 1.18) (*83*). The crystal structure of cholesterol oxidase from *Brevibacterium* with dehydroepiandrosterone (3β-hydroxyandrost-5-en-17-one; DHEA) bound reveals a hydrogen-bonding network that connects the water molecule in the active site to the conserved residues and the 3β-hydroxyl of the substrate (Figure 1.25) (*26, 27, 83*). His447 is positioned ~7 Å from the substrate hydroxyl, suggesting that it may act as a base to remove the 3-hydroxyl proton, along with Wat541, and catalyze the electron transfer to FAD. A previous study using site-directed mutagenesis to investigate the role of His447 concluded that His447 serves as the base for oxidation, assisted by Glu361 through hydrogen bonding mediated by Wat541 and Asn485. Since a neutral or positive

charge is required for this position, the imidazole is utilized. Details of the mechanisms were limited due to slower substrate isomerization occurring after the cholesterol oxidation. There were no solvent isotope effects observed, although a small deuterium isotope effect of ~ 2.2 with 3α-[^{2}H]-cholesterol for wild-type enzyme was noted (*83*). In the case of His447Asn, a solvent isotope effect of ~ 1.5 and a small substrate isotope effect were exhibited, indicating that the CH and OH bond cleavage becomes more concerted. Finally, comparison of the kinetic isotope effects of the wild-type and the His447Asn mutant highlight the important role of His447 in catalysis of the OH bond cleavage.

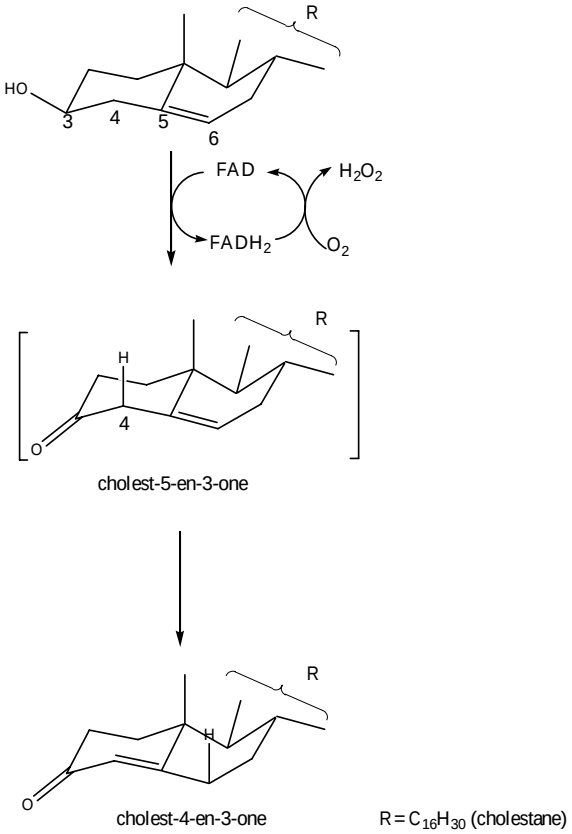

Scheme 1.3. Reaction catalyzed by cholesterol oxidase.
Modified from ref. (*83*).

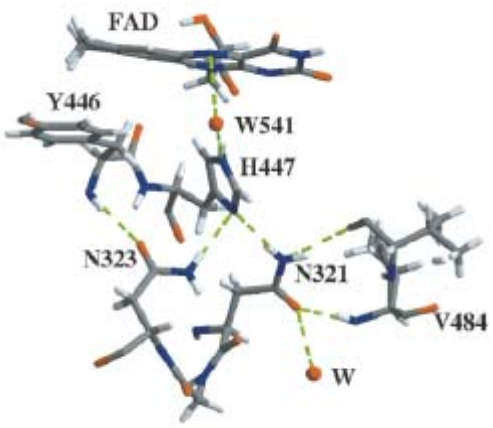

Figure 1.25. Stereoscopic representation of the hydrogen-bonding network around H447. Taken from Ref. (*94*).

Cellobiose dehydrogenase is an extracellular flavocytochrome produced by many lingo-cullulose-degrading fungi, such as the white-rot fungus *Phanerochaete chrysosposium*. The enzyme has an N-terminal cytochrome domain and a C-terminal dehydrogenase domain with FAD as a cofactor. The overall structure of the enzyme is similar to the glucose oxidase and cholesterol oxidase (*95*). There are two conserved residues, His689 and Asn732, that are positioned close to the isoalloxazine ring in the active site (Figure 1.18). Computational modeling reveals that the Wat1214 in the active site is expelled during substrate binding. This suggests that His689 contacts the substrate directly without the involvement of the water molecule. Asn732 plays a role in substrate binding and orientation, since the mutations in Asn732 resulted in weaker binding of lactose in comparison to the wild-type enzyme. Furthermore, Asn732Asp and Asn732Glu variants decrease the redox potential of FAD by altering the electrostatic environment. Therefore, another role of Asn732 is to stabilize the reduced FAD (*82*). In the crystal structure the cellobiose substrate was docked into the enzyme active site (*96*) and the glucose moiety of cellobiose was positioned within hydrogen bonding

distance of three residues: Asn732, His689, and Ser678 (*95*). This close distance between N5 of FAD and the α-carbon of cellobiose possibly enables both a base-catalyzed hydride transfer and a carbanion mechanism (*96*). Both mechanisms require a base, His689, to initiate the catalysis. The carbanion mechanism is difficult to reconcile with structural data, however, since the C-site glucosyl residue would have to tilt toward His689 by at least 45-90° to position the α-proton for the proton abstraction. On the other hand, the structure with docked cellobiose appears to be energetically unfavorable considering the spatially restricted active site (*96*). A radical mechanism is compatible with the structural observation in cellobiose dehydrogenase. With this mechanism, one electron is transferred from the substrate O1 to the flavin either at C4a or N5 position. This step occurs concomitantly with the abstraction of the α-hydroxyl proton by His689, resulting in a flavin radical and a substrate radical. Next, the hydrogen radical is transferred to N5 of the flavin (*96*). Biochemical studies have failed to provide evidence thus far for the formation of the two radical species involved in such a mechanism. Therefore, the hydride transfer mechanism is the preferred mechanism for the cellobiose dehydrogenase.

1.5. The reaction of alcohol activation catalyzed by choline oxidase from *Arthrobacter globiformis*

Choline oxidase from *A. globiformis* was cloned in our laboratory (*40*). The recombinant enzyme was expressed and isolated to a high degree of purity, allowing studies to be performed on the enzyme in order to further characterize it (*38, 40-42, 46, 47, 97-102*)**.** The results from these studies are summarized here and will be discussed in detail in Chapters II-IV.

As mentioned previously, choline oxidase catalyzes the two-step oxidation of choline to glycine betaine with the formation of betaine aldehyde as intermediate (Figure 1.12) (*44, 103*). The first oxidation step involves the oxidation of choline to betaine aldehyde yielding anionic

flavin hydroquinone (*42*); this is followed by the oxidation of flavin hydroquinone with concomitant reduction of molecular oxygen to yield hydrogen peroxide (*103*). Kinetic and mechanistic studies showed that the aldehyde intermediate is quickly hydrated to form the *gem*-diol (*104*), which stays bound to the active site during the first oxidation. In the second oxidation, the hydride equivalent is transferred from the *gem*-diol of aldehyde to the flavin. This process is followed by the oxidation of the reduced flavin by molecular oxygen (*104*).

The crystal structure of choline oxidase (to a resolution of 1.86 Å) supports previous observations that the enzyme is a 120 kDa homodimer (Figure 1.26). Each of its subunits contains FAD covalently bound to the C(8) methyl group and to the N(3) atom of His99 (*47*). The tertiary folding of the choline oxidase is similar to that of other enzymes in the GMC oxidoreductase enzyme superfamily (*26, 28, 55, 57, 64, 87, 94, 95, 105, 106*). The topologies of the FAD-and substrate binding domains are similar to those of glucose oxidase and the bacterial flavoenzyme *p*-hydroxybenzoate hydroxylase, called PHBH fold (*34*). The FAD binding domain consists of resides 1-159, 201-311, and 464-527 while the substrate binding domain is formed by residues 160-200 and 312-463 (Figure 1.26) (*47*). Another common feature of the GMC enzymes is a loop that forms a lid over the putative substrate binding site (*87, 94, 95, 106*). In the crystal structure of choline oxidase, the active site is adjacent to a loop and directly underneath a cluster of hydrophobic residues (Met62, Leu65, Val355, Phe357, and Met359). The results from molecular dynamics and Brownian dynamics simulations showed that these five hydrophobic residues form a gate and control access to the active site from the bulk solvent (*107*). The weak hydrophobic interactions between the gating residues permit the positively charged substrate choline to enter the highly electronegative active site easily (*107*). Figure 1.27 shows the active site of choline oxidase with DMSO ligand. The active site cavity has a volume of approximately

125 $Å^3$ and is adjacent to the *re* face of the FAD. This cavity is large enough to accommodate a choline molecule (93 $Å^3$). The hydrophobic residues (Trp61, Trp331, Phe357 and V464) and the polar residues (Glu312, His351, and His466) are surrounded in the cavity (Figure 1.27). His351 and His466 are near the FAD isoalloxazine ring. Glu312 is located on the top of the aromatic cage and is the only negatively charged residue in the active site. To gain insight into the enzyme-substrate interactions, the choline was manually docked into the active site cavity (Figure 1.27). Here, the side chain of Glu312 is ~3 Å from the positively charge trimethylammonium headgroup of choline, suggesting that it may be involved in the substrate binding. The choline hydroxyl O atom is ~ 4 Å from the side chain of His351 and His466. This leads us to believe that these residues could be potential candidates as catalytic bases. In addition, the side chain of Ser101 and the N5 of flavin are approximately 3 Å apart, indicating that Ser101 may play a role in the hydride transfer reaction.

Choline oxidase in the oxidized form shows typical UV-visible absorbance peaks at 359 and 452 nm at pH 8.0 (ε_{452} = 11.4 $mM^{-1}cm^{-1}$) (Figure 1.28) (*38*). Anaerobic substrate reduction reveals that the reduced enzyme is an anionic hydroquinone (Figure 1.28) which is stable in a solution with a pH ranging from 6 to 10 (*99*). At pH 8.0, the enzyme stabilizes the anionic species of the flavin semiquinone, which is non-reactive toward molecular oxygen (*38*). However, this anionic semiquinone can slowly be converted to a fully oxidized state under aerobic conditions at pH 6.0 and 4 °C. Site-directed mutagenesis studies supported the stabilization of the anionic species. The replacement of histidine with aspartate at the position 466 resulted in a lack of the intermediate flavosemiquinone formation and the neutral hydroquinone was stabilized instead of the anionic species. His466Asp has a low stoichiometry of FAD:protein and ~ 75% of the enzyme-bound flavin is bound noncovalently to the protein

(*99*). The X-ray structure shows that the side chain of both His466 and Asn510 is about 4 Å from the N(1)-C(2) locus of FAD (*47*). Therefore, Asn510 may, like His466, play an important role in the stabilization of the negative charge at the N(1)-C(2) locus of flavin and in the flavinylation of the protein in choline oxidase. More details of the role of Asn510 will be discussed in Chapter 3.

The steady-state kinetics of choline oxidase with choline as a substrate has been investigated and support a sequential steady-state kinetic mechanism (Scheme 1.5) (*44*). Upon replacement of the active site residues using site-directed mutagenesis at His351 (*102*), His466 (*46*), Val464 (*98*), Glu312 (*47*), His99 (*108*) and Ser101 (unpublished data), the order of the substrate binding to the enzyme is not affected. In all the mutants as in the wild- type enzyme, the overall turnover (k_{cat}) with choline as a substrate is limited by the two flavin reduction steps (k_3 and k_7 in Scheme 1.5).

The pH and kinetic isotope effect studies on the k_{cat}/K_m and k_{cat} values with 1,2-[$^2H_4$]-choline and 3,3-dimethylbutyraldehyde suggest that, after the enzyme-substrate complex is formed, the hydroxyl proton of the choline is abstracted by an unidentified base with thermodynamic pK_a of ~ 7.5 (Scheme 1.6) (*38, 41-43, 45, 104*), yielding an alkoxide species. This step is kinetically fast, followed by a slow hydride transfer step of α-carbon of the activated alkoxide species to the N(5) atom of flavin (Scheme 1.6). Studies of His466Ala, Val464Ala and Val464Thr concluded that the two residues His466 and Val464 contribute to the activation of the alcohol substrate, based on results in which the mutants showed the rate of the hydroxyl proton abstraction step was comparable to that of the hydride transfer step (*46, 98*). These results can be readily explained by the fact that replacement of the His with an Ala removes the positive charge that was required to support the negatively charge alkoxide species (*46*). Also, Val464

mutations result in the incorrect positioning of His466 because the environment becomes less hydrophobic(*98*).

As mentioned above, initiation of the reaction by choline oxidase requires the presence of a catalytic base. The active site of the enzyme reveals two histidine residues, His351 and His466, which are proposed to activate the oxidation of choline (Figure 1.27) (*47*). However, the results from the pH dependence profile of His466 revealed that there is a requirement for a base with a pK_a value of 9.0 (*46*). The imidazole rescuing experiment indicated that His466 is not likely to serve as a base in the reaction, because the His466Ala enzymatic activity can be partially restored in pH < 7 (imidazolium), but not in pH ≥ 7 (imidazole) (*46*). As there are no other ionizable groups in the active site (*47*), it is suspected that either His351 or both His351 and His466, may act as a base. Details of this investigation are discussed in Chapters 2 and 4. To date, there has been no strong evidence identifying a residue acting as a catalytic base among the flavin dependent enzymes which catalyze the oxidation of alcohol substrates.

Previous studies on the role of Glu312, His466, and Val464 suggested that these residues are important for the stabilization of the alkoxide intermediate that is formed during catalysis (*46, 47, 98, 102*). The stabilization of the intermediate is required through electrostatic and hydrogen bonding interactions of the trimethylammonium headgroup and the alkoxide oxygen atom with side chains of amino acids in the active site. It was shown that the Glu312Gln mutant, but not Glu312Asp, increased the choline K_d value about 500-fold (*47*). This is due to the fact that the negatively charged side chain of Glu312 interacts electrostatically with the positively charged trimethylammonium headgroup. Kinetic, spectroscopic, biochemical and mechanistic studies on His466Ala indicate that the protonated histidine electrostatically stabilizes the alkoxide intermediate and the transition state of the choline oxidation to betaine

aldehyde (Scheme 1.6) (*46*). Furthermore, the His466Ala mutant causes the CH and OH bond cleavages to have a concerted mechanism instead of the stepwise mechanism observed in the wild-type (*46*). Finally, the hydrophobic residue Val464 is required to stabilize the alkoxide intermediate indirectly by interacting with the side chain of His466 (*98*).

The hydride transfer in the oxidation of choline to betaine aldehyde occurs through a quantum tunneling mechanism with a preorganized enzyme-substrate complex. The studies on the effect of temperature on both k_{cat}/K_m for choline and 1,2-[$^2H_4$]-choline, and the associated kinetic isotope effect, $^D(k_{cat}/K_m)$, provide insights into this claim. At saturation of oxygen concentration, the hydride transfer is irreversible because $k_4/k_5[O_2]$ ratio is small (Scheme 1.5). It was then found that in wild-type the $^D(k_{cat}/K_m)$ value is large, 10.0 ± 0.6, and is temperature independent between 15 and 40 °C (*41*). Moreover, the Eyring preexponential factor ratio (A_H'/A_D') is larger than unity (14 ± 3). The enthalpy values of activation ($\Delta H^{\ddagger}$) for the hydride transfer reaction with choline and 1,2-[$^2H_4$]-choline are the same (18 ± 2 kJ/mol and 18 ± 5 kJ/mol, respectively). Lastly, the isotope effect on the activation energy for the reaction (ΔE) is negligible. These data are consistent with the hydride ion tunneling in a preorganized enzyme-substrate complex (*41*). Recent studies on the variants of choline oxidase suggest that the conformational change of the enzyme-substrate complex preorganizes the active site for the hydride transfer reaction and removal of the hydroxyl proton of the substrate occurs prior to the hydride transfer reaction (Scheme 1.7). The abstraction of hydroxyl proton of choline generates a negative charge on the alkoxide oxygen atom on the substrate. This negatively charged form is stabilized by the positively charged side chain of His466. A study on the role of the hydrophobic residue, Val464, showed that the replacement of Val464 with threonine or alanine is likely to affect the preorganization of the enzyme-substrate complex. Both Val464Ala and Val464Thr

showed that the solvent viscosity decreased the rate constant for the flavin reduction by ~ 40%. The effects of solvent viscosity must arise from a solvent-sensitive internal equilibrium between a choline-enzyme complex and a choline alkoxide-protonated enzyme complex (*98*). In addition, substituting Glu312 with an aspartate showed solvent viscosity effects on the k_{cat}/K_m value of choline substrate. The k_{cat}/K_m value increased monotonically with an increase of the viscosity in the solvent, suggesting a change in the conformation of the enzyme-substrate complex (*47*). Independent evidence for the presence of a kinetically relevant conformational change in the enzyme-substrate complex preceding the hydride transfer reaction comes from kinetic isotope effects on the k_{cat}/K_m value with choline as substrate, showing the pH independent and the average $^{D}(k_{cat}/K_m)$ value (7.1±1.3) are significant lower than the average $^{D}k_{cat}$ value (4.4 ± 1.2).

In conclusion, a number of mechanistic and structural studies have provided evidence that sheds light onto the alcohol oxidation catalyzed by *A. globiformis* choline oxidase. The reaction is initiated by a fast hydroxyl proton abstraction step from the alcohol substrate. This yields an intermediate alkoxide product, which is stabilized via electrostatic and hydrogen bonding interactions of the active site residues His466, His351, and Glu312 (Scheme 1.6). Next, a hydride ion is transferred quantum mechanically from the α-carbon of the activated alkoxide species to N(5) of flavin. Interestingly, the conformational change which occurs prior to the hydride transfer reaction results in a high degree of preorganization of the activated enzyme-substrate complex. This preorganization yields an efficient hydride transfer, and is therefore essential for the oxidation reaction catalyzed by choline oxidase.

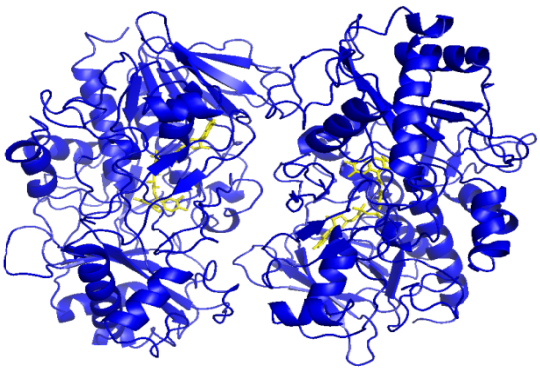

Figure 1.26. The X-ray structure of choline oxidase refined to a resolution of 1.86 Å (PDB code 2jbv). Taken from Ref. (*109*).

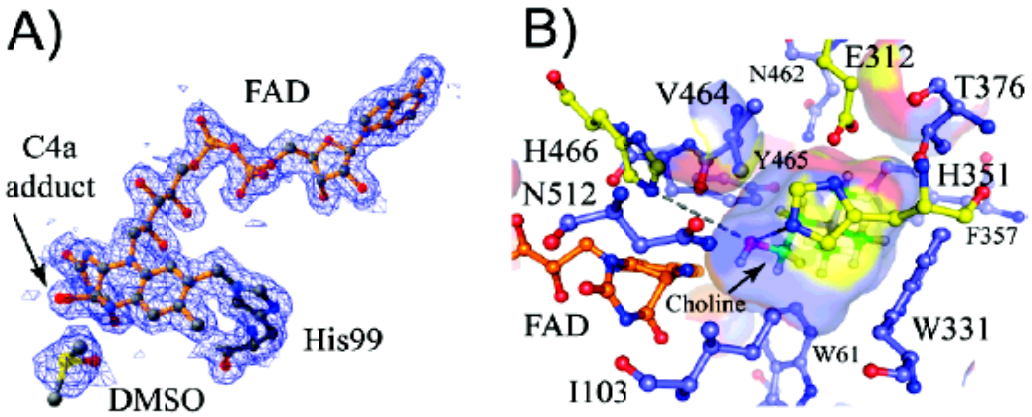

Figure 1.27. The active site of choline oxidase. (A) The typical 2mFo-DFc electron density at 1.86 Å resolution with DMSO ligand. (B) Solvent-excluded cavity with docking choline.

Taken from Ref. (*47*).

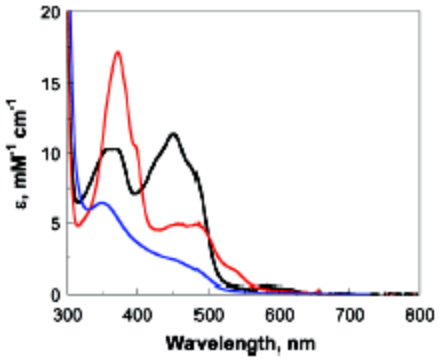

Figure 1.28. UV-visible absorbance spectra of choline oxidase in different states: oxidized (black), semiquinone (red), and hydroquinone (blue) state.

Taken from Ref. (*109*).

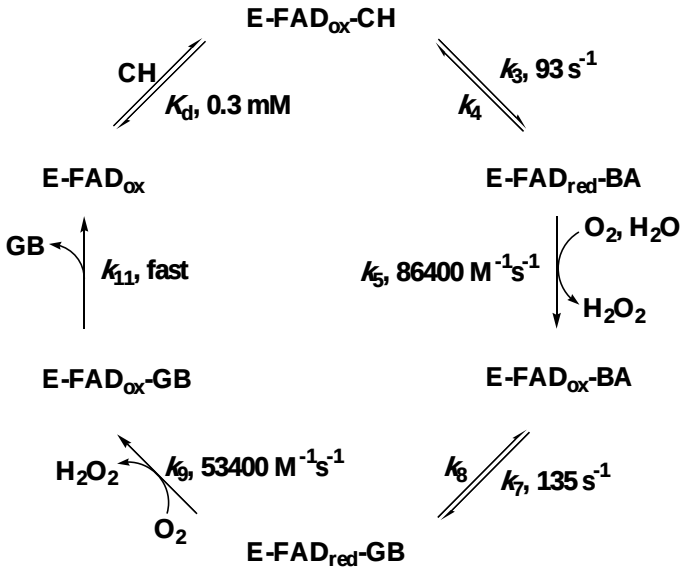

Scheme 1.4. State-state kinetic mechanism of choline oxidase at pH 10.0. E, enzyme; FADox, oxidize flavin; FADred, reduced flavin; CH, choline; BA, betaine aldehyde; GB, glycine betaine. Taken from Ref. (*109*).

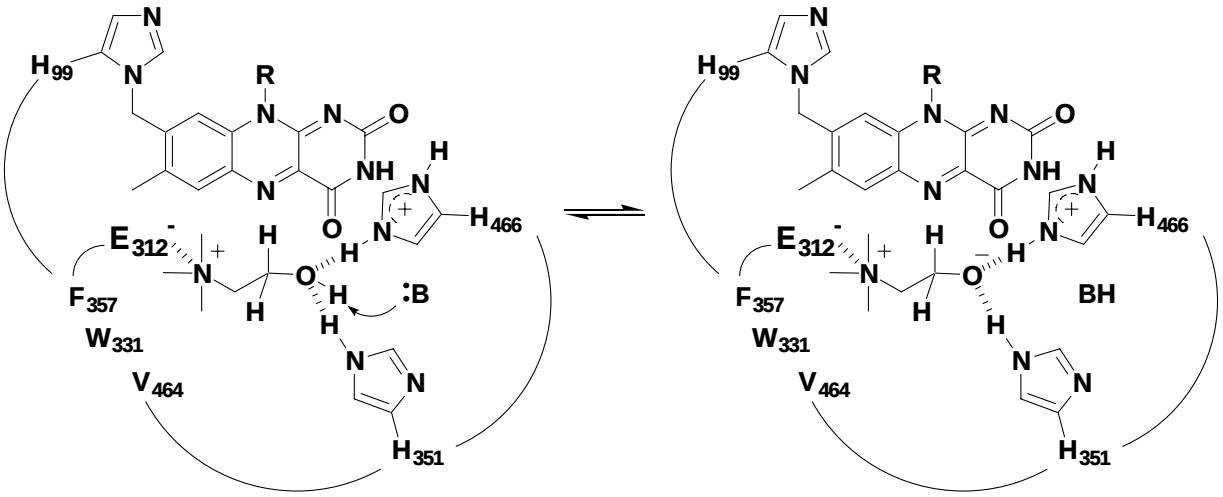

Scheme 1.5. The removal of hydroxyl proton of choline substrate in the reaction catalyzed by choline oxidase.
Taken from Ref. (*109*).

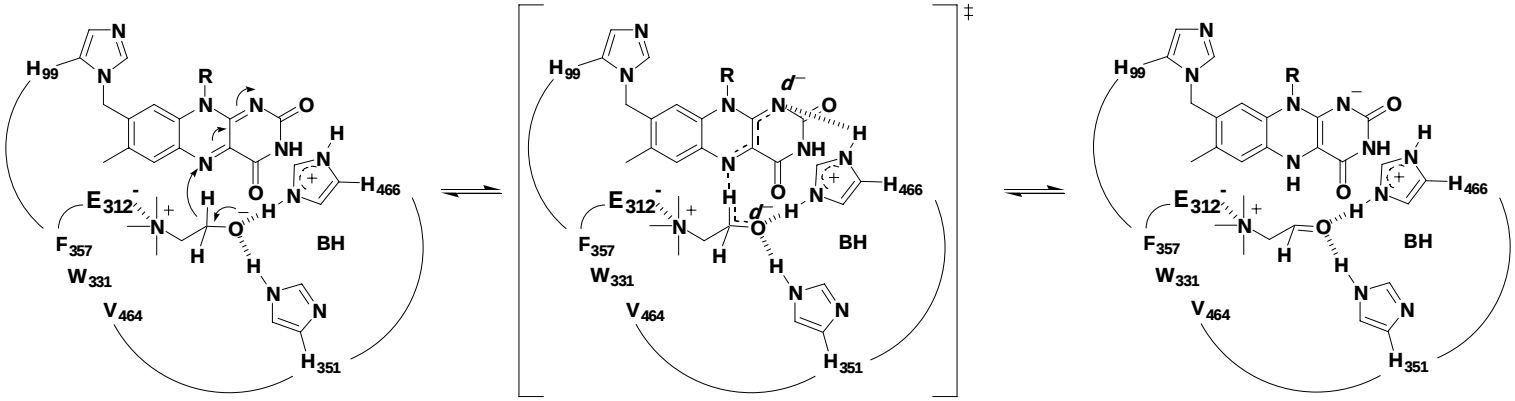

Scheme 1.6. Hydride ion transfer reaction from the choline substrate to N(5) atom of flavin.
Taken from Ref. (*109*).

1.6 Goals

The primary aim of this dissertation is to study the roles of the important amino acid residues His351, His466 and Asn510, of choline oxidase and the kinetic mechanism of pyranose 2-oxidase to gain more insight into the chemical mechanism of alcohol oxidation catalyzed by flavin-dependent enzymes.

Choline oxidase (E.C. 1.1.3.17) has been shown to catalyze the oxidation reaction of choline to glycine betaine with betaine aldehyde as intermediate and molecular oxygen acting as an electron acceptor, yielding hydrogen peroxide. The enzyme is a potential target for the development of therapeutic agents against bacteria, which are in need of high levels of glycine betaine to avoid dehydration (*47, 110*).

Choline oxidase has been studied extensively using a variety of biochemical, mechanistic, mutagenesis, and structural approaches (*38, 40-42, 45-47, 99, 104, 111, 112*)**.** The enzymatic catalysis is initiated by the kinetically fast hydroxyl proton removal from the enzyme-substrate complex (*42*). The hydroxyl proton abstraction requires an unprotonated group with a pK_a of ~ 7.5 (*43, 45*). To date, the identity of this unprotonated group remains unknown. Therefore, this study focuses on identifying this catalytic base in choline oxidase. The sequence alignment and crystal structure analysis of the choline oxidase have been compared against enzymes in the same family. The results point to a conserved histidine (His466) in the active site. This histidine is considered to be a potential base candidate for the reaction. Another study has shown, however, that it is unlikely that His466 behaves as a base based on pH dependence profile results. Another histidine residue in the active site, His351, is suspected to be the

responsible base because its position and orientation are suitable for the hydroxyl proton abstraction. Details of the studies of His351 will be discussed in Chapter 2. Since there are only two possible residues in the active site that could acts as a base, His466 and His351, the double mutants, His351Q/His466Ala and His351/466Ala, were prepared to test which of the two histidines is involved in the catalysis. This experiment will be described in detail in Chapter 4.

The crystal structure of choline oxidase reveals another conserved amino acid, Asn510, that is located near the N(1)-C(2) atom of flavin (4.7 Å), the imidazole side chain of His351 (3.0 Å) and His466 (4.0 Å) (*47*). This asparagine is also found in other GMC enzymes such as cholesterol oxidase, cellubiose dehydrogenase, pyranose 2-oxidase. Asn510 is found to display hydrogen bonding with a histidine residue (called His-Asn pair). It has been shown that the Asn510 residue sits close to N(1)-C(2) atom of flavin and the His466 in choline oxidase serves to stabilize the negative charge on the reduced flavin. In addition, His466 and His351 have been shown to be important for the electronic stabilization of the transient alkoxide species (*46, 102*). Disruption of the hydrogen bonds between the side chain at position 510 and two histidine residues may abrogate the required preorganization in the enzyme-substrate complex, resulting in the enzyme being devoid of enzymatic activity or changing the chemical mechanism. Therefore, this study also elucidates the role of conserved Asn510 in choline oxidase as described in Chapter 3.

Pyranose 2-oxidase (E.C.1.1.3.10), isolated from *Trametes ochracea,* is a member of GMC oxidoreductase enzyme superfamily. This enzyme catalyzes the oxidation of D-glucose and other pyranoses at the C2 position to yield 2-keto-sugars and hydrogen peroxide (*113*) (Scheme 1.8). The enzyme has become a target of interest to many biotechnology companies because its catalytic activity can be used produce rare sugars or drugs (*114*). The crystal structure

of pyranose 2-oxidase indicates that the enzyme is a tetramer with a total mass of 270 kDa. Each of its subunits contain FAD that covalently links the N(3) atom of histidine 167 to the C(8) methyl group of flavin (*87*). From biochemical and mechanical standpoints, several studies suggested that the kinetic mechanism of pyranose 2-oxidase occurs through a bi-bi ping-pong mechanism at pH 7.0. However, no experiments have been performed at other pH values. Therefore, a task of this study is to examine the steady-state kinetic mechanism of pyranose 2-oxidase (with D-glucose as a substrate) in solution with pH ranging from 5.5 to 8.5. The results will then be used to confirm the enzyme mechanism. Interestingly, the enzyme follows a ping-pong kinetic mechanism at pH < 7.0 whereas at pH > 7.0 it shows a ternary complex mechanism. These observations will be discussed together with the structural information in Chapter 5.

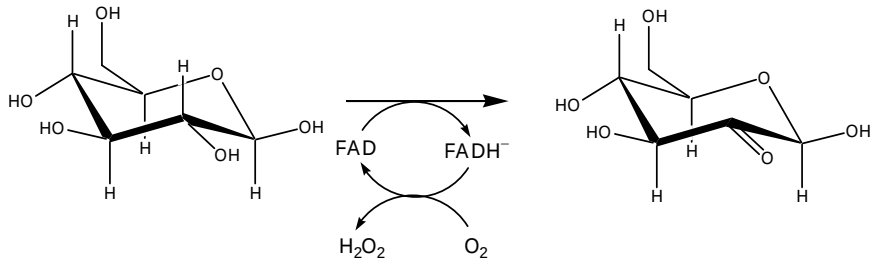

Scheme 1.7. Reaction catalyzed by pyranose 2-oxidase (113).

1.7 References

1. Massey, V. (1995) Introduction: Flavoprotein structure and mechanism, *FASEB. J. 9*, 473-475.
2. Hefti, M. H., Vervoort, J., and van Berkel, W. J. (2003) Deflavination and reconstitution of flavoproteins, *Eur. J. Biochem. 270*, 4227-4242.
3. Heuts, D. P., Scrutton, N. S., McIntire, W. S., and Fraaije, M. W. (2009) What's in a covalent bond? On the role and formation of covalently bound flavin cofactors, *FEBS. J. 276*, 3405-3427.
4. Joosten, V., and van Berkel, W. J. (2007) Flavoenzymes, *Curr. Opin. Chem. Biol. 11*, 195-202.
5. Mewies, M., McIntire, W. S., and Scrutton, N. S. (1998) Covalent attachment of flavin adenine dinucleotide (FAD) and flavin mononucleotide (FMN) to enzymes: The current state of affairs, *Protein. Sci. 7*, 7-20.
6. Huang, C. H., Lai, W. L., Lee, M. H., Chen, C. J., Vasella, A., Tsai, Y. C., and Liaw, S. H. (2005) Crystal structure of glucooligosaccharide oxidase from *Acremonium strictum*: A novel flavinylation of 6-S-cysteinyl, 8alpha-N1-histidyl FAD, *J. Biol. Chem. 280*, 38831-38838.
7. Winkler, A., Hartner, F., Kutchan, T. M., Glieder, A., and Macheroux, P. (2006) Biochemical evidence that berberine bridge enzyme belongs to a novel family of flavoproteins containing a bi-covalently attached FAD cofactor, *J. Biol. Chem. 281*, 21276-21285.

8. Massey, V. (2000) The chemical and biological versatility of riboflavin, *Biochem. Soc. Trans. 28*, 283-296.

9. Miura, R. (2001) Versatility and specificity in flavoenzymes: Control mechanisms of flavin reactivity, *Chem. Rec. 1*, 183-194.

10. Massey, V., and Palmer, G. (1966) On the existence of spectrally distinct classes of flavoprotein semiquinones. A new method for the quantitative production of flavoprotein semiquinones, *Biochemistry 5*, 3181-3189.

11. Hemmerich, P., Nagelschneider, G., and Veeger, C. (1970) Chemistry and molecular biology of flavins and flavoproteins, *FEBS. Lett. 8*, 69-83.

12. Palfey, B. A. a. M. V. (1996) *in Comprehensive Biochemical Catalysis*, Sinnott, M., Ed., Academic Press, New York.

13. Fitzpatrick, P. F., and Massey, V. (1983) The reaction of 8-mercaptoflavins and flavoproteins with sulfite. Evidence for the role of an active site arginine in D-amino acid oxidase, *J. Biol. Chem. 258*, 9700-9705.

14. Gadda, G., and Fitzpatrick, P. F. (1998) Biochemical and physical characterization of the active FAD-containing form of nitroalkane oxidase from *Fusarium oxysporum*, *Biochemistry 37*, 6154-6164.

15. Gadda, G., Wels, G., Pollegioni, L., Zucchelli, S., Ambrosius, D., Pilone, M. S., and Ghisla, S. (1997) Characterization of cholesterol oxidase from *Streptomyces hygroscopicus* and *Brevibacterium sterolicum*, *Eur. J. Biochem. 250*, 369-376.

16. Macheroux, P., Kieweg, V., Massey, V., Soderlind, E., Stenberg, K., and Lindqvist, Y. (1993) Role of tyrosine 129 in the active site of spinach glycolate oxidase, *Eur. J. Biochem*. *213*, 1047-1054.

17. Massey, V., Ghisla, S., and Moore, E. G. (1979) 8-Mercaptoflavins as active site probes of flavoenzymes, *J. Biol. Chem. 254*, 9640-9650.

18. Massey, V., Muller, F., Feldberg, R., Schuman, M., Sullivan, P. A., Howell, L. G., Mayhew, S. G., Matthews, R. G., and Foust, G. P. (1969) The reactivity of flavoproteins with sulfite. Possible relevance to the problem of oxygen reactivity, *J.Biol. Chem. 244*, 3999-4006.

19. Muller, F. (1972) On the interaction of flavins with phosphine-derivatives, *Z Naturforsch B 27*, 1023-1026.

20. Muller, F., and Massey, V. (1969) Flavin-sulfite complexes and their structures, *J. Biol. Chem. 244*, 4007-4016.

21. Wagner, M. A., Trickey, P., Chen, Z. W., Mathews, F. S., and Jorns, M. S. (2000) Monomeric sarcosine oxidase: 1. Flavin reactivity and active site binding determinants, *Biochemistry 39*, 8813-8824.

22. Ghisla, S., and Massey, V. (1986) New flavins for old: Artificial flavins as active site probes of flavoproteins, *Biochem. J. 239*, 1-12.

23. Massey, V., and Hemmerich, P. (1980) Active-site probes of flavoproteins, *Biochem. Soc. Trans. 8*, 246-257.

24. Mewies, M., Packman, L. C., Mathews, F. S., and Scrutton, N. S. (1996) Flavinylation in wild-type trimethylamine dehydrogenase and differentially charged mutant enzymes: A study of the protein environment around the N1 of the flavin isoalloxazine, *Biochem. J. 317 (Pt 1)*, 267-272.

25. Pennati, A., and Gadda, G. (2009) Involvement of ionizable groups in catalysis of human liver glycolate oxidase, *J. Biol. Chem. 284*, 31214-31222.

26. Li, J., Vrielink, A., Brick, P., and Blow, D. M. (1993) Crystal structure of cholesterol oxidase complexed with a steroid substrate: implications for flavin adenine dinucleotide dependent alcohol oxidases, *Biochemistry 32*, 11507-11515.

27. Vrielink, A., Lloyd, L. F., and Blow, D. M. (1991) Crystal structure of cholesterol oxidase from *Brevibacterium sterolicum* refined at 1.8 Å resolution, *J. Mol. Biol. 219*, 533-554.

28. Hecht, H. J., Kalisz, H. M., Hendle, J., Schmid, R. D., and Schomburg, D. (1993) Crystal structure of glucose oxidase from *Aspergillus niger* refined at 2.3 Å resolution, *J. Mol. Biol*. *229*, 153-172.

29. Su, Q., and Klinman, J. P. (1999) Nature of oxygen activation in glucose oxidase from Aspergillus niger: the importance of electrostatic stabilization in superoxide formation, *Biochemistry 38*, 8572-8581.

30. Ghisla, S., and Thorpe, C. (2004) Acyl-CoA dehydrogenases. A mechanistic overview, *Eur. J. Biochem. 271*, 494-508.

31. Ghisla, S., Thorpe, C., and Massey, V. (1984) Mechanistic studies with general acyl-CoA dehydrogenase and butyryl-CoA dehydrogenase: Evidence for the transfer of the beta-hydrogen to the flavin N(5)-position as a hydride, *Biochemistry 23*, 3154-3161.

32. Williams, C. H., Jr., Zanetti, G., Arscott, L. D., and McAllister, J. K. (1967) Lipoamide dehydrogenase, glutathione reductase, thioredoxin reductase, and thioredoxin, *J. Biol. Chem. 242*, 5226-5231.

33. Becker, K., Gromer, S., Schirmer, R. H., and Muller, S. (2000) Thioredoxin reductase as a pathophysiological factor and drug target, *Eur. J. Biochem. 267*, 6118-6125.

34. Fraaije, M. W., and Mattevi, A. (2000) Flavoenzymes: Diverse catalysts with recurrent features, *Trends. Biochem. Sci. 25*, 126-132.

35. Swoboda, B. E., and Massey, V. (1966) On the reaction of the glucose oxidase from *Aspergillus niger* with bisulfite, *J. Biol. Chem. 241*, 3409-3416.

36. Massey, V., Curti, B., and Ganther, H. (1966) A temperature-dependent conformational change in D-amino acid oxidase and its effect on catalysis, *J. Biol. Chem. 241*, 2347-2357.

37. Macheroux, P., Massey, V., Thiele, D. J., and Volokita, M. (1991) Expression of spinach glycolate oxidase in *Saccharomyces cerevisiae*: Purification and characterization, *Biochemistry 30*, 4612-4619.

38. Ghanem, M., Fan, F., Francis, K., and Gadda, G. (2003) Spectroscopic and kinetic properties of recombinant choline oxidase from *Arthrobacter globiformis*, *Biochemistry 42*, 15179-15188.

39. Trimmer, E. E., Ballou, D. P., Galloway, L. J., Scannell, S. A., Brinker, D. R., and Casas, K. R. (2005) Aspartate 120 of *Escherichia coli* methylenetetrahydrofolate reductase: evidence for major roles in folate binding and catalysis and a minor role in flavin reactivity, *Biochemistry 44*, 6809-6822.

40. Fan, F., Ghanem, M., and Gadda, G. (2004) Cloning, sequence analysis, and purification of choline oxidase from *Arthrobacter globiformis*: A bacterial enzyme involved in osmotic stress tolerance, *Arch. Biochem. Biophys. 421*, 149-158.

41. Fan, F., and Gadda, G. (2005) Oxygen- and temperature-dependent kinetic isotope effects in choline oxidase: Correlating reversible hydride transfer with environmentally enhanced tunneling, *J. Am. Chem. Soc. 127*, 17954-17961.

42. Fan, F., and Gadda, G. (2005) On the catalytic mechanism of choline oxidase, *J. Am. Chem. Soc. 127*, 2067-2074.

43. Gadda, G. (2003) pH and deuterium kinetic isotope effects studies on the oxidation of choline to betaine-aldehyde catalyzed by choline oxidase, *Biochim. Biophy.s Acta. 1650*, 4-9.

44. Gadda, G. (2003) Kinetic mechanism of choline oxidase from *Arthrobacter globiformis*, *Biochim. Biophys. Acta. 1646*, 112-118.

45. Gadda, G., Powell, N. L., and Menon, P. (2004) The trimethylammonium headgroup of choline is a major determinant for substrate binding and specificity in choline oxidase, *Arch. Biochem. Biophys*. *430*, 264-273.

46. Ghanem, M., and Gadda, G. (2005) On the catalytic role of the conserved active site residue His466 of choline oxidase, *Biochemistry 44*, 893-904.

47. Quaye, O., Lountos, G. T., Fan, F., Orville, A. M., and Gadda, G. (2008) Role of Glu312 in binding and positioning of the substrate for the hydride transfer reaction in choline oxidase, *Biochemistry 47*, 243-256.

48. Floss, H. G., Onderka, D. K., and Carroll, M. (1972) Stereochemistry of the 3-deoxy-D-arabino-heptulosonate 7-phosphate synthetase reaction and the chorismate synthetase reaction, *J. Biol. Chem. 247*, 736-744.

49. Morell, H., Clark, M. J., Knowles, P. F., and Sprinson, D. B. (1967) The enzymic synthesis of chorismic and prephenic acids from 3-enolpyruvylshikimic acid 5-phosphate, *J. Biol. Chem. 242*, 82-90.

50. Bornemann, S., Ramjee, M. K., Balasubramanian, S., Abell, C., Coggins, J. R., Lowe, D. J., and Thorneley, R. N. (1995) *Escherichia coli* chorismate synthase catalyzes the

conversion of (6S)-6-fluoro-5-enolpyruvylshikimate-3-phosphate to 6-fluorochorismate. Implications for the enzyme mechanism and the antimicrobial action of (6S)-6-fluoroshikimate, *J. Biol. Chem. 270*, 22811-22815.

51. Kitzing, K., Auweter, S., Amrhein, N., and Macheroux, P. (2004) Mechanism of chorismate synthase. Role of the two invariant histidine residues in the active site, *J. Biol. Chem. 279*, 9451-9461.

52. Macheroux, P., Schonbrunn, E., Svergun, D. I., Volkov, V. V., Koch, M. H., Bornemann, S., and Thorneley, R. N. (1998) Evidence for a major structural change in *Escherichia coli* chorismate synthase induced by flavin and substrate binding, *Biochem. J. 335 (Pt 2)*, 319-327.

53. Macheroux, P., Bornemann, S., Ghisla, S., and Thorneley, R. N. (1996) Studies with flavin analogs provide evidence that a protonated reduced FMN is the substrate-induced transient intermediate in the reaction of *Escherichia coli* chorismate synthase, *J. Biol. Chem*. *271*, 25850-25858.

54. Ferreira, P., Ruiz-Duenas, F. J., Martinez, M. J., van Berkel, W. J., and Martinez, A. T. (2006) Site-directed mutagenesis of selected residues at the active site of aryl-alcohol oxidase, an H_2O_2-producing ligninolytic enzyme, *FEBS. J. 273*, 4878-4888.

55. Cavener, D. R. (1992) GMC oxidoreductases. A newly defined family of homologous proteins with diverse catalytic activities, *J. Mol. Biol. 223*, 811-814.

56. Frederick, K. R., Tung, J., Emerick, R. S., Masiarz, F. R., Chamberlain, S. H., Vasavada, A., Rosenberg, S., Chakraborty, S., Schopfer, L. M., and et al. (1990) Glucose oxidase from *Aspergillus niger*. Cloning, gene sequence, secretion from *Saccharomyces cerevisiae* and kinetic analysis of a yeast-derived enzyme, *J. Biol. Chem. 265*, 3793-3802.

57. Kiess, M., Hecht, H. J., and Kalisz, H. M. (1998) Glucose oxidase from *Penicillium amagasakiense*. Primary structure and comparison with other glucose-methanol-choline (GMC) oxidoreductases, *Eur. J. Biochem. 252*, 90-99.

58. Ishizaki, T., Hirayama, N., Shinkawa, H., Nimi, O., and Murooka, Y. (1989) Nucleotide sequence of the gene for cholesterol oxidase from a *Streptomyces* sp, *J. Bacteriol. 171*, 596-601.

59. Ohta, T., Fujishiro, K., Yamaguchi, K., Tamura, Y., Aisaka, K., Uwajima, T., and Hasegawa, M. (1991) Sequence of gene choB encoding cholesterol oxidase of *Brevibacterium sterolicum*: Comparison with choA of *streptomyces* sp. SA-COO, *Gene 103*, 93-96.

60. Dreveny, I., Gruber, K., Glieder, A., Thompson, A., and Kratky, C. (2001) The hydroxynitrile lyase from almond: A lyase that looks like an oxidoreductase, *Structure 9*, 803-815.

61. Li, B., Nagalla, S. R., and Renganathan, V. (1996) Cloning of a cDNA encoding cellobiose dehydrogenase, a hemoflavoenzyme from *Phanerochaete chrysosporium*, *Appl Environ. Microbiol. 62*, 1329-1335.

62. Leskovac, V., Trivic, S., Wohlfahrt, G., Kandrac, J., and Pericin, D. (2005) Glucose oxidase from *Aspergillus niger*: The mechanism of action with molecular oxygen, quinones, and one-electron acceptors, *Int. J. Biochem. Cell. Biol. 37*, 731-750.

63. Bright, H. J., and Gibson, Q. H. (1967) The oxidation of 1-deuterated glucose by glucose oxidase, *J. Biol. Chem. 242*, 994-1003.

64. Wohlfahrt, G., Witt, S., Hendle, J., Schomburg, D., Kalisz, H. M., and Hecht, H. J. (1999) 1.8 and 1.9 Å resolution structures of the *Penicillium amagasakiense* and

Aspergillus niger glucose oxidases as a basis for modelling substrate complexes, *Acta. Crystallogr. D.Biol. Crystallogr. 55*, 969-977.

65. Roth, J. P., and Klinman, J. P. (2003) Catalysis of electron transfer during activation of O_2 by the flavoprotein glucose oxidase, *Proc. Natl. Acad. Sci. U S A 100*, 62-67.

66. Palfey, B. A., Ballou, D. P., and Massey, V. (1995) *Active Oxygen in Biochemistry*, Valentine, J.S., Foote, C.S., Greenberg, A. & Liebman, J.F. (Chapman & Hall, New York).

67. Fox, K. M., and Karplus, P. A. (1994) Old yellow enzyme at 2 Å resolution: overall structure, ligand binding, and comparison with related flavoproteins, *Structure 2*, 1089-1105.

68. Brown, B. J., Deng, Z., Karplus, P. A., and Massey, V. (1998) On the active site of Old Yellow Enzyme. Role of histidine 191 and asparagine 194, *J. Biol. Chem. 273*, 32753-32762.

69. Messiha, H. L., Munro, A. W., Bruce, N. C., Barsukov, I., and Scrutton, N. S. (2005) Reaction of morphinone reductase with 2-cyclohexen-1-one and 1-nitrocyclohexene: proton donation, ligand binding, and the role of residues histidine 186 and asparagine 189, *J. Biol. Chem. 280*, 10695-10709.

70. Barna, T., Messiha, H. L., Petosa, C., Bruce, N. C., Scrutton, N. S., and Moody, P. C. (2002) Crystal structure of bacterial morphinone reductase and properties of the C191A mutant enzyme, *J. Biol. Chem. 277*, 30976-30983.

71. Craig, D. H., Barna, T., Moody, P. C., Bruce, N. C., Chapman, S. K., Munro, A. W., and Scrutton, N. S. (2001) Effects of environment on flavin reactivity in morphinone

reductase: analysis of enzymes displaying differential charge near the N-1 atom and C-2 carbonyl region of the active-site flavin, *Biochem. J. 359*, 315-323.

72. Saito, K., Thiele, D. J., Davio, M., Lockridge, O., and Massey, V. (1991) The cloning and expression of a gene encoding Old Yellow Enzyme from *Saccharomyces carlsbergensis*, *J. Biol. Chem. 266*, 20720-20724.

73. Stott, K., Saito, K., Thiele, D. J., and Massey, V. (1993) Old Yellow Enzyme. The discovery of multiple isozymes and a family of related proteins, *J. Biol. Chem. 268*, 6097-6106.

74. Niino, Y. S., Chakraborty, S., Brown, B. J., and Massey, V. (1995) A new old yellow enzyme of *Saccharomyces cerevisiae*, *J. Biol. Chem. 270*, 1983-1991.

75. Miranda, M., Ramirez, J., Guevara, S., Ongay-Larios, L., Pena, A., and Coria, R. (1995) Nucleotide sequence and chromosomal localization of the gene encoding the Old Yellow Enzyme from *Kluyveromyces lactis*, *Yeast 11*, 459-465.

76. Madani, N. D., Malloy, P. J., Rodriguez-Pombo, P., Krishnan, A. V., and Feldman, D. (1994) Candida albicans estrogen-binding protein gene encodes an oxidoreductase that is inhibited by estradiol, *Proc. Natl. Acad. Sci. U S A 91*, 922-926.

77. Snape, J. R., Walkley, N. A., Morby, A. P., Nicklin, S., and White, G. F. (1997) Purification, properties, and sequence of glycerol trinitrate reductase from *Agrobacterium radiobacter*, *J. Bacteriol. 179*, 7796-7802.

78. Miura, K., Tomioka, Y., Suzuki, H., Yonezawa, M., Hishinuma, T., and Mizugaki, M. (1997) Molecular cloning of the nemA gene encoding N-ethylmaleimide reductase from *Escherichia coli*, *Biol. Pharm. Bull. 20*, 110-112.

79. Schaller, F., and Weiler, E. W. (1997) Molecular cloning and characterization of 12-oxophytodienoate reductase, an enzyme of the octadecanoid signaling pathway from *Arabidopsis thaliana*. Structural and functional relationship to yeast old yellow enzyme, *J. Biol. Chem. 272*, 28066-28072.

80. French, C. E., Nicklin, S., and Bruce, N. C. (1996) Sequence and properties of pentaerythritol tetranitrate reductase from *Enterobacter cloacae* PB2, *J. Bacteriol. 178*, 6623-6627.

81. French, C. E., and Bruce, N. C. (1995) Bacterial morphinone reductase is related to Old Yellow Enzyme, *Biochem. J. 312 (Pt 3)*, 671-678.

82. Rotsaert, F. A., Renganathan, V., and Gold, M. H. (2003) Role of the flavin domain residues, His689 and Asn732, in the catalytic mechanism of cellobiose dehydrogenase from *Phanerochaete chrysosporium*, *Biochemistry 42*, 4049-4056.

83. Kass, I. J., and Sampson, N. S. (1998) Evaluation of the role of His447 in the reaction catalyzed by cholesterol oxidase, *Biochemistry 37*, 17990-18000.

84. Yamashita, M., Toyama, M., Ono, H., Fujii, I., Hirayama, N., and Murooka, Y. (1998) Separation of the two reactions, oxidation and isomerization, catalyzed by *Streptomyces* cholesterol oxidase, *Protein. Eng. 11*, 1075-1081.

85. Yin, Y., Sampson, N. S., Vrielink, A., and Lario, P. I. (2001) The presence of a hydrogen bond between asparagine 485 and the π system of FAD modulates the redox potential in the reaction catalyzed by cholesterol oxidase, *Biochemistry 40*, 13779-13787.

86. Sanner, C., Macheroux, P., Ruterjans, H., Muller, F., and Bacher, A. (1991) ^{15}N- and ^{13}C-NMR investigations of glucose oxidase from *Aspergillus niger*, *Eur. J. Biochem. 196*, 663-672.

87. Hallberg, B. M., Leitner, C., Haltrich, D., and Divne, C. (2004) Crystal structure of the 270 kDa homotetrameric lignin-degrading enzyme pyranose 2-oxidase, *J.Mol. Biol. 341*, 781-796.

88. Lederer, F. (1991) Flavocytochrome b_2, in *Chemistry and Biochemistry of Flavoenzymes* Muller. F., Ed., pp 153-242, CRC Press, Boca Raton, FL.

89. Xia, Z., and Mathews, F. S. (1990) Molecular structure of flavocytochrome b_2 at 2.4 Å resolution, *J. Mol. Biol. 212*, 837-863.

90. Lindqvist, Y., Branden, C. I., Mathews, R., and Lederer, F. (1991) Spinach glycolate oxidase and yeast flavocytochrome b_2 are structurally homologous and evolutionarily related enzymes with distinctly different fundtion and flavin mononucleotide binding, *J. Biol. Chem. 266*, 3198-3207.

91. Balme, A., Brunt, C. E., Pallister, R. L., Cahapman, S. K., and Reid, G. A. (1995) Isolation and characterization of the flavin binding domain of flavocytochrome b_2 expressed independently in *Escherichia coli*, *Biochem. J. 309*, 601-605.

92. Sobrado, P., and Fitzpatrick, P. F. (2003) Solvent and primary deuterium isotope effects show that lactate CH and OH bond cleavages are concerted in Y254F flavocytochrome b_2, consistent with a hydride transfer mechanism, *Biochemistry 42*, 15208-15214.

93. Tsai, C. T., Gokulan, K., Sobrado, P., Sacchettini, J. C., and Fitzpatrick, P. F. (2007) Mechanistic and structural studies of H373Q flavocytochrome b_2: Effects of mutating the active site base, *Biochemistry 46*, 7844-7851.

94. Yue, Q. K., Kass, I. J., Sampson, N. S., and Vrielink, A. (1999) Crystal structure determination of cholesterol oxidase from *Streptomyces* and structural characterization of key active site mutants, *Biochemistry 38*, 4277-4286.

95. Hallberg, B. M., Henriksson, G., Pettersson, G., and Divne, C. (2002) Crystal structure of the flavoprotein domain of the extracellular flavocytochrome cellobiose dehydrogenase, *J. Mol. Biol. 315*, 421-434.

96. Hallberg, B. M., Henriksson, G., Pettersson, G., Vasella, A., and Divne, C. J. (2003) Mechanism of the reductive-half reaction in cellobiose dehydrogenase, *J. Biol. Chem. 278*, 7160-7166.

97. Fan, F., and Gadda, G. (2007) An internal equilibrium preorganizes the enzyme-substrate complex for hydride tunneling in choline oxidase, *Biochemistry 46*, 6402-6408.

98. Finnegan, S., and Gadda, G. (2008) Substitution of an active site valine uncovers a kinetically slow equilibrium between competent and incompetent forms of choline oxidase, *Biochemistry 47*, 13850-13861.

99. Ghanem, M., and Gadda, G. (2006) Effects of reversing the protein positive charge in the proximity of the flavin N(1) locus of choline oxidase, *Biochemistry 45*, 3437-3447.

100. Hoang, J. V., and Gadda, G. (2007) Trapping choline oxidase in a nonfunctional conformation by freezing at low pH, *Proteins 66*, 611-620.

101. Orville, A. M., Lountos, G. T., Finnegan, S., Gadda, G., and Prabhakar, R. (2009) Crystallographic, spectroscopic, and computational analysis of a flavin C4a-oxygen adduct in choline oxidase, *Biochemistry 48*, 720-728.

102. Rungsrisuriyachai, K., and Gadda, G. (2008) On the role of histidine 351 in the reaction of alcohol oxidation catalyzed by choline oxidase, *Biochemistry 47*, 6762-6769.

103. Ikuta, S., Imamura, S., Misaki, H., and Horiuti, Y. (1977) Purification and characterization of choline oxidase from *Arthrobacter globiformis*, *J. Biol. Chem. 82*, 1741-1749.

104. Fan, F., Germann, M. W., and Gadda, G. (2006) Mechanistic studies of choline oxidase with betaine aldehyde and its isosteric analogue 3,3-dimethylbutyraldehyde, *Biochemistry 45*, 1979-1986.

105. Albrecht, M., and Lengauer, T. (2003) Pyranose oxidase identified as a member of the GMC oxidoreductase family, *Bioinformatics 19*, 1216-1220.

106. Bannwarth, M., Bastian, S., Heckmann-Pohl, D., Giffhorn, F., and Schulz, G. E. (2004) Crystal structure of pyranose 2-oxidase from the white-rot fungus *Peniophora* sp, *Biochemistry 43*, 11683-11690.

107. Xin, Y., Gadda, G., and Hamelberg, D. (2009) The cluster of hydrophobic residues controls the entrance to the active site of choline oxidase, *Biochemistry 48*, 9599-9605.

108. Quaye, O., Cowins, S., and Gadda, G. (2009) Contribution of flavin covalent linkage with histidine 99 to the reaction catalyzed by choline oxidase, *J. Biol. Chem. 284*, 16990-16997.

109. Gadda, G. (2008) Hydride transfer made easy in the reaction of alcohol oxidation catalyzed by flavin-dependent oxidases, *Biochemistry 47*, 13745-13753.

110. O'Callaghan, J., and Condon, S. (2000) Growth of Lactococcus lactis strains at low water activity: Correlation with the ability to accumulate glycine betaine, *Int. J. Food. Microbiol. 55*, 127-131.

111. Gadda, G., Fan, F., and Hoang, J. V. (2006) On the contribution of the positively charged headgroup of choline to substrate binding and catalysis in the reaction catalyzed by choline oxidase, *Arch. Biochem. Biophys. 451*, 182-187.

112. Gadda, G., and McAllister-Wilkins, E. E. (2003) Cloning, expression, and purification of choline dehydrogenase from the moderate halophile *Halomonas elongata*, *Appl. Environ. Microbiol. 69*, 2126-2132.

113. Rungsrisuriyachai, K., and Gadda, G. (2009) A pH switch affects the steady-state kinetic mechanism of pyranose 2-oxidase from *Trametes ochracea*, *Arch. Biochem. Biophys. 483*, 10-15.

114. Giffhorn, F. (2000) Fungal pyranose oxidases: Occurrence, properties and biotechnical applications in carbohydrate chemistry, *Appl. Microbiol. Biotechnol. 54*, 727-740.

115. Mowat, CG., Gazur, B., Campbell, LP., and Chapman, SK. (2010) Flavin-containing heme enzymes, *Arch. Biochem. Biophys.* 493, 37-52.

Chapter 2

On the Role of Histidine 351 in the Reaction of Alcohol Oxidation Catalyzed by Choline Oxidase

(This chapter has been published verbatim in Rungsrisuriyachai, K., and Gadda, G., (2008), *Biochemistry 4*7, 6762-6769.)

2.1 Abbreviations

His351Ala enzyme, choline oxidase variant with His351 replaced with Ala; His466Ala enzyme, choline oxidase variant with His466 replaced with Ala.

2.2 Abstract

Choline oxidase catalyzes the four-electron, flavin-linked oxidation of choline to glycine betaine with transient formation of an enzyme-bound aldehyde intermediate. The recent determination of the crystal structure of choline oxidase to a resolution of 1.86 Å established the presence of two histidine residues in the active site, which may participate in catalysis. His466 was the subject of a previous study [Ghanem, M., and Gadda, G. (2005), *Biochemistry*, 44, 893-904]. In this study, His351 was replaced with alanine using site-directed mutagenesis, and the resulting mutant enzyme was purified and characterized in its mechanistic properties. The results presented establish that His351 contributes to substrate binding and positioning, and stabilizes the transition state for the hydride transfer reaction to the flavin, as suggested by anaerobic substrate reduction stopped-flow data. Furthermore, His351 contributes to the overall polarity of the active site by modulating the pK_a of the group that deprotonates choline to the alkoxide species, as indicated by pH profiles of the steady-state kinetic parameters with the substrate or a competitive inhibitor. Surprisingly, His351 is not involved in the activation of the reduced flavin for reaction with oxygen. The latter observation, along with previous mutagenesis data on

His466, allow to conclude that choline oxidase must necessarily utilize a strategy for oxygen reduction different from that established for glucose oxidase, where other authors showed that the catalytic effect almost entirely arises from a protonated histidine residue.

2.3 Introduction

Choline oxidase (E.C. 1.1.3.17) catalyzes the four-electron, flavin-linked oxidation of choline to glycine betaine with transient formation of an enzyme-bound aldehyde. The overall reaction includes two reductive half-reactions in which a protein-bound flavin accepts a hydride ion from the alcohol substrate (step a in Scheme 2.1) and the hydrated betaine aldehyde intermediate (step c in Scheme 2.1). Each reductive half-reaction is followed by an oxidative half-reaction in which a hydride equivalent and a proton are transferred from the reduced flavin and the protein to molecular oxygen with formation and release of hydrogen peroxide (*1-4*). The enzyme-bound aldehyde produced in the first oxidation reaction is rapidly hydrated in the active site of the enzyme to the *gem*-diol species (step b in Scheme 2.1), which is the form acting as substrate in the second oxidation reaction catalyzed by the enzyme (*2*). The first reductive half-reaction in which choline is oxidized to betaine aldehyde has been studied extensively using a variety of mechanistic, biochemical, mutagenesis, and structural approaches using choline and choline analogs (*1-11*). Catalysis is initiated in the enzyme-substrate complex by a kinetically fast removal of the hydroxyl proton of the alcohol substrate by an as yet unidentified catalytic base with pK_a of ~7.5 (step a in Scheme 2.2) as suggested by kinetic isotope effect (*3, 10*). The resulting zwitterionic, choline alkoxide species is stabilized in the enzyme-substrate complex through electrostatic bonds with the charged side chains of His466 and Glu312 at the opposite ends of the molecule (*4, 6, 9*). These interactions, along with the limited mobility of the flavin cofactor that is covalently linked through its CM 8 group to His99 (*9*), likely contribute to

preorganize the enzyme-substrate complex for an efficient oxidation reaction (*9*). The hydride transfer reaction between the alkoxide α-carbon and the N(5) atom of the flavin then occurs quantum mechanically as a result of environmental vibrations of the reaction coordinate that permit a tunneling distance between the hydride donor and acceptor within a highly preorganized enzyme-complex Michaelis (steps b and c in Scheme 2.2) (*8*). The resulting reduced flavin finally reacts with molecular oxygen to yield hydrogen peroxide, before a second oxidation reaction will produce glycine betaine from betaine aldehyde. In agreement with a highly preorganized enzyme-substrate complex, recent mutagenesis studies showed that replacement of Glu312 with aspartate results in a 260-fold decrease in the rate of hydride transfer to the flavin (*9*).

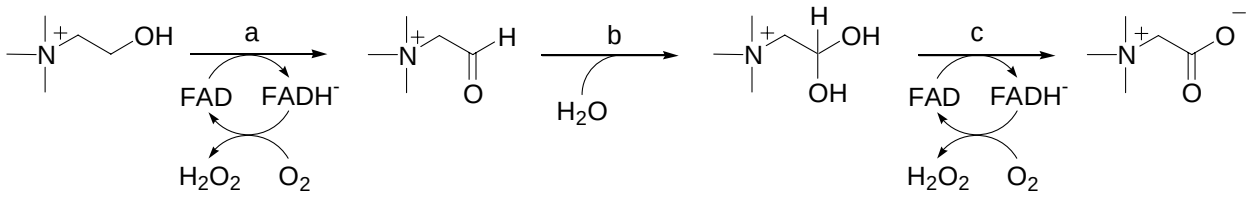

Scheme 2.1. Reaction catalyzed by choline oxidase.

The oxidative half-reaction in which a hydride equivalent and a proton are transferred from the reduced flavin and the protein to molecular oxygen to yield hydrogen peroxide in choline oxidase is less understood. However, this reaction has been well-characterized in another member of the Glucose-Methanol-Choline oxidoreductase enzyme superfamily to which choline oxidase belongs, namely glucose oxidase (*12-15*). In that enzyme, several mechanistic probes

have been used by other authors on the wild-type and a mutant variant of the enzyme in which His516 was replaced with alanine to convincingly conclude that the catalytic effect of glucose oxidase in the reduction of oxygen arises almost entirely from a single positive charge located on His516 (*13*). In this context, previous mechanistic studies indicated that in choline oxidase the reactivity of the reduced flavin toward oxygen is not affected upon replacement of His466 with alanine, which is equivalent to the His516Ala mutation in glucose oxidase (*4*). Moreover, in contrast to the observations reported for glucose oxidase, where there is a marked effect of pH on the reactivity of the reduced flavin with oxygen (*12, 13, 15*), the wild-type form of choline oxidase shows similar reactivity in the pH range from 6 to 10 (*10*). As illustrated in Figure 2.1, the recent determination of the crystal structure of choline oxidase to a resolution of 1.86 Å shows that a second histidine residue, namely His351, is located in the active site in a location that suggests its possible involvement in the oxygen reduction reaction. His351 may therefore play catalytic roles similar to those of His516 in glucose oxidase.

The present study was conducted with the dual goal of evaluating whether His351 participates in the reductive and the oxidative half-reactions catalyzed by choline oxidase. In the former His351 could catalyze the abstraction of the hydroxyl proton of the alcohol substrate that results in the activation of choline. In the latter it could provide the necessary stabilization that is required for the reaction of the reduced flavin with oxygen. Toward these goals, His351 was replaced with alanine using site-directed mutagenesis, and the resulting mutant enzyme was purified and characterized in its kinetic and mechanistic properties. The results presented are consistent with His351 being important for the proper binding and positioning of the substrate so that the subsequent hydride transfer reaction occurs efficiently, for stabilization of the transition state developed during choline oxidation, and for fine-tuning the polarity of the active site that is

required for choline activation. However, the results of the present study do not support the notions that His351 is solely responsible for the abstraction of the hydroxyl proton of choline and that it participates in the activation of the reduced flavin for reaction with oxygen.

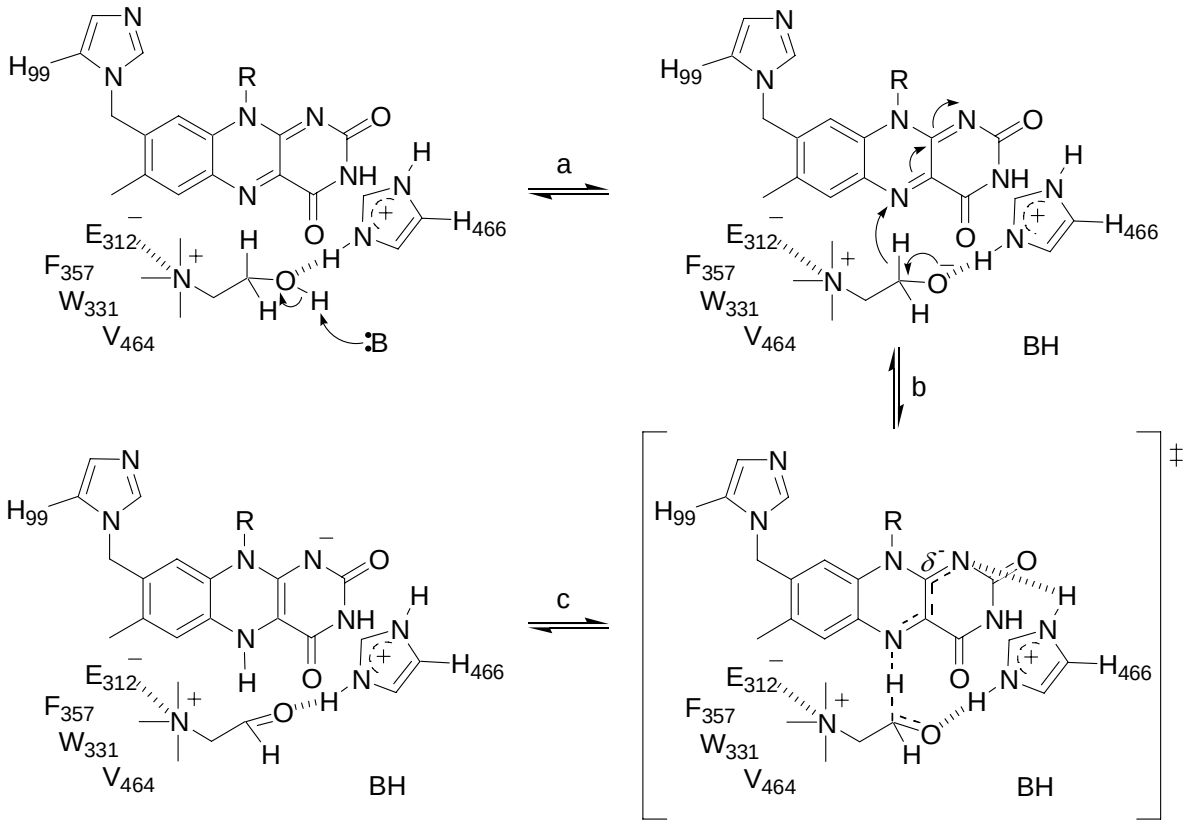

Scheme 2.2. The oxidation of choline catalyzed by choline oxidase.

Figure 2.1. The active site of wild-type choline oxidase at a resolution of 1.86 Å (PDB 2jbv). Selected amino acids are shown, along with DMSO (cyan), an additive used in the crystallization process. Note the distortion of the flavin ring, which is due to the presence of an c4a flavin adduct (not shown here), whose nature is currently under investigation.

2.4 Experimental procedures

Materials. *Escherichia coli* strain Rosetta(DE3)pLysS was from Novagen (Madison, WI). DNase was from Roche. The QuikChange site-directed mutagenesis kit was from Stratagene (La Jolla, CA). The QIAprep Spin Miniprep kit was from Qiagen (Valencia, CA). Oligonucleotides used for sequencing of the mutant gene were custom synthesized by Sigma Genosys (Woodland, TX). Bovine serum albumin, chloramphenicol, tetracycline, DMSO, isopropyl-β-D-thiogalactopyranoside (IPTG), phenylmethylsulfonyl fluoride (PMSF), lysozyme, sodium hydrosulfite, betaine aldehyde, glycine betaine, Luria-Bertani agar and broth were from Sigma (St. Louis, MO). EDTA was from Fisher. Choline chloride and ampicillin were from ICN Pharmaceutical Inc. 1,2-[$^{2}H_{4}$]-Choline bromide (98%) and sodium deuteroxide (99%) were from Isotec Inc. (Miamisburg, OH). Wild-type choline oxidase from *Arthrobacter globiformis* strain ATCC 8010 was expressed from plasmid pET/*codA*1 and purified to homogeneity as described previously (*1*). All other reagents were of the highest purity commercially available.

Site-Directed Mutagenesis. A QuikChange kit was used to prepare the mutant enzyme His351Ala. The experiment was performed by following the manufacturer's instructions in the presence of 2% DMSO using the pET/CodAmg1 plasmid harboring the wild-type gene (CodA) for choline oxidase as a template and forward and reverse oligonucleotides as primers for site-directed mutagenesis. The resulting mutant gene (*codA*mg1-H351A) was sequenced at the DNA core Facility at Georgia State University using an Applied Biosystems Big Dye Kit on an Applied Biosystems model ABI 377 DNA sequencer. Sequencing confirmed the presence of the mutant gene in the correct orientation. Finally, *E. coli* strain Rosetta(DE3)pLysS competent cells were transformed with the mutant plasmid pET/*codA*mg1-H351A by electroporation, and permanent stocks of the transformed cells were prepared and stored at -80 ^{o}C.

Expression and Purification of His351Ala Variant of Choline Oxidase. Permanent stocks of *E. coli* Rosetta(DE3)pLysS cells harboring plasmid pET/*codA*mg1-H351A were used to inoculate 4.5 L of Luria-Bertani broth medium containing 50 μg/mL ampicillin and 34 μg/mL chloramphenicol. The liquid cultures were grown for 12-14 h at 37 °C, before inducing protein expression with 0.05 mM IPTG for 5 h at 22 °C. The mutant enzyme was purified to homogeneity using the same procedure described previously for the purification of the wild-type enzyme (*1*).

Enzyme Assays. The enzymatic activity of the His351Ala enzyme variant was measured by the method of initial rates as described for the wild-type enzyme (*1*) using a computer-interfaced Oxy-32 oxygen-monitoring system (Hansatech Instrument Ltd). The steady-state kinetic parameters of the mutant enzyme were determined by varying the concentration of oxygen (in the range from 0.02 to 0.1 mM) and choline (in the range from 0.5 to 50 mM) in 50 mM sodium pyrophosphate, pH 10 and 25 °C. The assay reaction mixture was equilibrated at the desired oxygen concentration by bubbling with a O_2/N_2 gas mixture for at least 15 min before the reaction was started with the addition of the enzyme. Product inhibition studies were carried out by measuring enzymatic activity at vary concentrations of choline at several fixed concentrations of glycine betaine (from 0 to 80 mM) in air-saturated 50 mM sodium pyrophosphate at 25 °C over a pH range of 6 to 9.5. The pH dependences of the steady-state kinetic parameters of the His351Ala enzyme variant were determined by measuring enzymatic activity at varying concentrations at both organic substrate and oxygen in the pH range between 5 to 10 in 50 mM sodium pyrophosphate at 25 °C with the exception of pH 7 where sodium phosphate was used. The pH dependence of the primary kinetic isotope effect with 1,2-[$^2H_4$]-choline as substrate was determined by measuring the kinetic parameters of the mutant enzyme with labeled and

unlabeled substrate in air-saturated 50 mM sodium pyrophosphate at 25 °C in pH range 7 to 10. Pre-steady-state kinetic measurements were carried out by using a Hi-Tech SF-61 stopped-flow spectrophotometer thermostated at 25 °C, pH 10. The rate of flavin reduction was measured by monitoring the decrease in absorbance at 453 nm which results from the anaerobic mixing of the mutant enzyme with the organic substrate as described in ref (*3*) for the wild-type enzyme. The mutant enzyme was mixed anaerobically with an equal volume of substrate, obtaining a final reaction mixture of ~15 μM enzyme and 0.2 to 10 mM choline or 1 to 25 mM betaine aldehyde. For each concentration of substrate, the rates of flavin reduction were recorded in triplicate, with measurements usually differing by ≤ 5%.

Data Analysis. Kinetic data were fit with the KaleidaGraph (Synergy Software, Reading, PA) and the Enzfitter (Biosoft, Cambridge, U.K.) softwares. Apparent kinetic parameters in atmospheric oxygen were determined by fitting initial rates at different substrate concentration to the Michaelis-Menten equation for one substrate. The steady-state kinetic parameters at varying concentrations of both choline and oxygen were determined by fitting the initial rates to eq 1, which describes a steady-state kinetic mechanism with formation of a ternary complex. K_a and K_b are the Michaelis constants for choline (*A*) and oxygen (*B*), respectively, and k_{cat} is the turnover number of the enzyme (*e*).

$$\frac{v}{e} = \frac{k_{cat} AB}{K_a B + K_b A + AB + K_{ia} K_b} \qquad (1)$$

The pH profiles of the k_{cat} and k_{cat}/K_m values were determined by fitting initial rate data to eq 2, which describes a curve with a slope of +1 and a plateau region at high pH. C is the pH independent value of the kinetic parameter of interest. Product inhibition data were fit to eq 3, which describes a competitive inhibition mechanism of the organic substrate and the product. K_{is} is the inhibition constant and *P* is the concentration of glycine betaine. The pH profile of enzyme

inhibition by glycine betaine was determined by fitting the initial rate data to eq 4, which describes a curve with a slope of -1 and a plateau region at low pH. Kinetic isotope effects were determined by taking the ratio of the kinetic parameters obtained with choline to that obtained with 1,2-[$^2H_4$]-choline.

$$\log Y = \log \frac{C}{1 + \frac{10^{-pH}}{10^{-pKa}}} \tag{2}$$

$$\frac{v}{e} = \frac{k_{cat} A}{K_a \left(1 + \frac{P}{K_{is}}\right) + A} \tag{3}$$

$$\log Y = \log \frac{C}{1 + \frac{10^{-pK_a}}{10^{-pH}}} \tag{4}$$

Stopped-flow data traces were fit with eq 5, which describes a single-exponential process, in which k_{obs} is the apparent first-order rate constant for flavin reduction, A is the value of absorbance at the specific wavelength of interest at time t, B is the amplitude of the absorbance change, and C is an offset value that accounts for the non-zero absorbance value at infinite time. Pre-steady-state kinetic parameters were determined by using eq 6, where k_{obs} is the observed first-order rate for the reduction of the enzyme-bound flavin at any given concentration of substrate, k_{red} is the limiting first-order rate constant for flavin reduction at saturated substrate concentration, and K_d is the macroscopic dissociation constant for binding of the substrate to the enzyme.

$$A = B \exp(-k_{obs} t) + C \tag{5}$$

$$k_{obs} = \frac{k_{red} A}{K_d + A} \tag{6}$$

2.5 Results

Purification of the His351Ala Variant of Choline Oxidase. The His351Ala variant of choline oxidase in which His351 was replaced with alanine was engineered using site-directed mutagenesis, expressed in *E. coli* strain Rosetta(DE3)pLysS, and purified by anionic exchange chromatography at pH 8 using the same protocol established for the wild-type enzyme (*1*). The purified enzyme had about 50 to 70% of the enzyme-bound flavin cofactor as an air-stable anionic flavosemiquinone, which was slowly converted to the oxidized state by extensive dialysis at pH 6 and 4 ^{o}C (Figure S1)**.** In this respect, the His351Ala enzyme behaved like the wild-type enzyme, which was previously shown to stabilize the anionic flavosemiquinone in air at pH 8 (*1, 10*). The UV-visible absorbance spectrum of the oxidized form of the His351Ala variant at pH 8 showed peaks at 367 and 454 nm with a ε_{454nm} value of 11.7 $mM^{-1}cm^{-1}$, in agreement with the value of 11.4 $mM^{-1}cm^{-1}$ previously observed with the wild-type enzyme (*10*). Acid denaturation of the enzyme using 10% TCA, followed by centrifugation to remove the unfolded protein, yielded a supernatant that was devoid of absorbance in the visible region of the spectrum, consistent with the flavin cofactor being covalently bound to the protein. The fully oxidized form of the His351Ala enzyme had a specific activity of 0.04 μmol O_2 $min^{-1}mg^{-1}$ with 10 mM choline as substrate at pH 7, which was ~200-fold lower than that of the wild-type enzyme, suggesting that His351 is important for catalysis in choline oxidase.

Steady-State Kinetics. The steady-state kinetic parameters of the His351Ala enzyme were determined using choline as substrate at 25 ^{o}C, by monitoring the rate of oxygen consumption at varying concentrations of both the organic substrate and oxygen. The determination was carried out at pH 10 because all of the kinetic parameters for the wild-type (*10*) and the His351Ala mutant enzymes (this study) were independent of the pH in this region,

thereby allowing for a direct comparison of the values obtained with the two enzymes. As for the case previously reported for the wild-type form of choline oxidase (*3*), the best fits of the data were obtained with eq 1, consistent with the order of the kinetic steps involving substrate binding and product release being the same in the two enzymes. Substitution of histidine with alanine at position 351 resulted in a decrease in the overall turnover with choline of 60-fold with respect to the turnover of the wild-type enzyme (Table 2.1). A 360-fold decrease in the k_{cat}/K_m value with choline was also observed, suggesting that the histidine to alanine mutation affects the reductive half-reaction in which the organic substrate is oxidized by choline oxidase. In contrast, the k_{cat}/K_{O2} value which directly reported on the oxidative half-reaction in which the reduced flavin reacts with molecular oxygen (*16*) was only 1.2-times lower in the His351Ala than in wild-type choline oxidase. These data are consistent with His351 playing a minimal role in the oxidative half-reaction in which the reduced flavin reacts with molecular oxygen.

Table 2.1. Comparison of the Kinetic Parameters of His351Ala[a] and Wild-Type[b] Choline Oxidase at pH 10

Kinetic parameters	His351Ala	Wild-type
Choline		
k_{cat}, s^{-1}	1.00 ± 0.01	60 ± 1
K_m, mM	1.50 ± 0.30	0.25 ± 0.01
K_{O_2}, μM	16 ± 2	690 ± 30
k_{cat}/K_m, $M^{-1}s^{-1}$	660 ± 120	237000 ± 9000
k_{cat}/K_{O_2}, $M^{-1}s^{-1}$	70000 ± 10000	86400 ± 3600
K_{ia}, mM	7.1 ± 1.6	0.14 ± 0.01
k_{red}, s^{-1}	1.2 ± 0.1	93 ± 1
K_d, mM	2.6 ± 0.3	0.29 ± 0.01
$^D(k_{cat}/K_m)$	7.8 ± 0.2	10.7 ± 2.6
$^Dk_{cat}$	5.0 ± 0.2	7.5 ± 0.3
Betaine aldehyde		
k_{red}, s^{-1}	4.4 ± 0.4	135 ± 4
K_d, mM	12.0 ± 2.2	0.45 ± 0.03

[a] Enzymatic activity was measured at varying concentrations of both organic substrate and oxygen in 50 mM sodium pyrophosphate, pH 10, at 25 °C. [b] From ref 3. The steady-state and pre-steady-state kinetic parameters were determined by using by eqs 1 and 6, respectively.

Reductive Half-Reactions with Choline or Betaine Aldehyde. The reductive half-reactions with choline or betaine aldehyde as substrate were investigated further in a stopped-flow spectrophotometer by mixing anaerobically the His351Ala enzyme with different concentrations of choline or betaine aldehyde at pH 10 and 25 °C. In all cases, the decrease in absorbance at 453 nm associated with the reduction of the enzyme-bound flavin was fit best to a single exponential process, as illustrated in the example of Figure 2A. Full reduction of the enzyme-bound flavin to the neutral hydroquinone species was observed in all cases, as suggested by the poorly defined absorbance peak in the 350 nm region of the UV-visible absorbance spectrum and the prominent shoulder centered at 400 nm (Figure 2.2 B). The observed rates of flavin reduction (k_{obs}) were hyperbolically dependent on the concentration of the organic substrate (Figure 2.2 C, D), which allowed for the determination of the limiting rate constants for flavin reduction (k_{red}) and the macroscopic equilibrium constants for substrate binding at the active site of the enzyme (K_d). As summarized in Table 1, the k_{red} values for the His351Ala enzyme were 80- and 30-fold lower with choline and betaine aldehyde with respect to the wild-type enzyme. In addition, replacement of His351 with alanine resulted in 10- and 25-fold increases in the K_d values for choline and betaine aldehyde. Thus, His351 plays significant roles for both substrate binding and the hydride transfer reaction catalyzed by choline oxidase.

pH Dependence of the k_{cat} and k_{cat}/K_m Values. The pH profiles of the steady-state kinetic parameters of the His351Ala enzyme were determined in the pH range from 5 to 10, at varying concentrations of both choline and oxygen. Both the k_{cat} and k_{cat}/K_m values with choline increased with increasing pH and reached limiting values at high pH (Figure 2.3A, B), consistent with the requirement for an unprotonated group in the reductive half-reaction of the mutant enzyme. The apparent pK_a values determined from the plots of log k_{cat}/K_m and k_{cat} versus pH

were 7.8 ± 0.2 and 6.6 ± 0.1. For comparison, the wild-type enzyme was previously shown to have pK_a values of 7.6 and 7.1 in the k_{cat}/K_m and k_{cat} pH profiles with choline as substrate (*10*).

In the pH range from 7 to 10 the K_m values for oxygen were all less than 15 μM (Table S2 in Supporting Information), yielding pH-independent k_{cat}/K_{O2} values in the lower 10^5 $M^{-1}s^{-1}$ range. At pH lower than 7 the K_m values for oxygen decreased further, thereby preventing the determination of the k_{cat}/K_{O2} values at low pH due to the enzyme being fully saturated with oxygen at the lowest concentrations of oxygen attainable in the steady-state experiments, i.e., 10 μM.

Substrate Kinetic Isotope Effects. Due to the His351Ala enzyme being saturated with oxygen under atmospheric condition[1], the kinetic isotope effects on the steady-state kinetic parameters were determined with 1,2-[$^2H_4$]-choline in air-saturated buffer. As shown in Figure 4, both the $^D(k_{cat}/K_m)$ and $^Dk_{cat}$ values with the His351Ala enzyme were pH-independent in the pH range from 7 to 10, with average values of 7.8 ± 0.2 and 5.0 ± 0.2, respectively. These values were only slightly lower than those of 10.6 and 7.5 previously reported for the wild-type enzyme (*3*), for which the cleavage of the CH bond of choline was shown to be fully rate-limiting for the reductive half-reaction and partially rate-limiting for the overall turnover of the enzyme along with the subsequent step of CH bond cleavage of the aldehyde intermediate (*3*).

Binding of Glycine Betaine. Previous studies showed that glycine betaine inhibits the wild-type form of choline oxidase by binding at the active site of enzyme, with a limiting K_{is} value of 13 mM at low pH and a pK_a value of 7.5 (*10, 11*). Consequently, the pH dependence of the inhibition by glycine betaine was determined to obtain the thermodynamic pK_a value for the group in the active site of the His351Ala enzyme that participates in the reductive-half reaction.

[1] At 25 °C the concentration of oxygen dissolved in aqueous solution is 253 μM. In the pH range from 7 to 10 the K_m value for oxygen of the His351Ala enzyme was ≤15 μM. Consequently the mutant enzyme is ≥94% saturated with oxygen throughout the pH interval that was studied.

As shown in Figure 3C, His351Ala enzyme inhibition was maximal at low pH (K_{is} value of 21 ± 3 mM) and decreased with increasing pH, yielding a pK_a value of 8.0 ± 0.1. Thus, replacement of His351 with alanine resulted in a 0.5-unit increase in the macroscopic, thermodynamic pK_a value for the ionizable group(s) in the active of the enzyme.

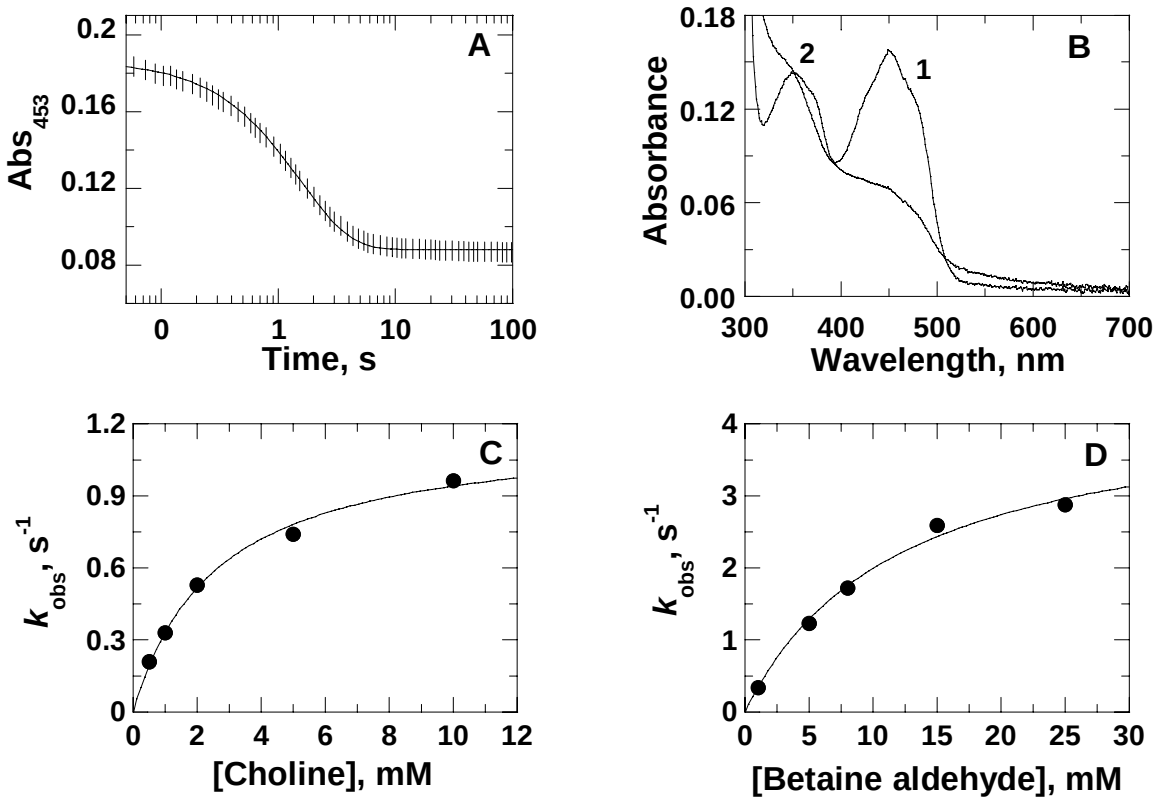

Figure 2.2. Anaerobic substrate reduction of the His351Ala enzyme with choline and betaine aldehyde as substrate. Panel A: stopped-flow trace obtained upon mixing anaerobically the His351Ala enzyme variant with 15 mM betaine aldehyde in 50 mM sodium phosphate, sodium pyrophosphate buffer, pH 10, at 25 °C. The curve represents the fit of the data with eq. 5. Time indicated is after the end of flow, i.e., 2.2 ms. For clarity, one experimental point every 10 is shown (vertical lines). Panel B: The UV-visible absorbance spectra of the oxidized (curve 1) and reduced (curve 2) species of the His351Ala enzyme variant obtained by mixing anaerobically the oxidized enzyme with buffer and 15 mM betaine aldehyde in 50 mM sodium phosphate, sodium pyrophosphate buffer, pH 10, at 25 °C. Panels C and D, observed rates of anaerobic flavin reduction (k_{obs}) as a function of the concentrations of choline and betaine aldehyde, respectively. Data were fit to eq 6.

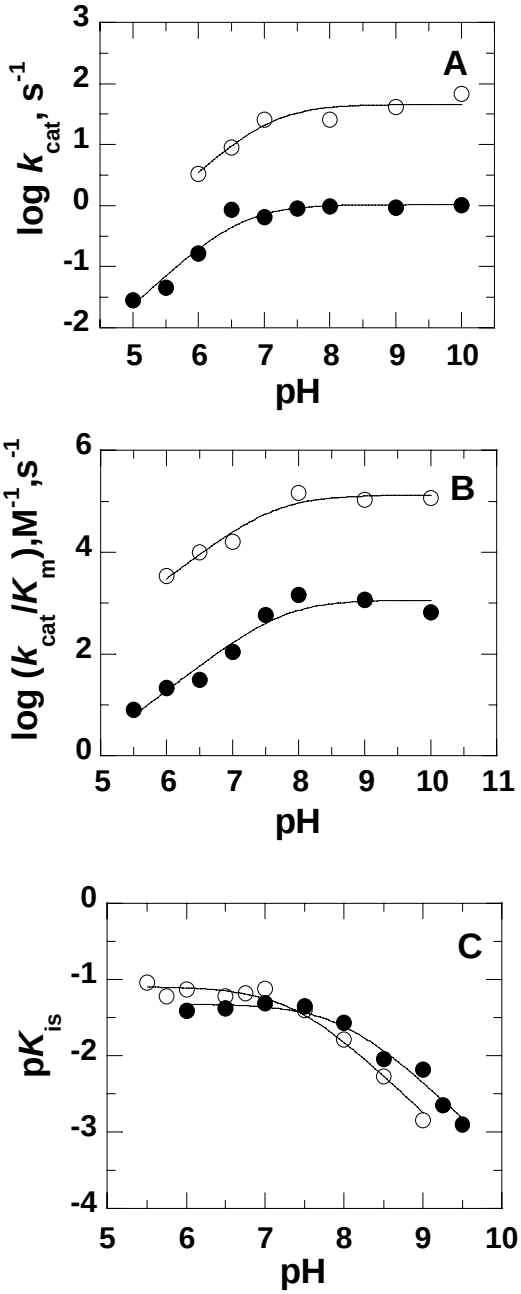

Figure 2.3. pH dependence of the k_{cat} (panel A), k_{cat}/K_m values for choline (panel B), and glycine betaine inhibition (panel C) for the His351Ala (●) and the wild-type (○) enzymes. Panel A and B, activity assays were measured at varying concentration of both choline and oxygen between pH 5 and 10, at 25 °C. The data were fit with eq 2. Panel C, activity assays were measured at varying concentrations of choline and glycine betaine in air-saturated buffer between pH 6 to 9.5, at 25 °C. The lines were fit of the data to eq. 4. The K_{is} value for glycine betaine was determined by fitting the initial rate data to eq 3. Data for wild-type enzyme are from ref (*10*).

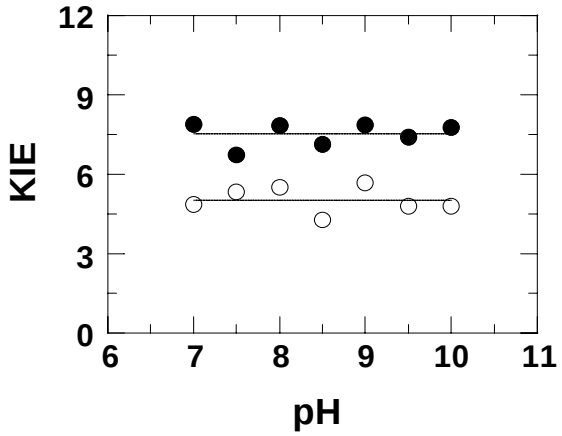

Figure 2.4. pH dependence of substrate deuterium isotope effects on the k_{cat}/K_m values (●) and k_{cat} (○) values with choline as substrate for the His351Ala enzyme variant. Enzymatic activities were measured in air-saturated 50 mM sodium pyrophosphate buffer with choline and 1,2-[$^2H_4$]-choline as substrates between pH 7 to 10, at 25 °C. Data were fit by y = 7.78 and y = 5.15, for k_{cat}/K_m and k_{cat} values, respectively.

2.6 Discussion

The variant of choline oxidase in which His351 has been replaced with alanine was prepared in this study to investigate the role played by this residue in the enzyme-catalyzed reaction of choline oxidation. The mutant enzyme is properly folded and is similar to the wild-type enzyme with respect to *a*) a flavin covalently linked to the protein; *b*) the stabilization of an air-stable, anionic flavosemiquinone, which can be slowly oxidized upon prolonged treatment at pH 6 and 4 ^oC; *c*) a sequential steady-state kinetic mechanism in which oxygen reacts in a second-order fashion with the enzyme-bound reduced flavin before the release of the organic product of reaction; *d*) a chemical step for cleavage of the substrate CH bond that is fully rate limiting for the reductive half-reaction and partially rate limiting for the overall turnover of the enzyme; *e*) the requirement for an unprotonated group in the reductive half-reaction; and *f*) the absence of ionizable groups with pK_a in the range from 7 to 10 for the oxidative half-reaction

with choline as substrate. Consequently, the comparison of the mechanistic properties that differ from and are similar to one another in the His351Ala and wild-type enzymes can be used to gain insights on the catalytic role exerted by His351 in the active site of choline oxidase.

The active site residue His351 is important for substrate binding, most likely by acting as a hydrogen bond donor to the hydroxyl oxygen of the alcohol substrate, as illustrated schematically in Figure 2.5. Evidence supporting this conclusion comes from anaerobic substrate reduction experiments using a stopped-flow spectrophotometer, showing that in the His351Ala variant the K_d values for choline and betaine aldehyde binding are 9- and 17-times larger than the corresponding values in the wild-type enzyme (*10*). The decreases in the chemical affinity of the His351Ala enzyme variant for the substrates correspond to an energetic contribution of the side chain of His351 of 5 to 8 kJ mol^{-1}, which agrees well with the expected value for a hydrogen bonding interaction (*17*). Structural data independently support an involvement of His351 in binding to the hydroxyl moiety of the alcohol substrate(s). Indeed, the crystal structure of choline oxidase resolved to 1.86 Å shows that His351 is 3.5 Å from the methyl groups of DMSO, an additive that was used in the crystallization solution and that was proposed to mimic the substrate, and 6.7 Å from the N(5) atom of the flavin (*9*), which is the site acting as the acceptor of the hydride ion originating from the α-carbon of the choline alkoxide species in the reaction catalyzed by the enzyme (Scheme 2) (*3*).

His351 facilitates the hydride transfer reaction between the activated alkoxide intermediate and the flavin N(5) atom (Scheme 2.2), likely by hydrogen bonding to the oxygen atom of the alkoxide species in the transition state for the reaction. This conclusion is supported by the 75-fold decrease in the rate constant for flavin reduction (k_{red}) that accompanies the replacement of His351 with alanine determined in anaerobic substrate reduction experiments

using a stopped-flow spectrophotometer. A decrease of 30-fold in the k_{red} value is also observed when hydrated betaine aldehyde is used instead of choline as substrate, further consistent with His351 stabilizing the transition state for the reaction. In agreement with this conclusion the substrate kinetic isotope effect that is associated with CH bond cleavage is ~ 30% lower than in the wild-type enzyme with a $^{D}(k_{cat}/K_m)$ value of 7.8 as compared to 10.6 (*3*). Recent mechanistic studies on the wild-type form of choline oxidase showed that the hydride transfer reaction occurs quantum mechanically within a highly pre-organized active site, with little independent movement of the alkoxide species acting as hydride donor and the N(5) atom of the flavin acting as hydride acceptor (*8*). In this context, it is attractive to hypothesize that the decreased rates of hydride transfer with choline and hydrated betaine aldehyde seen in the His351Ala enzyme variant may originate from disruption of pre-organization in the enzyme-substrate complex, which would allow for the alkoxide donor and the flavin acceptor more independent movement in the His351Ala enzyme-substrate complex with respect to the wild-type enzyme. This hypothesis is the focus of a current investigation of the enzyme.

Replacement of the histidine residue at position 351 with alanine results in the increase from 7.5 to ~8 of the thermodynamic pK_a value for the catalytic base that activates choline to the alkoxide species, as indicated by the pH profile of glycine betaine inhibition with the His351Ala enzyme. A larger increase in the thermodynamic pK_a value for the catalytic base of choline oxidase, to a value of ~9, was previously observed upon replacing the only other histidine residue located in the active site of the enzyme with alanine (e.g., His466) (*4*). These data are consistent with both active site histidine residues contributing to the overall polarity of the active site, which is essential for an efficient deprotonation of the hydroxyl proton of the alcohol substrate during enzymatic turnover. However, neither of the two histidine residues is essential

for the deprotonation reaction (Scheme 2.2), since the pH profiles for the k_{cat}/K_m values unequivocally show the requirement for a catalytic base in both the His351Ala (this study) and the His466Ala enzyme variants (*4*). Since no ionizable side chains other than His351 and His466 are present in the active site of the enzyme, a rationale that explains the site-directed mutagenesis results is that either one of the two histidines acts as catalytic base in the wild-type enzyme, whereas the other residue would pick up the catalytic role in the absence of the "original" base in the site-directed mutagenized enzyme. Alternatively, one should contemplate the possibility of multiple residues in the active site of the enzyme acting synergistically, and not singlehandedly, to promote acidification of the substrate hydroxyl group through electrostatic and hydrogen bonds. In the active site of choline oxidase, such a synergistic role may be played by Ser101, His351, His466, possibly the C4 oxygen atom of the flavin and water. In the latter case, the quest for the "catalytic base" using a classical site-directed mutagenesis approach in which a single residue is selectively replaced and the function of the resulting enzyme is investigated would be hampered by the fact that the typical behavior associated with the presence of a catalytic base would still be observed in the pH profiles irrespective of the site of mutagenesis, as it has been the case for the His351 and His466 mutant forms of choline oxidase.

His351 does not participate in the activation of the reduced flavin for reaction with molecular oxygen, as demonstrated by the minimal decrease of 1.2-fold in the k_{cat}/K_m value for oxygen in the His351Ala enzyme as compared to the wild-type enzyme (*10*). Interestingly, a similar decrease of 1.5-fold was recently reported in the k_{cat}/K_m value for oxygen for another active site variant of choline oxidase in which the conserved His466 was replaced with alanine (*4*). These results, along with the lack of pH dependence of the k_{cat}/K_m value for oxygen reported in this study for the His351Ala enzyme and in a previous study for the wild-type form of choline

oxidase (*10*), are in stark contrast with a mechanistic model recently presented by Klinman and co-workers for the reaction of reduced flavoproteins with oxygen (*13, 15*). Based on studies using a variety of mechanistic probes on the wild-type and an active site mutant form of glucose oxidase in which His516 was replaced by alanine, which is equivalent to the His466 to alanine substitution in choline oxidase, the authors concluded that "virtually all of the catalytic effect in the glucose oxidase reduction of oxygen can be assigned to a single protonated histidine!" (*18*). Although the features that activate the reduced flavin for reaction with oxygen in choline oxidase have not been yet elucidated, at this stage of the investigation it can be confidently concluded that a molecular mechanism different from that proposed for glucose oxidase must necessarily operate in choline oxidase. Caution should therefore be exerted in extending *a priori* conclusions that apply to well-characterized systems, such as glucose oxidase, to other oxidases that reduce oxygen in the absence of metal ions.

The neutral hydroquinone species of the flavin is stabilized in the His351Ala enzyme at pH 10, as suggested by the UV-visible absorbance spectrum of the enzyme observed after anaerobic reduction with choline in the stopped-flow spectrophotometer. Stabilization of the neutral flavin hydroquinone at high pH was previously observed in other variants of choline oxidase in which His466 was replaced with alanine or aspartate (*6*). These results contrast to the behavior of the wild-type form of choline oxidase, which stabilizes the anionic hydroquinone species between pH 6 and 10 (*6*). All taken together these data are consistence with a minimal difference in the reactivity of the neutral and anionic flavin hydroquinone species with molecular oxygen, as suggested by the similar k_{cat}/K_m values for oxygen of the wild-type, His351Ala and His466Ala enzymes. In this regard, previous mechanistic studies showed that a major determinant for reduced flavin reactivity with molecular oxygen in choline oxidase is provided

instead by the positively charged trymethylammonium moiety of the organic substrate, which is bound at the active site (*7, 11*).

The large, pH independent substrate kinetic isotope effect of 7.8 determined in this study on the second-order rate constant k_{cat}/K_m with 1,2-[$^2H_4$]-choline as substrate is consistent with the chemical step of hydride ion transfer from the alkoxide substrate to the flavin being the slowest step in the reductive half-reaction catalyzed by the His351Ala enzyme (*3*). Independent evidence for choline being a slow substrate for the His351Ala enzyme comes from the similarity between the thermodynamic pK_a value for the catalytic group in the active site of the enzyme determined in the pH profile of glycine betaine inhibition, with a value of 8.0 ± 0.1, and the kinetic pK_a value of 7.8 ± 0.2 determined from the pH profile of the k_{cat}/K_m value with choline. In this respect, the His351Ala enzyme behaves like the wild-type enzyme, for which it was previously shown that the chemical step of CH bond cleavage is fully rate limiting for the reductive half-reaction (*3*).

The overall turnover in the His351Ala enzyme with choline as substrate is limited primarily by the chemical step of hydride ion transfer from the alcohol substrate to the enzyme-bound flavin, with a minor contribution of the second hydride ion transfer reaction involving the aldehyde intermediate and the flavin. This conclusion is supported by both steady-state kinetics and anaerobic substrate reduction data, showing that the k_{cat} value of 1 s^{-1} experimentally determined at pH 10 is approximated fairly well by eq 7, where $k_{red(CH)}$ represents the limiting rate constant for hydride transfer reaction between choline and the enzyme-bound flavin, with a value of 1.2 ± 0.1 s^{-1}, and $k_{red(BA)}$ is the corresponding limiting rate constant for the hydride transfer reaction from the aldehyde intermediate to the flavin, with a value of 4.4 ± 0.4 s^{-1}.

$$k_{cat} = \frac{k_{red(CH)} k_{red(BA)}}{k_{red(CH)} + k_{red(BA)}} = 0.94 \pm 0.11 \text{ s}^{-1} \qquad (7)$$

In summary, the results presented in this study on the mutant form of choline oxidase in which His351 has been replaced with alanine allow to support the notion that His351 is an important, but not an essential, residue for the reductive half-reaction of choline oxidation catalyzed by choline oxidase. In contrast, His351 has a minimal role in the subsequent oxidative half-reaction in which the reduced flavin reacts with oxygen. In the reductive half-reaction, His351 contributes to substrate binding by providing a hydrogen bond with its imidazole side chain to the hydroxyl group of choline. This hydrogen bonding interaction is important for the subsequent reaction of hydride transfer from the α-carbon of the activated, alkoxide substrate to the N(5) atom of the enzyme-bound flavin, in that it most likely contributes to the correct positioning of the hydride donor and acceptor in the enzyme-substrate complex. In this respect, the large substrate kinetic isotope effect seen here on the k_{cat}/K_m value is an important prerequisite for future mechanistic investigations aimed at the elucidation of the importance of His351 in the hydride transfer reaction catalyzed by choline oxidase. Furthermore, His351 contributes to the overall polarity of the active site, by modulating the macroscopic pK_a value for the group that activates choline to the alkoxide species, whose identity still remains elusive. Finally, neither His351 nor His466, which are the only ionizable residues in the active site of the enzyme with the potential to gain a positive charge, play a role in the reaction between the reduced flavin and molecular oxygen. Thus, important questions that pertain to the molecular mechanisms for alkoxide formation by the enzyme and oxygen reduction by the flavin will have to be addressed in future investigations.

2.7 Appendix

SUPPORTING INFORMATION

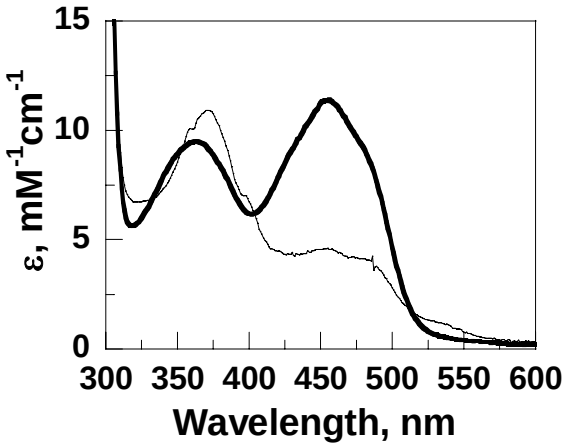

Figure A2.1. UV- visible absorbance absorbance spectrum of the His351Ala enzyme as purified.

Table A2.1. Observed rates and amplitudes of the changes at 453 nm associated with the anaerobic flavin reduction of the His351Ala enzyme with choline or betaine aldehyde as substrate at pH 10, 25 °C [a]

	Choline				Amp			
[Substrate] mM	k_{obs} A s^{-1}	k_{obs} B s^{-1}	k_{obs} C s^{-1}	Ave k_{obs} [b] s^{-1}	Amp A s^{-1}	Amp B s^{-1}	Amp C s^{-1}	Ave Amp [c] s^{-1}
0.5	0.21	0.21	0.21	0.21 ± 0.01	0.10	0.10	0.10	0.10 ± 0.001
1	0.33	0.33	0.33	0.33 ± 0.01	0.10	0.10	0.10	0.10 ± 0.001
2	0.53	0.53	0.52	0.53 ± 0.01	0.09	0.09	0.09	0.09 ± 0.001
5	0.71	0.72	0.78	0.74 ± 0.04	0.08	0.08	0.08	0.08 ± 0.002
10	0.96	0.99	0.91	0.95 ± 0.04	0.06	0.06	0.06	0.06 ± 0.002
	Betaine aldehyde				Amp			
[Substrate] mM	k_{obs} A s^{-1}	k_{obs} B s^{-1}	k_{obs} C s^{-1}	Ave k_{obs} s^{-1}	Amp A s^{-1}	Amp B s^{-1}	Amp C s^{-1}	Ave Amp s^{-1}
1	0.34	0.36	0.35	0.34 ± 0.01	0.10	0.10	0.09	0.10 ± 0.005
5	1.21	1.24	1.24	1.24 ± 0.01	0.10	0.10	0.10	0.10 ± 0.001
8	1.74	1.71	1.72	1.72 ± 0.02	0.10	0.10	0.10	0.10 ± 0.001
15	2.61	2.55	2.59	2.60 ± 0.03	0.09	0.09	0.09	0.09 ± 0.002
25	2.80	2.85	2.98	2.90 ± 0.10	0.07	0.07	0.08	0.075 ± 0.002

[a]Pre-steady-state kinetic data were measured under anaerobic conditions at varying concentrations of organic substrate in 50 mM sodium phosphate and sodium pyrophosphate, pH 10, at 25 °C. The stopped-flow traces were fit to eq 5. [b]Ave k_{obs} is the mean average of k_{obs} A, k_{obs} B and k_{obs} C. [c]Ave Amp is the mean average of Amp A, Amp B and Amp C.

Table A2.2. Steady-State Kinetic Parameters with Choline as Substrate for the His351Ala Enzyme at 25 ˚C [a]

pH	k_{cat}, s^{-1}	K_a, mM[b]	k_{cat}/K_a, $M^{-1}s^{-1}$[b]	Ko_2,μM	k_{cat}/Ko_2, $M^{-1}s^{-1}$	K_{ia}, mM	R^2
5.0	0.03 ± 0.01	1.5 ± 0.2	18.2 ± 2.2	-	-	-	-
5.5	0.045 ± 0.1	5.6 ± 0.8	8.1 ± 0.2	-	-	-	-
6.0	0.2 ± 0.1	7.7 ± 0.1	21.6 ± 0.13	-	-	-	-
6.5	0.8 ± 0.1	27.6 ± 0.1	31.2 ± 0.16	-	-	-	-
7.0	0.7 ± 0.1	5.8 ± 0.1	110.6 ± 0.2	3.3 ± 0.01	195,454 ± 610	35.8 ± 0.2	0.981
7.5	0.9 ± 0.1	1.6 ± 0.2	581 ± 71	5.5 ± 0.4	165,454 ± 1,230	19.5 ± 2.0	0.977
8.0	1.0 ± 0.1	0.6 ± 0.1	1,643 ± 69	10.7 ± 0.1	93,018 ± 955	18.2 ± 0.2	0.989
9.0	0.9 ± 0.1	0.8 ± 0.4	1,151 ± 616	9.1 ± 3.6	101,320 ± 40,700	6.8 ± 4.3	0.969
10.0	1.0 ± 0.1	1.5 ± 0.2	661 ± 121	14.9 ± 2.1	68,037 ± 10,000	7.1 ± 1.6	0.994

[a] Enzymatic activity was measured by varying the concentrations of both choline and oxygen in 50 mM sodium phosphate and sodium pyrophosphate, at 25 ˚C.
[b] K_a and k_{cat}/K_a are the K_m and k_{cat}/K_m values for choline, respectively.

Table A2.3. pH Dependence of Product Inhibition of the His351Ala Enzyme with Glycine Betaine and Choline as Substrate[a]

Substrate	pH	$^{app}k_{cat}$, s^{-1}	$^{app}K_m$, mM	K_{is}, mM	R^2
Choline	6.0	0.11 ± 0.1	22.1 ± 0.3	25.7 ± 4.0	0.993
	6.5	0.28 ± 0.1	21.2 ± 4.0	24.5 ± 4.3	0.986
	7.0	0.41 ± 0.1	11.5 ± 0.6	20.1 ± 1.8	0.998
	7.5	0.46 ± 0.1	3.3 ± 0.1	16.6 ± 0.4	0.986
	8.0	0.46 ± 0.1	2.2 ± 0.1	36.7 ± 2.4	0.995
	8.5	0.48 ± 0.1	2.1 ± 0.1	110 ± 2	0.996
	9.0	0.47 ± 0.1	1.6 ± 0.2	152 ± 47	0.978
	9.25	0.48 ± 0.1	1.5 ± 0.1	440 ± 73	0.991
	9.5	0.48 ± 0.1	1.8 ± 0.2	793 ± 246	0.979

[a]Enzyme activity was measured at varying concentrations of choline substrate and glycine betaine in air-saturated 50 mM sodium phosphate and sodium pyrophosphate at 25 °C.

2.7 Acknowledgement

The authors thank Dr. Mahmoud Ghanem for his initial assistance in the site-directed mutagenesis experiments.

2.8 References

1. Fan, F., Ghanem, M., and Gadda, G. (2004) Cloning, sequence analysis, and purification of choline oxidase from *Arthrobacter globiformis*: a bacterial enzyme involved in osmotic stress tolerance, *Arch. Biochem. Biophys. 421*, 149-158.
2. Fan, F., Germann, M. W., and Gadda, G. (2006) Mechanistic studies of choline oxidase with betaine aldehyde and its isosteric analogue 3,3-dimethylbutyraldehyde, *Biochemistry 45*, 1979-1986.
3. Fan, F., and Gadda, G. (2005) On the catalytic mechanism of choline oxidase, *J. Am. Chem. Soc. 127*, 2067-2074.
4. Ghanem, M., and Gadda, G. (2005) On the catalytic role of the conserved active site residue His_{466} of choline oxidase, *Biochemistry 44*, 893-904.
5. Gadda, G., and McAllister-Wilkins, E. E. (2003) Cloning, expression, and purification of choline dehydrogenase from the moderate halophile Halomonas elongata, *Appl. Environ. Microbiol. 69*, 2126-2132.
6. Ghanem, M., and Gadda, G. (2006) Effects of reversing the protein positive charge in the proximity of the flavin N(1) locus of choline oxidase, *Biochemistry 45*, 3437-3447.
7. Gadda, G., Fan, F., and Hoang, J. V. (2006) On the contribution of the positively charged headgroup of choline to substrate binding and catalysis in the reaction catalyzed by choline oxidase, *Arch. Biochem. Biophys. 451*, 182-187.

8. Fan, F., and Gadda, G. (2005) Oxygen- and temperature-dependent kinetic isotope effects in choline oxidase: correlating reversible hydride transfer with environmentally enhanced tunneling, *J. Am. Chem. Soc. 127*, 17054-17061.

9. Quaye, O., Lountos, G. T., Fan, F., Orville, A. M., and Gadda, G. (2008) Role of Glu312 in binding and positioning of the substrate for the hydride transfer reaction in choline oxidase, *Biochemistry 47*, 243-256.

10. Ghanem, M., Fan, F., Francis, K., and Gadda, G. (2003) Spectroscopic and kinetic properties of recombinant choline oxidase from *Arthrobacter globiformis*, *Biochemistry 42*, 15179-15188.

11. Gadda, G., Powell, N., and Menon, P. (2004) The trimethylammonium headgroup of choline is a major determinant for substrate binding and specificity in choline oxidase, *Arch. Biochem. Biophys. 430*, 264-273.

12. Wohlfahrt, G., Witt, S., Hendle, J., Schomburg, D., Kalisz, H. M., and Hecht, H. J. (1999) 1.8 and 1.9 A resolution structures of the Penicillium amagasakiense and Aspergillus niger glucose oxidases as a basis for modelling substrate complexes, *Acta. Crystallogr. D. Biol. Crystallogr*. *55*, 969-977.

13. Roth, J. P., and Klinman, J. P. (2003) Catalysis of electron transfer during activation of O2 by the flavoprotein glucose oxidase, *Proc. Natl. Acad. Sci. U S A 100*, 62-67.

14. Kiess, M., Hecht, H. J., and Kalisz, H. M. (1998) Glucose oxidase from Penicillium amagasakiense. Primary structure and comparison with other glucose-methanol-choline (GMC) oxidoreductases, *Eur. J. Biochem*. *252*, 90-99.

15. Su, Q., and Klinman, J. P. (1999) Nature of oxygen activation in glucose oxidase from Aspergillus niger: the importance of electrostatic stabilization in superoxide formation, *Biochemistry 38*, 8572-8581.

16. Gadda, G. (2003) Kinetic mechanism of choline oxidase from Arthrobacter globiformis, *Biochim. Biophys. Acta. 1646*, 112-118.

17. Sheu, S. Y., Schlag, E. W., Selzle, H. L., and Yang, D. Y. (2008) Molecular dynamics of hydrogen bonds in protein-D2O: the solvent isotope effect, *J. Phys. Chem. A 112*, 797-802.

18. Klinman, J. P. (2007) How do enzymes activate oxygen without inactivating themselves?, *Acc. Chem. Res. 40*, 325-333.

CHAPTER 3

Role of Asparagine 510 in the Relative Timing of Substrate Bond Cleavages in the Reaction Catalyzed by Choline Oxidase

(This chapter has been published verbatim in Rungsrisuriyachai, K. and Gadda, G., (2010), *Biochemistry 49:* 2483-2490*)*

3.1. Abbreviations

Asn510Ala, Asn510His, Asn510Leu, and Asn510Asp enzymes, choline oxidase variants with asparagine at position 510 replaced with alanine, histidine, leucine, and aspartate.

3.2. Abstract

The flavoprotein choline oxidase catalyzes the oxidation of choline to glycine betaine with transient formation of an aldehyde intermediate and molecular oxygen as final electron acceptor. The enzyme has been grouped in the Glucose-Methanol-Choline oxidoreductase enzyme superfamily, which shares a highly conserved His-Asn catalytic pair in the active site. In this study, the conserved asparagine residue at position 510 in choline oxidase was replaced with alanine, aspartate, histidine, or leucine by site-directed mutagenesis and the resulting mutant enzymes were purified and characterized in their biochemical and mechanistic properties. All of the substitutions resulted in low incorporation of FAD into the protein. The Asn510Asp enzyme was not catalytically active with choline and had 75% of the flavin associated non-covalently. The most notable changes in the catalytic parameters with respect to wild-type choline oxidase were seen in the Asn510Ala enzyme, with decreases of 4,300-fold in the $k_{cat}/K_{choline}$, 600-fold in

the k_{red}, 660-fold in the k_{cat}, and 50-fold in the k_{cat}/K_{oxygen} values. Smaller, but nonetheless similar, changes were seen also in the Asn510His enzyme. Both the K_d and K_m values for choline changed ≤7-fold. These data are consistent with Asn510 participating in both the reductive and oxidative half-reactions, but having minimal role in substrate binding. Substrate, solvent and multiple kinetic isotope effects on the k_{red} values indicated that the substitution of Asn510 with alanine, but not with histidine, resulted in a change from stepwise to concerted mechanisms for the cleavages of the OH and CH bonds of choline catalyzed by the enzyme.

3.3. Introduction

The flavoenzyme choline oxidase (E.C.1.1.3.17; choline-oxygen 1-oxidoreductase) catalyzes the two-step oxidation of choline to glycine betaine with the formation of an aldehyde as reaction intermediate (Scheme 3.1). The study of the biophysical and mechanistic properties of choline oxidase is interesting for medical and biotechnological applications because accumulation of the biocompatible solute glycine betaine in many pathogens and plants enables their stress resistance toward hyperosmotic environments (*1, 2*). Mechanistic studies on choline oxidase have been carried out by using pH, kinetic isotope, and temperature effects (*3-7*), as well as site-directed mutagenesis on a number of active site residues (*8-12*), mainly to address the mechanism of alcohol oxidation. Catalysis is initiated with the deprotonation of the hydroxyl group of choline to yield a zwitterionic alkoxide species, which is stabilized in the enzyme active site through electrostatic and hydrogen bonding interactions with the charged side chains of His351, His466, and Glu312 (*9-12*). A hydride ion subsequently transfers from the alkoxide α-carbon of the activated substrate to the flavin N(5) atom (*4*). After the reduced flavin reacts with oxygen to yield hydrogen peroxide and regenerate oxidized flavin, the enzyme undergoes a

second oxidation step that involves the hydrated form of the aldehyde to generate glycine betaine and hydrogen peroxide (*13*).

Choline oxidase has been grouped in the glucose-methanol-choline (GMC) oxidoreductase enzyme superfamily (*14, 15*), which comprises choline dehydrogenase (*16*), cellobiose dehydrogenase (*17*), glucose oxidase (*18*), pyranose 2-oxidase (*19, 20*), methanol oxidase and cholesterol oxidase (*21*). The active sites of representative enzymes within the superfamily reveal the presence of a conserved His-Asn pair, except for glucose oxidase where the asparagine residue is replaced with histidine (*20*). Site-directed mutagenesis studies on the role of the conserved asparagine residues are limited to cholesterol oxidase and cellobiose dehydrogenase. In cholesterol oxidase, Asn485 has been shown to hydrogen bond to the flavin π-system, thereby modulating the electrostatic potential of the flavin to enhance the oxidation reaction (*22*). In cellobiose dehydrogenase, Asn732 has been implicated in substrate binding (*23*). In choline oxidase, the side chain of Asn510 interacts with the imidazole side chains of His351 (3.0 Å) and His466 (4.0 Å), and it is 4.7 Å from both the flavin O(2) and N(3) atoms (Figure 3.1). In a recent study, His351 was shown to participate in substrate binding and in the hydride ion transfer reaction, as suggested by the effect on the K_d and k_{red} values with choline as substrate for the mutant enzyme containing alanine at position 351 (*12*). Site-directed mutagenesis studies allowed the authors to propose multiple roles for His466 in modulating the electrophilicity of the flavin and the polarity of the active site, and contributing to the stabilization of the transient alkoxide species that is formed in the oxidation of choline (*9*).

In this study, we assess the mechanistic role of Asn510 in choline oxidase using site-directed mutagenesis, biochemical, steady state and rapid kinetics techniques. Four mutant variants where Asn510 is replaced with alanine, leucine, aspartate, and histidine were prepared

using site-directed mutagenesis and the resulting proteins were purified to high levels and investigated in their biochemical and mechanistic properties. The results of the spectroscopic and mechanistic investigations presented here establish the importance of Asn510 in both the reductive and oxidative half-reactions catalyzed by choline oxidase. Interestingly, the relative timing of cleavages of the substrate OH and CH bonds in the mutant enzymes differed among mutated enzymes, depending upon which substitution is used to replace Asn510.

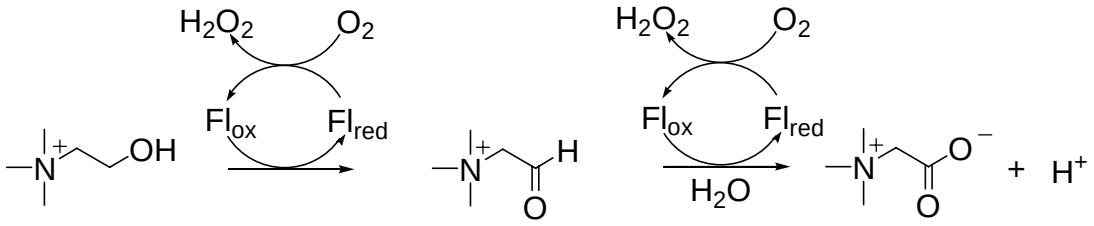

Scheme 3.1. Reaction Catalyzed by Choline Oxidase.

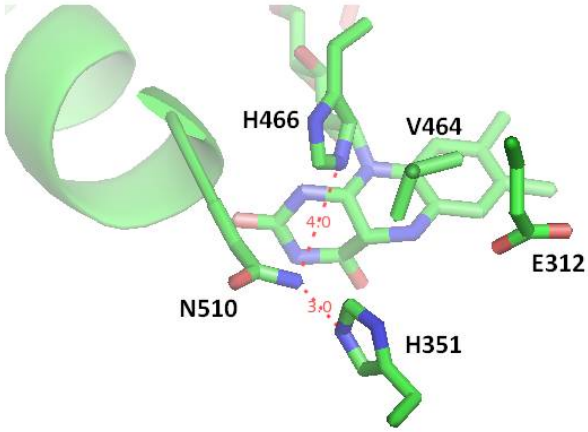

Figure 3.1. The active site of wild-type choline oxidase with selected amino acids at a resolution of 1.86 Å (PDB 2jbv). Dashed, red lines represent interactions of the side chain of Asn510 with the side chains of His351 and His466.

3.4. Experimental procedures

Materials. *Escherichia coli* strain Rosetta(DE3)pLysS was from Novagen (Madison, WI). DNase was from Roche. The QuikChange site-directed mutagenesis kit was from Stratagene (La Jolla, CA). The QIAprep Spin Miniprep kit was from Qiagen (Valencia, CA). Oligonucleotides used for sequencing of the mutant gene were custom synthesized by Sigma Genosys (Woodland, TX). Bovine serum albumin, chloramphenicol, tetracycline, DMSO, isopropyl-β-D-thiogalactopyranoside (IPTG), phenylmethylsulfonyl fluoride (PMSF), lysozyme, sodium hydrosulfite, betaine aldehyde, glycine betaine, Luria-Bertani agar and broth were from Sigma (St. Louis, MO). EDTA was from Fisher. Choline chloride and ampicillin were from ICN

Pharmaceutical Inc. 1,2-[$^2H_4$]-Choline bromide (98%) and sodium deuterioxide (99%) were from Isotec Inc. (Miamisburg, OH). All other reagents were of the highest purity commercially available.

Site-Directed Mutagenesis. Mutant genes for the choline oxidase variants Asn510Ala, Asn510Asp, Asn510His and Asn510Leu were prepared using the pET/codAmg1 plasmid for the wild-type enzyme as a template (*24*) and forward and reverse oligonucleotides as primers for site-directed mutagenesis. A QuikChange kit was used to prepare the mutant enzymes and the experiment was performed by following the manufacturer's instructions in the presence of 2% DMSO. The resulting mutant genes were sequenced at the DNA core Facility at Georgia State University using an Applied Biosystems Big Dye Kit on an Applied Biosystems model ABI 377 DNA sequencer. Sequencing confirmed the presence of the mutant genes in the correct orientation.

Expression and Purification of Choline Oxidase Variants. Permanent stocks of *E. coli* Rosetta(DE3)pLysS cells harboring plasmids pET/*codA*mg1-Asn510Ala, -Asn510Asp, -Asn510His or -Asn510Leu were used to inoculate 4.5 L of Luria-Bertani broth medium containing 50 μg/mL ampicillin and 34 μg/mL chloramphenicol. The liquid cultures were grown for 4 to 6 h at 37 °C, before inducing protein expression with 0.1 mM IPTG for 20 h at 20 °C. The variant enzymes were expressed and purified to homogeneity using the same procedure described previously for the purification of the wild-type enzyme (*24*).

Spectrophotometric Studies. The extinction coefficients of the mutant enzymes were determined in Tris-Cl, pH 8.0, after denaturation of the enzymes by treatment with 4 M urea at 40 °C for 30 min, based upon the ε_{450} value of 11.3 $mM^{-1}cm^{-1}$ for free FAD (*25*). To determine the amount of covalently bound flavin, the purified enzymes were incubated on ice for 30 min

after the addition of 10% trichloroacetic acid, followed by removal of precipitated protein by centrifugation. The UV-visible absorbance spectra of the supernatants were recorded again to check the presence of unbound FAD. All UV-visible absorbance spectra were recorded using an Agilent Technologies diode-array model HP 8453 spectrophotometer.

Steady State Kinetics. The enzymatic activity of choline oxidase mutants was measured by the method of initial rates as described for the wild-type enzyme (*7, 24*) using a computer-interfaced Oxy-32 oxygen-monitoring system (Hansatech Instrument Ltd.). The steady state kinetic parameters of the Asn510Ala and Asn510His enzymes were determined at varying concentrations of choline between 1 to 10 mM and oxygen between 0.05 to 0.75 mM in 50 mM sodium pyrophosphate, pH 10.0 and 25 °C. Each reaction mixture was equilibrated at the desired oxygen concentration by sparging the appropriate O_2/N_2 gas mixture for a minimum of 15 min before the reaction was started with the addition of the enzyme.

Reductive Half-reactions. Reductive half-reactions were carried out by using a Hi-Tech SF-61 stopped-flow spectrophotometer thermostated at 25 °C, pH or pD 10.0. The rate of flavin reduction was measured by monitoring the decrease in absorbance at 454 nm that results from the anaerobic mixing of choline oxidase with choline or betaine aldehyde, as previously described for the wild-type enzyme (*3*). Glucose (5 mM) and glucose oxidase (0.5 μM) were added to the substrate and enzyme solutions to scavenge possible trace amounts of oxygen. The mutant enzymes Asn510Ala and Asn510His were mixed anaerobically with an equal volume of substrate, obtaining reaction mixtures with 20 μM enzyme and 0.5-25 mM choline or 1,2-[$^2H_4$]-choline or 20 μM enzyme and 0.1-5 mM betaine aldehyde. For the determination of solvent isotope effects, buffers were prepared using 99.9% deuterium oxide by adjusting the pD value with NaOD. The pD values were determined by adding 0.4 to the pH electrode readings (*26*). For

each concentration of the substrates, the rate constants for flavin reduction were recorded in triplicate, with measurements usually differing by ≤5 %. Solvent viscosity effects were measured in the presence of 0.0211 g/mL PEG-6000 as viscosigen, in both the tonometer containing the enzyme and the syringes containing the organic substrates. The resulting relative viscosity at 25 °C was 1.26 which is slightly above the value of 1.23 representing a 100% solution of D_2O (*27, 28*).

Data Analysis. Kinetic data were fit with the KaleidaGraph (Synergy Software, Reading, PA) and the Enzfitter (Biosoft, Cambridge, U.K.) softwares. The steady state kinetic parameters at varying concentrations of both choline and oxygen were determined by fitting the initial rates to eq 1, which describes a steady state kinetic mechanism with formation of a ternary complex. Here, K_a and K_b are the Michaelis constants for choline (*A*) and oxygen (*B*), respectively, and k_{cat} is the turnover number of the enzyme (*e*) at saturating concentrations of both substrates. For kinetic isotope effects with choline as substrate, data obtained were divided into two sets, one with unlabeled substrate or solvent and one with isotopically labeled substrate or solvent and kinetic isotope effects were determined by taking the ratio of the kinetic parameters obtained with normal substrate or solvent to that obtained with labeled substrate or solvent. Stopped-flow traces were fit to eq 2, which describes a single exponential process where k_{obs} is the observed first-order rate constant for flavin reduction, *A* is the value of absorbance at the specific wavelength of interest at time *t*, *B* is the amplitude of the absorbance change, and *C* is an offset value that accounts for the non-zero absorbance value at infinite time. Kinetic parameters for the reductive half-reactions were determined by using eq 3, where k_{obs} is the observed first-order rate constant for the reduction of the enzyme-bound flavin at any given concentration of substrate, k_{red} is the limiting first-order rate constant for flavin reduction at

saturated substrate concentration, and K_d is the macroscopic dissociation constant for binding of the substrate to the enzyme.

$$\frac{v}{e} = \frac{k_{cat} AB}{K_a B + K_b A + AB + K_{ia} K_b} \quad (1)$$

$$A = B \exp(-k_{obs} t) + C \quad (2)$$

$$k_{obs} = \frac{k_{red} A}{K_d + A} \quad (3)$$

3.5. Results

Expression and Purification of Asn510 Variants of Choline Oxidase. The mutant proteins containing alanine, aspartate, histidine or leucine at position 510 were expressed and purified at pH 8.0 to high levels as judged by SDS-PAGE using the same protocol that was devised for the wild-type enzyme (*24*). Glycerol (10%) was present in all the buffered solutions throughout the purification process to increase the stability of the enzymes (*29*). With the exception of the Asn510His enzyme, which stabilized aerobically the anionic form of the flavin semiquinone as previously reported for the wild-type enzyme (*7*), the Asn510Ala, Asn510Asp, and Asn510Leu enzymes were in the oxidized state throughout the purification process at pH 8.0.

The Asn510Asp enzyme showed no oxygen consumption at concentrations as high as 20 μM and up to 0.6 M choline at pH 7.0 and 25 ^{o}C [for comparison the wild-type enzyme typically shows maximal velocities in the ~90 nmol O_2 $mL^{-1}min^{-1}$ when assayed at a concentration of 0.1 μM]. The apparent steady state kinetic parameters for all of the other mutant enzymes were determined with choline at atmospheric oxygen concentration, yielding apparent turnover numbers ($^{app}k_{cat}$) at least 25-fold lower than the wild-type enzyme and $^{app}K_{choline}$ values that were at least 100-fold higher than the wild-type enzyme (Table 3.1). Thus, Asn510 is an important residue for catalysis in the active site of choline oxidase.

Flavin Content. The UV-visible absorbance spectra of the Asn510 mutant enzymes as purified had maxima in the 360 nm and 450 nm regions[1], as expected for flavoproteins with the flavin in the oxidized state (Figure 3.2). The Asn510Asp enzyme showed the most dramatic changes with a hypsochromic shift of 6 nm of the low energy band of the flavin and a 22 nm bathochromic shift of the high energy band of the flavin with respect to the wild-type enzyme

(Figure 3.2). The Asn510Asp enzyme also had 75% of the total flavin non-covalently associated with the protein, as established through acid denaturation with 10% trichloroacetic acid followed by centrifugation to remove denatured protein. In contrast, the Asn510His, Asn510Ala, and Asn510Leu enzymes showed small bathochromic shifts (≤4 nm) of the low energy flavin band and small hypsochromic shifts (≤8 nm) of the high energy flavin band (Figure 3.2). These mutant enzymes had the flavin covalently linked to the protein, as for the case of the wild-type enzyme (*7, 24*). With all the mutant enzymes, a flavin to protein ratio between 0.16 and 0.26 was determined, which was significantly lower than the value of 0.90 determined for the wild-type enzyme (Table 3.2). Collectively, these results suggest that substitution of Asn510 with other amino acids results in low incorporation of the flavin in the protein, an altered protein microenvironment around the flavin and, for the case of the Asp510 enzyme, impairment of protein flavinylation.

Kinetic Properties. A detailed kinetic characterization was carried out for the Asn510His and Asn510Ala enzymes by using steady state and rapid kinetics approaches, but not for the Asn510Leu and Asn510Asp enzymes for which enzymatic activity was too low to obtain meaningful data. The steady state kinetic parameters were determined by monitoring the initial rates of oxygen consumption at varying concentrations of both choline and oxygen at pH 10.0 and 25 ^{o}C. The choice of pH 10.0 was dictated by previous investigations on the wild-type and various mutant forms showing that the k_{cat} and the $k_{cat}/K_{choline}$ values of choline oxidase are pH-independent at high pH (*3, 4, 6, 7, 9, 11-13*). With both the Asn510His and Asn510Ala enzymes, the best fit of the data was observed with a sequential steady state kinetic mechanism as seen also in the wild-type enzyme (*3, 5, 6*). The most notable changes in the kinetic parameters with respect to the wild-type enzyme were seen in the Asn510Ala enzyme, with decreases of 4,300-

fold in the $k_{cat}/K_{choline,}$ 660-fold in the k_{cat}, and 50-fold in the k_{cat}/K_{oxygen} values (Table 3.3). For comparison, the Asn510His enzyme showed smaller decreases of 30-fold in the $k_{cat}/K_{choline,}$ and ~15-fold in both the k_{cat} and k_{cat}/K_{oxygen} values (Table 3.3). These data suggest that replacing Asn510 with alanine or histidine negatively affects both the reductive and oxidative half-reactions catalyzed by choline oxidase.

The reductive half-reactions of the Asn510His and Asn510Ala enzymes were also investigated in a stopped-flow spectrophotometer by mixing anaerobically the enzyme with choline or betaine aldehyde at pH 10.0 and 25 ^{o}C. The time-resolved changes in the absorbance at ~455 nm were best fit to a single exponential process, as illustrated in the example of Figure 3.3. Full reduction to the anionic hydroquinone species of the flavin was observed (Figure 3.3). The observed rate constants for flavin reduction showed hyperbolic dependence on the concentration of choline or betaine aldehyde, allowing the determination of the limiting rate constants for flavin reduction (k_{red}) and the equilibrium constants for substrate binding (K_d). As illustrated in Table 3, significant decreases in the k_{red} values with respect to the wild-type enzyme were seen in both enzymes with both substrates. The K_d value for choline and betaine aldehyde were ≤13-fold larger than the value of wild-type choline oxidase, consistent with replacement of Asn510 with alanine or histidine having only a minor effect on substrate binding.

Kinetic Isotope Effects. The relative timing for the cleavage of the OH and CH bonds of choline in the reactions catalyzed by the Asn510His and Asn510Ala enzymes was investigated with substrate, solvent and multiple kinetic isotope effects on the reductive half-reaction in a stopped-flow spectrophotometer at pL 10.0 and 25 ^{o}C. Substitution of choline with 1,2-[$^{2}H_4$]-choline yielded $^{D}k_{red}$ values >4 with both the Asn510His and Asn510Ala enzymes (Table 3.4), indicating that the cleavage of the CH bond of choline is at least partially rate-limiting in the

reductive half-reaction. Substitution of water with deuterium oxide resulted in $^{D2O}k_{red}$ values >1.3 with both enzymes (Table 3.4), suggesting that the cleavage of the OH bond of choline is also at least partially rate-limiting in the reductive half-reaction. These data are significantly different from those with the wild-type form of choline oxidase, for which the $^{D}k_{red}$ values are large and the $^{D2O}k_{red}$ values are unity (*3*).

With the Asn510His enzyme, a significant decrease in the magnitude of the substrate kinetic isotope effect was observed upon substituting water with deuterium oxide (cfr: $^{D}(k_{red})_{D2O}$ and $^{D}k_{red}$ values in Table 4). Analogously, the magnitude of the solvent kinetic isotope effect also decreased when 1,2-[$^{2}H_4$]-choline was used instead of choline (cfr: $^{D2O}(k_{red})_{D}$ and $^{D2O}k_{red}$ values in Table 4). Finally, multiple kinetic isotope effects were smaller than the product of the individual substrate and solvent kinetic isotope effects (cfr: $^{D,D2O}k_{red}$ and the product of the $^{D}k_{red}$ and $^{D2O}k_{red}$ values in Table 3.4).

With the Asn510Ala enzyme, the substrate kinetic isotope effect increased upon substituting water with deuterium oxide (cfr $^{D}(k_{red})_{D2O}$ and $^{D}k_{red}$ values in Table 4), as did the solvent kinetic isotope effect when 1,2-[$^{2}H_4$]-choline was used instead of choline (cfr: $^{D2O}(k_{red})_{D}$ and $^{D2O}k_{red}$ values in Table 3.4). Furthermore, the $^{D,D2O}k_{red}$ value was slightly larger than the product of the $^{D}k_{red}$ and $^{D2O}k_{red}$ values.

To establish whether the observed solvent kinetic isotope effects originated from the cleavage of the OH bond of choline rather than being due to an increased viscosity of D_2O with respect to H_2O, the effects of solvent viscosity on the reductive half-reactions of the Asn510His and Asn510Ala enzymes were investigated. The experiment was performed at pH 10.0 and 25 °C in solutions containing 0.0211 g/mL PEG-6000, which provides a relative solvent viscosity equivalent to a 100% solution of D_2O. In both enzymes, similar k_{red} values were observed in the

presence and absence viscosigen (i.e., 4.3 ± 0.2 s^{-1} versus 4.4 ± 0.2 s^{-1} in the Asn510His enzyme, and 0.13 ± 0.01 s^{-1} versus 0.13 ± 0.01 s^{-1} in the Asn510Ala enzyme). Similarly, the K_d values were not affected by the increased relative viscosity of the solvent (data not shown). These data indicate that the solvent kinetic isotope effects determined in D_2O were directly associated with the cleavage of the substrate OH bond in the reaction catalyzed by Asn510His and Asn510Ala enzymes.

Table 3.1. Apparent Steady State Kinetic Parameters for Choline Oxidase Variants Substituted at Asn510[a]

	wild-type[b]	Asn510His	Asn510Ala	Asn510Leu	Asn510Asp
$^{app}k_{cat}$, s^{-1}	13.4 ± 0.5	0.51 ± 0.01	0.06 ± 0.01	0.02 ± 0.01	nd[c]
$^{app}K_{choline}$, mM	0.6 ± 0.1	60 ± 4	155 ± 34	213 ± 22	nd
$^{app}(k_{cat}/K_{choline})$, $M^{-1}s^{-1}$	22000 ± 3760	8.5 ± 0.6	0.4 ± 0.1	0.09 ± 0.01	nd

[a] Initial rates determined as oxygen consumption with choline as substrate at fixed atmospheric [oxygen] in 50 mM potassium phosphate, pH 7.0 and 25 °C. [b] From ref (*11*). [c] Not determined.

Table 3.2. Comparison of the Spectral Parameters for Choline Oxidase Variants Substituted at Asn510 at pH 8.0

	wild-type[a]	Asn510His	Asn510Ala	Asn510Leu	Asn510Asp
UV-visible absorbance (λ_{max}, nm)	366, 452	360, 456	358, 454	364, 455	384, 446
ε (mM^{-1} cm^{-1})	9.8, 11.4	11.1, 11.8	10.6, 13.0	11.5, 12.1	10.5, 12.4
stoichiometry (no. of FAD/protein)	0.9 ± 0.1	0.16 ± 0.01	0.26 ± 0.01	0.22 ± 0.01	0.18 ± 0.01
% of FAD non-covalently bound	0	0	0	0	75

[a] From ref (*7*).

Table 3.3. Comparison of the Kinetic Parameters of the Asn510Ala and Asn510His Enzymes with Wild-type Choline Oxidase [a]

	kinetic parameter	wild-type [b]	Asn510His	Asn510Ala
choline	k_{cat}, s^{-1}	60 ± 1	3.4 ± 0.2	0.090 ± 0.003
	$K_{choline}$, mM	0.25 ± 0.01	0.48 ± 0.08	1.7 ± 0.2
	K_{oxygen}, μM	690 ± 30	535 ± 60	55 ± 12
	$k_{cat}/K_{choline}$, $M^{-1}s^{-1}$	237000 ± 9000	7100 ± 1250	55 ± 6
	k_{cat}/ K_{oxygen}, $M^{-1}s^{-1}$	86400 ± 3600	6360 ± 805	1700 ± 370
	K_{ia}, mM	0.14 ± 0.01	0.23 ± 0.06	3.45 ± 1.37
	k_{red}, s^{-1}	93 ± 1	4.3 ± 0.2	0.13 ± 0.01
	K_d, mM	0.29 ± 0.01	1.2 ± 0.2	0.95 ± 0.06
betaine aldehyde	k_{red}, s^{-1}	135 ± 4	17.0 ± 0.6	0.88 ± 0.01
	K_d, mM	0.45 ± 0.03	1.0 ± 0.1	5.9 ± 0.2

[a] Steady state parameters were measured at varying concentrations of both choline and oxygen in 50 mM sodium pyrophosphate, pH 10, at 25 °C. [b] From ref (*3*).

Table 3.4. Substrate and Solvent Kinetic Isotope Effects with Choline as Substrate[a]

Parameter	wild-type[b]	Asn510His	Asn510Ala
$^{D}k_{red}$	8.9 ± 0.2	4.2 ± 0.1	5.5 ± 1.2
$^{D}(k_{red})_{D2O}$	8.7 ± 0.2	1.9 ± 0.1	7.2 ± 0.4
$^{D2O}k_{red}$	0.99 ± 0.02	2.6 ± 0.1	1.28 ± 0.04
$^{D2O}(k_{red})_{D}$	0.94 ± 0.03	1.23 ± 0.04	1.7 ± 0.4
$^{D,D2O}k_{red}$	8.4 ± 0.2	5.2 ± 0.2	9.2 ± 0.6

[a] Conditions: 50 mM sodium pyrophosphate, pH or pD 10, at 25 °C. [b] From ref. (*3*).

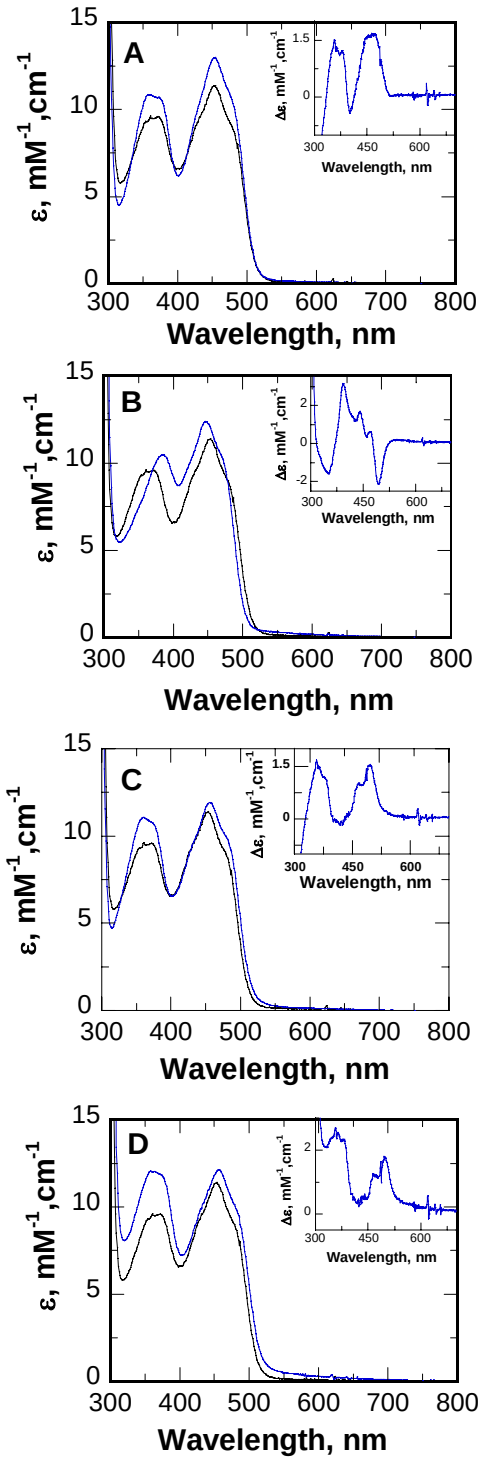

Figure 3.2. Comparison of the UV-visible absorbance spectra of the oxidized wild-type (black curve) and Asn510 mutants (blue curves) in 20 mM Tris-Cl pH 8.0. (A) Asn510Ala, (B) Asn510Asp, (C) Asn510His, and (D) Asn510Leu enzymes. The insets show the difference absorbance spectra of the Asn510 mutant enzymes minus the wild-type enzyme.

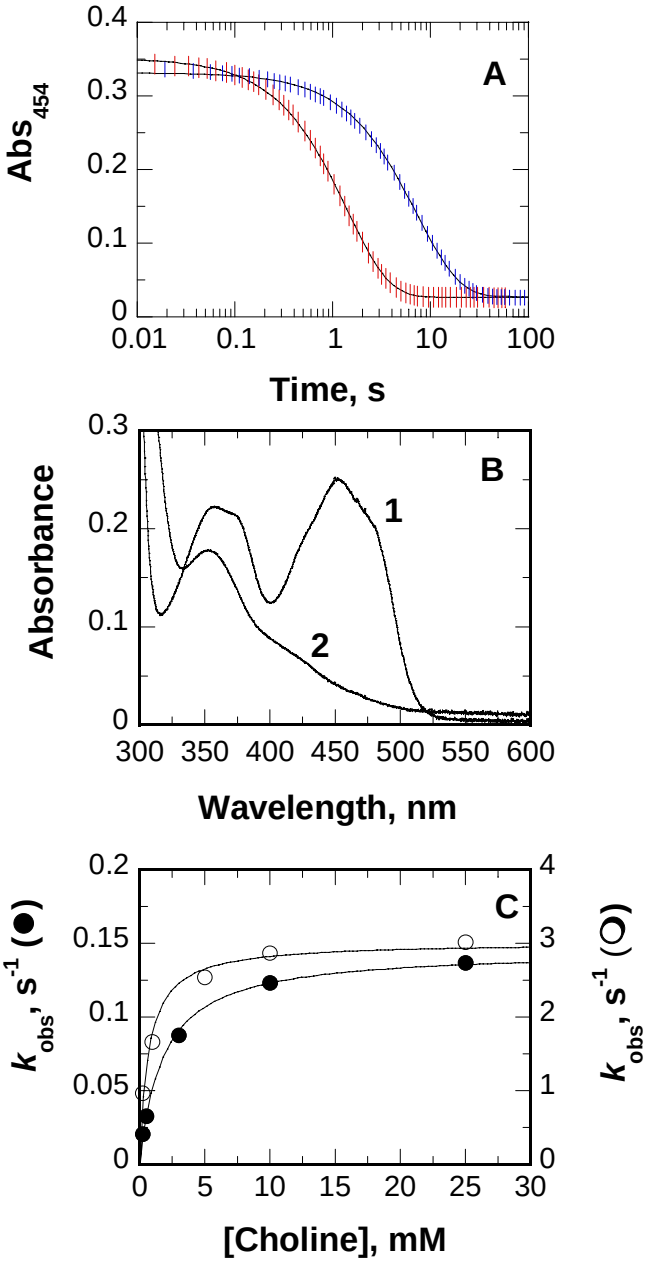

Figure 3.3. Anaerobic substrate reductions of the Asn510Ala and Asn510His enzymes with choline as substrate. (A) Stopped-flow traces obtained upon mixing anaerobically the Asn510Ala (blue) and Asn510His (red) enzymes with 25 mM choline in 50 mM sodium pyrophosphate buffer, pH 10.0, at 25 °C. The curves represent the fit of the data with eq 2. Time indicated is after the end of flow, i.e., 2.2 ms, and one experimental point in every 10 is shown (vertical lines). (B) UV-visible absorbance spectra of the oxidized (curve 1) and reduced (curve 2) species of the Asn510Ala enzyme after mixing anaerobically the oxidized enzyme with buffer and 25 mM choline in 50 mM sodium pyrophosphate buffer, pH 10.0, at 25 °C. (C) The observed rate constants of anaerobic flavin reduction (k_{obs}) of the Asn510Ala (●) and Asn510His (○) enzymes as a function of the concentrations of choline. Data were fit to eq 3.

3.6. Discussion

The variants of choline oxidase in which the conserved residue Asn510 was replaced with alanine, aspartate, histidine or leucine were prepared in this study to investigate the role of this residue in enzyme catalysis. The mutant enzymes maintained a number of biophysical and kinetic properties that are in common with the wild-type form of choline oxidase. The Asn510Ala, Asn510His and Asn510Leu enzymes contained FAD covalently linked to the protein moiety, as does the wild-type enzyme. The Asn510Ala and Asn510His enzymes displayed a sequential steady state kinetic mechanism as does the wild-type enzyme, and had K_m and K_d values for choline that differed by less than 7-times from the values of the wild-type enzyme. Moreover, large substrate kinetic isotope effects with values ≥4 were determined in the reductive half-reactions of the Asn510Ala, Asn510His, and wild-type enzymes. Finally, the small perturbations of the UV-visible absorbance spectra of all of the four mutant enzymes from the features observed in the wild-type enzyme can be rationalized with the effects that a substituted protein microenvironment have on the spectroscopic properties of the enzyme-bound flavin (*see below*), further suggesting that the enzymes maintain an overall fold that is similar to that of the wild-type enzyme. These observations allowed conclusions on the role of Asn510 in the reaction catalyzed by choline oxidase to be drawn from the comparison of the biophysical, kinetic, and mechanistic properties of the enzyme variants containing amino acids other than asparagine at position 510 with those of the wild-type enzyme.

The active site residue Asn510 is important for the oxidation of both choline and the reduced flavin, but plays a minor role in the binding of the alcohol substrate. Evidence supporting this conclusion comes from the comparison of the steady state and rapid reaction kinetic data of the Asn510His and Asn510Ala enzymes with the wild-type form of choline

oxidase. Both the bimolecular rate constant for the reductive half-reactions ($k_{cat}/K_{choline}$) and the limiting rate constant for anaerobic flavin reduction (k_{red}) were decreased by >600-fold and >30-fold upon replacing Asn510 with alanine and histidine. The second-order rate constant for oxygen capture on the enzyme (k_{cat}/K_{oxygen}) decreased 15-fold in the Asn510His enzyme and 50-fold in the Asn510Ala enzyme. Finally, the equilibrium constant for substrate binding (K_d) increased by ≤6-fold when the mutant enzymes were compared to wild-type choline oxidase. Small increases in the K_m values were reported for mutant variants of another member of the glucose-methanol-choline oxidoreductase superfamily, cellobiose dehydrogenase, where Asn732 was replaced with alanine (no changes), histidine or glutamine (2.5-fold), aspartate (10-fold) and glutamate (14-fold). In that case the authors concluded that the main role of Asn732 is in the binding of the substrate (*23*).

The overall turnover in the Asn510 variants with choline as substrate is limited primarily by the chemical step of hydride transfer from the alcohol substrate to enzyme-bound flavin, with contribution of the second hydride transfer involving the aldehyde intermediate and the flavin. This conclusion is supported by steady state and rapid kinetic data and the use of eq 4, where $k_{red(CH)}$ and $k_{red(BA)}$ represent the limiting rate constants for the hydride transfer reactions between choline and betaine aldehyde and the enzyme-bound flavin. The k_{cat} values calculated by using eq 4 were 0.1 s^{-1} and 3.4 s^{-1} for the Asn510Ala and Asn510His enzymes, in excellent agreement with the experimentally measured k_{cat} values of 0.09 s^{-1} and 3.4 s^{-1} with choline as substrate. The overall turnover being limited by both hydride transfer reactions implies that choline is oxidized to glycine betaine in the reaction catalyzed by the Asn510 mutant enzymes, as for the case previously reported for the wild-type enzyme (*3*).

$$k_{cat} = \frac{k_{red(CH)}\ k_{red(BA)}}{k_{red(CH)} + k_{red(BA)}} \qquad (4)$$

In the reductive half-reaction, replacement of Asn510 with histidine or alanine decreases the rate of cleavage of the substrate OH bond catalyzed by choline oxidase. This conclusion is supported by the solvent kinetic isotope effects on the limiting rate constant for anaerobic flavin reduction at saturating concentration of choline, $^{D2O}k_{red}$, being significantly larger than unity, with values of 2.6 and 1.3 in the Asn510His and Asn510Ala enzymes. This is not the case for the wild-type form of choline oxidase, for which it was shown that the cleavage of the substrate OH bond is significantly faster than the subsequent cleavage of the CH bond, as indicated by a $^{D2O}(k_{red})$ value of 0.99 (*3*). Slower rates of hydroxyl proton abstraction with respect to the wild-type enzyme were recently reported for other variants of choline oxidase where Val464 is replaced with threonine or alanine, where the $^{D2O}k_{red}$ values were >4 (*8*). Interestingly, the side chains of Val464 and Asn510 are both in spatial proximity of His466 (i.e., ≤4 Å), a residue that in choline oxidase has been implicated in the electrostatic stabilization of the transient alkoxide species that originates from the cleavage of the substrate OH bond (*9*). Thus, it is likely that the much slower rate of hydroxyl proton abstraction in these mutant enzymes is due to a non-optimal orientation of the side chain of His466 with respect to either the base that abstracts the substrate proton, the alcohol substrate, or both. In support of a disrupted preorganization in the enzyme-substrate complexes of the mutant enzymes is the observation of a substrate kinetic isotope effect that is significantly lower than the value of 9 that is seen in the wild-type enzyme (*3*).

The relative timing for cleavages of the substrate OH and CH bonds is affected upon replacing Asn510 with alanine, but not when Asn510 is substituted with histidine (Scheme 3.2). Evidence for this conclusion comes from the comparison of the multiple kinetic isotope effects determined on the limiting rate constants for flavin reduction at saturating concentrations of

choline for the Asn510Ala, Asn510His and wild-type enzymes. With the Asn510Ala enzyme, both the substrate and solvent kinetic isotope effects increased upon slowing down the cleavage of the other bond by replacing water with D_2O and choline with 1,2-[$^2H_4$]-choline, respectively. This immediately rules out a stepwise mechanism for cleavage of the substrate OH and CH bonds, in which upon slowing down the cleavage of the other bond a decrease in the magnitudes of the substrate and solvent kinetic isotope effects is expected (*30*). Consistent with a concerted mechanism for the cleavages of the OH and CH bonds, the multiple kinetic isotope effects, with a $^{D,D2O}k_{red}$ value of ~9, were not smaller than the product of the individual substrate and solvent kinetic isotope effects, with a value of ~7 (i.e., $^{D}k_{red}$ x $^{D2O}k_{red}$) (*30*). In contrast, the Asn510His enzyme catalyzed the cleavage of the substrate OH and CH bonds with a stepwise mechanism, as indicated by the decreases in the substrate and solvent kinetic isotope effects upon slowing down the cleavage of the other bond per effect of deuteration and the $^{D,D2O}k_{red}$ value of ~5 being smaller than the product of the individual substrate and solvent kinetic isotope effects, with a value of ~11 (i.e., $^{D}k_{red}$ x $^{D2O}k_{red}$) (*30*). Finally, previous studies using kinetic isotope effects established a stepwise mechanism for the cleavages of the OH and CH bonds in the wild-type enzyme (*3*). The change in the timing for the cleavages of the OH and CH bonds of choline catalyzed by the Asn510Ala enzyme probably stems from the mutated enzyme having likely lost the capability of the wild-type and the Asn510His enzymes to form a hydrogen bond interaction between the side chain at position 510 and a reaction intermediate or a transition state or, alternatively, a neighboring residue such as His466 that directly interacts with a reaction intermediate and transition state (*9*).

The effect of the mutation of Asn510 on the reactivity of the reduced flavin with oxygen in choline oxidase is difficult to rationalize with the data at hand. In choline oxidase, activation

of oxygen for reaction with the flavin is exerted by the positive charge harbored on the quaternary ammonium group of choline rather than by side chains of histidine and lysine residues like in the case of glucose oxidase and monomeric sarcosine oxidase (*31-37*). In this respect, mutation of either His351 or His466 with alanine does not affect the oxidative half-reaction in choline oxidase, as suggested by lack of effects on the k_{cat}/K_{oxygen} values (*9, 12*). This suggests that the low reactivity of the flavin with oxygen in the mutant enzymes is likely not mediated by the residues neighboring Asn510. An interesting alternative is that the mutation of Asn510 to histidine or alanine may alter the pattern of hydrogen bonds between the protein microenvironment and the flavin, since the side chain of Asn510 is less than 5 Å from the flavin O(2) and N(3) atoms of the isoalloxazine ring. In this respect, replacement of the analogous Asn485 in cholesterol oxidase with leucine has been associated with the loss of a hydrogen bond involving the π-system of the flavin (*22*). Current efforts are aimed at the elucidation of the three-dimensional structures of the Asn510 mutant enzymes by using X-ray crystallography.

Asn510 is important for the flavinylation reaction in which FAD is covalently attached to the protein moiety in choline oxidase. Evidence in support of this conclusion comes from the stoichiometry of FAD to protein in the Asn510 mutant enzymes that is 5-fold lower than that of the wild-type enzyme, where a 1:1 stoichiometry was established (*7, 24*). Furthermore, upon introducing by mutation a negative charge on residue 510 (i.e., Asn→Asp mutant enzyme), ~75% of the flavin that is bound to the protein has a non-covalent association. Since Asn510 sits less than 5 Å from the flavin N(1)-C(2) atoms, a ready explanation is that in the Asn510His, Asn510Ala and Asn510Leu enzymes there is a decreased stabilization of the negative charge that is required on the flavin N(1)-C(2) atoms for the formation of the covalent attachment to the protein (*38*). In agreement with this conclusion is the observation that the anionic

flavosemiquinone is not observed during the purification of the Asn510Asp, Asn510Ala, and Asn510Leu enzymes, in contrast to what occurs in the wild-type enzyme (*7, 24*). In the Asn510Asp enzyme, where the side chain of the residue is negatively charged, such a lack of stabilization of the negative charge on the flavin is even more dramatic, to the extent that the reaction of covalent attachment of the flavin to the protein is also impaired. Lack of stabilization of the negative charge on the reduced flavin is also consistent with the Asn510Asp enzyme being devoid of enzymatic activity with choline, since the enzyme would not be able to stabilize the anionic hydroquinone during turnover with choline. Previously, we have shown that in choline oxidase the replacement of His466 with aspartate also results in an enzyme that is unable to consume oxygen in the presence of choline, has a low stoichiometry of FAD:protein, and has ~75% of the enzyme-bound flavin being non-covalently linked to the protein (*10*). Collectively, the results strongly support the importance of the protein microenvironment in proximity of the flavin N(1)-C(2) atoms as being important for the flavinylation of the protein in choline oxidase.

In conclusion, the results of the biochemical and mechanistic investigation of active site mutant enzymes where the conserved residue Asn510 is substituted by site-directed mutagenesis with alanine, histidine, leucine or aspartate are consistent with Asn510 being important for both choline and FAD oxidations. Substitution of Asn510 with alanine or histidine yields enzymes with a significant decrease in the rate of hydroxyl proton abstraction with respect to wild-type choline oxidase. Moreover, the Asn510Ala enzyme lost the ability of the wild-type or the Asn510His enzymes to stabilize the alkoxide intermediate that is formed in the oxidation of choline, displaying a concerted mechanism for the cleavages of the OH and CH bonds of choline. Minimal changes in the K_d values for choline in the Asn510Ala and Asn510His enzymes suggest no direct involvement of Asn510 in substrate binding. Finally, all of the

mutations introduced at residue 510 resulted in enzymes with much lower levels of FAD incorporation, with most of the flavin being associated non-covalently upon replacing Asn510 with aspartate. These studies therefore represent an example of how the relative timing for cleavages of multiple bonds in an enzymatic reaction can be modulated depending upon the type of mutation that is introduced at a specific active site position.

Asn510Ala enzyme:

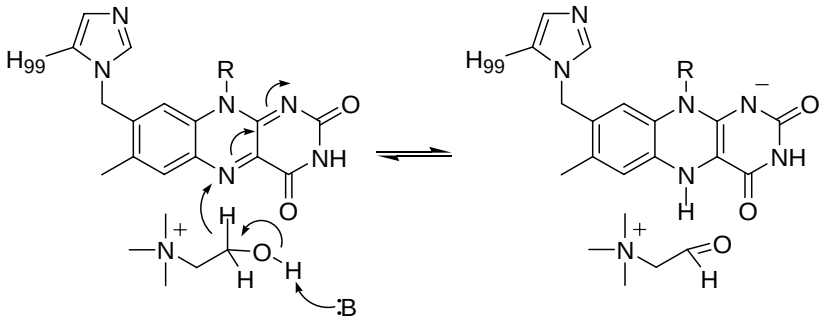

Asn510His enzyme:

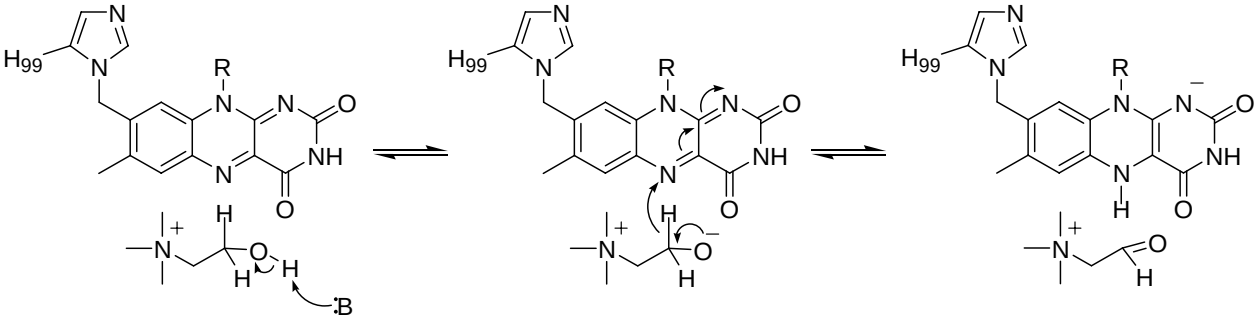

Scheme 3.2. Relative Timing for the Cleavages of the OH and CH bonds of Choline in the reactions Catalyzed by the Ans510His and Asn510Ala Enzymes.

3.7. Acknowledgements

We are very grateful to Ms. Hongling Yuan for her assistance in the solvent viscosity on the reductive half-reaction experiments and the reviewers for their insightful suggestions.

3.8. References

1. Burg, M. B., Kwon, E. D., and Kultz, D. (1997) Regulation of gene expression by hypertonicity, *Annu. Rev. Physiol. 59*, 437-455.
2. McNeil, S. D., Nuccio, M. L., and Hanson, A. D. (1999) Betaines and related osmoprotectants. Targets for metabolic engineering of stress resistance, *Plant Physiol. 120*, 945-950.
3. Fan, F., and Gadda, G. (2005) On the catalytic mechanism of choline oxidase, *J. Am. Chem. Soc. 127*, 2067-2074.
4. Fan, F., and Gadda, G. (2005) Oxygen-and temperature-dependent kinetic isotope effects in choline oxidase: Correlating reversible hydride transfer with environmentally enhanced tunneling, *J. Am. Chem. Soc. 127*, 17954-17961.
5. Gadda, G. (2003) Kinetic mechanism of choline oxidase from *Arthrobacter globiformis*, *Biochim. Biophys. Acta 1646*, 112-118.
6. Gadda, G. (2003) pH and deuterium kinetic isotope effects studies on the oxidation of choline to betaine-aldehyde catalyzed by choline oxidase, *Biochim. Biophys. Acta 1650*, 4-9.
7. Ghanem, M., Fan, F., Francis, K., and Gadda, G. (2003) Spectroscopic and kinetic properties of recombinant choline oxidase from *Arthrobacter globiformis*, *Biochemistry 42*, 15179-15188.

8. Finnegan, S., and Gadda, G. (2008) Substitution of an active site valine uncovers a kinetically slow equilibrium between competent and incompetent forms of choline oxidase, *Biochemistry 47*, 13850-13861.

9. Ghanem, M., and Gadda, G. (2005) On the catalytic role of the conserved active site residue His466 of choline oxidase, *Biochemistry 44*, 893-904.

10. Ghanem, M., and Gadda, G. (2006) Effects of reversing the protein positive charge in the proximity of the flavin N(1) locus of choline oxidase, *Biochemistry 45*, 3437-3447.

11. Quaye, O., Lountos, G. T., Fan, F., Orville, A. M., and Gadda, G. (2008) Role of Glu312 in binding and positioning of the substrate for the hydride transfer reaction in choline oxidase, *Biochemistry 47*, 243-256.

12. Rungsrisuriyachai, K., and Gadda, G. (2008) On the role of histidine 351 in the reaction of alcohol oxidation catalyzed by choline oxidase, *Biochemistry 47*, 6762-6769.

13. Fan, F., Germann, M. W., and Gadda, G. (2006) Mechanistic studies of choline oxidase with betaine aldehyde and its isosteric analogue 3,3-dimethylbutyraldehyde, *Biochemistry 45*, 1979-1986.

14. Ikuta, S., Imamura, S., Misaki, H., and Horiuti, Y. (1977) Purification and characterization of choline oxidase from *Arthrobacter globiformis*, *J. Biochem*. *82*, 1741-1749.

15. Ohishi, N., and Yagi, K. (1979) Covalently bound flavin as prosthetic group of choline oxidase, *Biochem. Biophys. Res. Commun*. *86*, 1084-1088.

16. Tsuge, H., Nakano, Y., Onishi, H., Futamura, Y., and Ohashi, K. (1980) A novel purification and some properties of rat liver mitochondrial choline dehydrogenase, *Biochim. Biophys. Acta 614*, 274-284.

17. Hallberg, B. M., Henriksson, G., Pettersson, G., Vasella, A., and Divne, C. (2003) Mechanism of the reductive half-reaction in cellobiose dehydrogenase, *J. Biol. Chem. 278*, 7160-7166.

18. Gibson, Q. H., Swoboda, B. E., and Massey, V. (1964) Kinetics and Mechanism of Action of Glucose Oxidase, *J. Biol. Chem*. *239*, 3927-3934.

19. Albrecht, M., and Lengauer, T. (2003) Pyranose oxidase identified as a member of the GMC oxidoreductase family, *Bioinformatics 19*, 1216-1220.

20. Hallberg, B. M., Leitner, C., Haltrich, D., and Divne, C. (2004) Crystal structure of the 270 kDa homotetrameric lignin-degrading enzyme pyranose 2-oxidase, *J. Mol. Biol. 341*, 781-796.

21. Kamei, T., Takiguchi, Y., Suzuki, H., Matsuzaki, M., and Nakamura, S. (1978) Purification of 3beta-hydroxysteroid oxidase of *Streptomyces violascens* origin by affinity chromatography on cholesterol, *Chem. Pharm. Bull. (Tokyo) 26*, 2799-2804.

22. Yin, Y., Sampson, N. S., Vrielink, A., and Lario, P. I. (2001) The presence of a hydrogen bond between asparagine 485 and the pi system of FAD modulates the redox potential in the reaction catalyzed by cholesterol oxidase, *Biochemistry 40*, 13779-13787.

23. Rotsaert, F. A., Renganathan, V., and Gold, M. H. (2003) Role of the flavin domain residues, His689 and Asn732, in the catalytic mechanism of cellobiose dehydrogenase from *phanerochaete chrysosporium*, *Biochemistry 42*, 4049-4056.

24. Fan, F., Ghanem, M., and Gadda, G. (2004) Cloning, sequence analysis, and purification of choline oxidase from *Arthrobacter globiformis*: a bacterial enzyme involved in osmotic stress tolerance, *Arch. Biochem. Biophys*. *421*, 149-158.

25. Whitby, L. G. (1953) A new method for preparing flavin-adenine dinucleotide, *Biochem. J. 54*, 437-442.

26. Schowen, K. B., and Schowen, R. L. (1982) Solvent Isotope Effects on Enzyme Systems, in *Methods Enzymol.* (Purich, D. L., Ed.), pp 551-606, Academic Press, New York.

27. Lide, D. R. (2000) *Handbook of Chemistry and Physics*, CRC Press, Boca Raton, FL.

28. Stanislava Kirini, C. K. (1999) Viscosity of aqueous solutions of poly(ethylene glycol) at 298.15K., *Fluid Phase Equilib 155*, 311-325.

29. Raibekas, A. A., and Massey, V. (1997) Glycerol-assisted restorative adjustment of flavoenzyme conformation perturbed by site-directed mutagenesis, *J. Biol. Chem. 272*, 22248-22252.

30. Cleland, W. W. (1991) *in Enzyme Mechanism from Isotope Effects (Cook, P.R., Ed.)*, CRC Press, Boca Raton, FL.

31. Gadda, G., Powell, N. L., and Menon, P. (2004) The trimethylammonium headgroup of choline is a major determinant for substrate binding and specificity in choline oxidase, *Arch. Biochem. Biophys*. *430*, 264-273.

32. Gadda, G., Fan, F., and Hoang, J. V. (2006) On the contribution of the positively charged headgroup of choline to substrate binding and catalysis in the reaction catalyzed by choline oxidase, *Arch. Biochem. Biophys. 451*, 182-187.

33. Klinman, J. P. (2007) How do enzymes activate oxygen without inactivating themselves? *Acc. Chem. Res*. *40*, 325-333.

34. Roth, J. P., Wincek, R., Nodet, G., Edmondson, D. E., McIntire, W. S., and Klinman, J. P. (2004) Oxygen isotope effects on electron transfer to O_2 probed using chemically modified flavins bound to glucose oxidase, *J. Am. Chem. Soc*. *126*, 15120-15131.

35. Roth, J. P., and Klinman, J. P. (2003) Catalysis of electron transfer during activation of O2 by the flavoprotein glucose oxidase, *Proc. Natl. Acad. Sci. U S A 100*, 62-67.

36. Su, Q., and Klinman, J. P. (1998) Probing the mechanism of proton coupled electron transfer to dioxygen: the oxidative half-reaction of bovine serum amine oxidase, *Biochemistry 37*, 12513-12525.

37. Zhao, G., Bruckner, R. C., and Jorns, M. S. (2008) Identification of the oxygen activation site in monomeric sarcosine oxidase: role of Lys265 in catalysis, *Biochemistry 47*, 9124-9135.

38. Hassan-Abdallah, A., Bruckner, R. C., Zhao, G., and Jorns, M. S. (2005) Biosynthesis of covalently bound flavin: isolation and in vitro flavinylation of the monomeric sarcosine oxidase apoprotein, *Biochemistry 44*, 6452-6462.

CHAPTER 4

On the Role of His466: Possibly the Catalytic Base in Choline Oxidase?

4.1. Abstract

Choline oxidase from *Arthrobacter globiformis* is an FAD-dependent enzyme that oxidizes choline to glycine betaine with molecular oxygen as final electron acceptor. Mechanistic studies suggested that the reaction occurs through hydride transfer mechanism in which the reaction is initiated by the abstraction of the hydroxyl proton from the substrate by a catalytic base. The conserved His466 proposed to be the active site base in choline oxidase was mutated to glutamine. In addition, His351Gln, His351Gln/His466Ala, and His351/466Gln mutant variants were also prepared to support the hypothesis that either one of the two histidines can act as catalytic base in the wild-type enzyme, whereas the other residue plays the catalytic role in the absence of the original base in the mutant enzyme. The kinetic parameters of the mutant enzymes indicated that His466 id essential for catalysis, stabilizes the intermediate during the oxidation reaction and may be a catalytic base in choline oxidase.

4.2. Introduction

The FAD-dependent enzyme choline oxidase catalyzes the oxidation of choline to glycine betaine with betaine aldehyde as intermediate and molecular oxygen as electron acceptor. In the first reductive half-reaction, choline is oxidized to betaine aldehyde to give reduced flavin. The first oxidation-reduction is completed when the reduced flavin is reoxidized by molecular oxygen yielding H_2O_2. Then, the second oxidation-reduction takes place which finally produce glycine betaine as the final product (*1*).

Previous studies showed that in choline oxidase the turnover is initiated by a kinetically fast removal of the hydroxyl proton of the alcohol substrate by an unidentified base with pK_a ~ 7.5 (*2-4*). The process of proton abstraction requires a catalytic base residue located close to the hydroxyl group of the substrate in the enzyme-substrate complex. The crystal structure reveals that there are only two ionizable groups which could act as catalytic base in the active site, His466 and His351 (Figure 4.1). In addition, mechanistic studies on GMC enzymes suggested that histidine residue is fully conserved within the family and might act as the active site base that participates in the oxidation of the alcohol substrate (*5-10*). This residue corresponds to His466 in choline oxidase. To date, the evidence for a single histidine residue being responsible for the activation of the alcohol substrate is not conclusive. Studies from a number of flavin-dependent enzymes such as glucose oxidase (*9, 11-13*), pyranose 2-oxidase (*14-17*), glycolate oxidase (*18*), lactate monooxygenase (*19*), and flavocytochrome b_2 (*20-22*) investigated either the structures or the kinetic parameters of mutant enzymes, but did not implicated or having strong evidences supporting that histidine residue being a catalytic base. Only in the case of mandelate dehydrogenase it had been showed the enzymatic activity of the mutant enzyme was rescued in rescuing experiment on pH-dependence profile.

In this work, we report the results of the single amino acid substitution in which histidine 351 and 466 have been replaced to glutamine. Since either one of the two histidine residues could act as a catalytic base in the wild-type enzyme (*23*), double mutant enzymes in which His351 was replaced to glutamine and His466 to alanine and both histidine residues were mutated to glutamine were obtained. In accord with the proposed catalytic role of His466, His466Gln and His351Gln/His466Ala showed dramatic decrease in activity, especially in the rate of flavin reduction of His466Gln. Moreover, our data supported the previous results that these two histidine residues provide stabilization of alkoxide intermediate during the oxidation of choline substrate.

Figure 4.1. The active site of wild-type choline oxidase with DMSO ligand and selected amino acids at a resolution of 1.86 Å.

4.3. Experimental procedures

Materials. *Escherichia coli* strain Rosetta(DE3)pLysS was from Novagen (Madison, WI). DNase was from Roche. The QuikChange site-directed mutagenesis kit was from Stratagene (La Jolla, CA). The QIAprep Spin Miniprep kit was from Qiagen (Valencia, CA). Oligonucleotides used for sequencing of the mutant gene were custom synthesized by Sigma Genosys (Woodland, TX). Bovine serum albumin, chloramphenicol, tetracycline, DMSO, isopropyl-β-D-thiogalactopyranoside (IPTG), phenylmethylsulfonyl fluoride (PMSF), lysozyme, sodium hydrosulfite, betaine aldehyde, glycine betaine, Luria-Bertani agar and broth were from Sigma (St. Louis, MO). EDTA was from Fisher. Choline chloride and ampicillin were from ICN Pharmaceutical Inc. 1,2-[$^{2}H_{4}$]-Choline bromide (98%) and sodium deuteroxide (99%) were from Isotec Inc. (Miamisburg, OH). Wild-type choline oxidase from *Arthrobacter globiformis* strain ATCC 8010 was expressed from plasmid pET/*codA*1 and purified to homogeneity as described previously (*1*). All other reagents were of the highest purity commercially available.

Site-Directed Mutagenesis. A QuikChange kit was used to prepare the mutant variants: His351Gln, His466Gln, His351Gln/His466Ala, and His351/466Gln. The experiment was performed by following the manufacturer's instructions in the presence of 2% DMSO using the pET/CodAmg1 plasmid harboring the wild-type gene (CodA) for choline oxidase as a template and forward and reverse oligonucleotides as primers for site-directed mutagenesis. The resulting mutant genes were sequenced at the DNA core Facility at Georgia State University using an Applied Biosystems Big Dye Kit on an Applied Biosystems model ABI 377 DNA sequencer. Sequencing confirmed the presence of the mutant gene in the correct orientation. Finally, *E. coli* strain Rosetta(DE3)pLysS competent cells were transformed with the mutant plasmid i.e.,

pET/*codA*mg1-H351A by electroporation, and permanent stocks of the transformed cells were prepared and stored at -80 ^{o}C.

Expression and Purification of His351Gln, His466Gln, His351Gln/His466Ala and His351/His466Gln Variants of Choline Oxidase. Permanent stocks of *E. coli* Rosetta(DE3)pLysS cells harboring plasmid corresponding to the mutants were used to inoculate 4.5 L of Luria-Bertani broth medium containing 50 μg/mL ampicillin and 34 μg/mL chloramphenicol. The liquid cultures were grown for 5 h at 37 °C, before inducing protein expression with 0.05 mM IPTG for 12-14 h at 22 °C. The mutant enzymes were purified to homogeneity using the same procedure described previously for the purification of the wild-type enzyme (*1*).

Enzyme Assays. The enzymatic activity of His351Gln mutants were measured by the method of initial rates as described for the wild-type enzyme (*1*) using a computer-interfaced Oxy-32 oxygen-monitoring system (Hansatech Instrument Ltd). The apparent steady-state kinetic was performed with choline as substrate in 50 mM potassium phosphate buffer, pH 7.0 and 25 °C. The rate of flavin reduction of His466Gln and His351Gln/His466Ala were performed anaerobically using an anaerobic cuvette with two side arms. Choline in buffer, at a desired final concentration, was initially loaded into one sidearm, whereas the other side arm was loaded with the enzyme. The cuvette was made anaerobic by repeated cycles of vacuuming and flushing with ultra-pure argon for at least 15 times, before mixing the enzyme with the choline substrate in the buffer. The rate of flavin reduction was determined by acquiring the UV-visible spectra every 2 min until no changing in the spectra of the reduced flavin were observed. The substrate and solvent kinetic isotope effects on the rate of flavin reduction were carried out at the same procedure with normal choline, except the use of substrate, 1,2-[$^{2}H_{4}$]-choline, and deuterium

oxide. In solvent kinetic isotope effect experiment, buffers were prepared using 99.9% deuterium oxide by adjusting the pD value with NaOD. The pD values were determined by adding 0.4 to the pH electrode reading (*24*).

Crystallization of His351/466Gln enzyme. Crystals of the His351/466Gln enzyme were grown aerobically at room temperature by hanging drop vapor diffusion with different buffers, precipitants, additives, cryoprotectant, and pH such as 10-15% (v/v) polyethylene glycol MW 6000, 50-200 mM Magnesium acetate, 1-0.05 M sodium cacodylate, 5-20% 1, 4-dioxane, 0.05-0.1 M MES, 0.5-2 M ammonium sulfate, and pH range from 5.0 to 8.0.

Data Analysis. Kinetic data were fit with the KaleidaGraph (Synergy Software, Reading, PA) and the Enzfitter (Biosoft, Cambridge, U.K.) softwares. Apparent kinetic parameters in atmospheric oxygen were determined by fitting initial rates at different substrate concentration to the Michaelis-Menten equation for one substrate. For kinetic isotope effects with choline as substrate, data obtained were separated in two sets, one with unlabeled substrate or solvent and one with labeled substrate or solvent, and kinetic isotope effects were determined by taking the ratio of the kinetic parameters obtained with normal substrate or solvent to that obtained with labeled substrate or solvent. Kinetic parameters for the reductive half-reactions were determined by using eq 1, where k_{obs} is the observed first-order rate for the reduction of the enzyme-bound flavin at any given concentration of substrate, k_{red} is the limiting first-order rate constant for flavin reduction at saturated substrate concentration, and K_d is the macroscopic dissociation constant for binding of the substrate to the enzyme.

$$k_{obs} = \frac{k_{red} A}{K_d + A} \qquad (1)$$

4.4. Results

Expression and purification of His351Gln, His466Gln, His351Gln/His466Ala and His351/His466Gln variants of choline oxidase. The mutant enzymes were expressed and purified at pH 8.0 to homogeneity as judged by SDS-PAGE using the same protocol developed for the wild-type enzyme (*1*). Glycerol at final 10% was added in all of the buffered solutions throughout the purification process to increase the stability of the enzymes (*25*). His466Gln, His351Gln/His466Ala and His351/His466Gln showed no oxygen consumption at concentrations as high as 30 μM and choline up to 0.5 M at pH 7.0 and 25 °C. The apparent steady-state kinetic parameters for His351Gln mutant enzyme were obtained with different choline concentrations at atmospheric oxygen, yielding apparent k_{cat} and K_m values for choline (Table 4.1). Since all mutant enzymes showed effects on both k_{cat} and K_m values, histidine residues at position 351 and 466 are important for catalysis in the reaction catalyzed by choline oxidase.

Crystallization of His351/466Gln enzyme. Crystals of His351/466Gln were grown by the hanging drop vapor diffusion method with the same crystallization conditions as wild-type, 0.1 M Bis-Tris propane, pH 8.5, 1.2 M ammonium sulfate, and 10% (v/v) dimethyl sulfoxide (DMSO), and Val464Ala, 0.08 M sodium cacodylate, pH 6.0, 50-200 mM magnesium acetate and 10-15% (v/v) polyethylene glycol. However, diffraction-quality crystals still could not be obtained.

Kinetic properties. The rates of flavin reduction of His466Gln and His351Gln/His466Ala mutants were measured with the method of the initial rate (*30*) by monitoring the spectral changes over time in UV-visible spectrophotometer after mixing enzyme with different concentration of choline under anaerobiosis. The observed rate constants for flavin reduction showed hyperbolic dependence on choline concentration, allowing for the

determination of limiting rate constants for flavin reduction (k_{red}) and the equilibrium constants for substrate binding (K_d). The double mutant His351Gln/His466Ala showed a limiting observed rate for flavin reduction (k_{red}) value of 0.012 s^{-1} which is 8000-fold lower compared to wild-type at pH 10.0 (Figure 4.2). In addition, The His466Gln variant was more impaired, in which at pH 8.0 the k_{red} is 9 order magnitudes lower than wild-type enzyme (2.0×10^{-7} s^{-1} in His466Gln compared to 93 s^{-1} in wild-type enzyme) (Figure 4.3). Interestingly, the reoxidation of the reduced flavin of His466Gln is kinetically fast since the enzyme is fully oxidized only a few minutes after allowing oxygen to get in the reaction mixture. This result suggested that the His466 is involved in the oxidation of choline, but not with the reduced flavin.

Kinetic Isotope Effects. Substrate, solvent, and multiple kinetic isotope effects on the reductive half-reaction catalyzed by the His351Gln/His466Ala enzyme were determined at pH 10.0. Substitution of water with deuterium oxide resulted in a $^{D_2O}k_{red}$ value that was slightly greater than unity (Table 4.2) indicating that the cleavage of OH bond of choline is at least partially rate limiting in the reductive half-reaction. In contrast, the wild-type choline oxidase showed no solvent kinetic isotope effect in which the $^{D}k_{red}$ values are large (8.9 ± 0.2) and the ^{D_2O} k_{red} values are unity (0.99 ± 0.02) (*2*). For multiple kinetic isotope effect, the substrate kinetic isotope effect increased upon substituting water with deuterium oxide ($^{D}(k_{red})_{D_2O}$ compared to $^{D}k_{red}$ value in Table 4.2) and in a similar fashion, the solvent kinetic isotope effect value increased when 1,2-[$^{2}H_4$]-choline was used instead of choline ($^{D_2O}(k_{red})_{D}$ compared to $^{D_2O}k_{red}$ value in Table 4.2). All taken together, these data are consistent with hydroxyl proton abstraction and hydride transfer occurring in the same transition state in His351Gln/His466Ala enzyme.

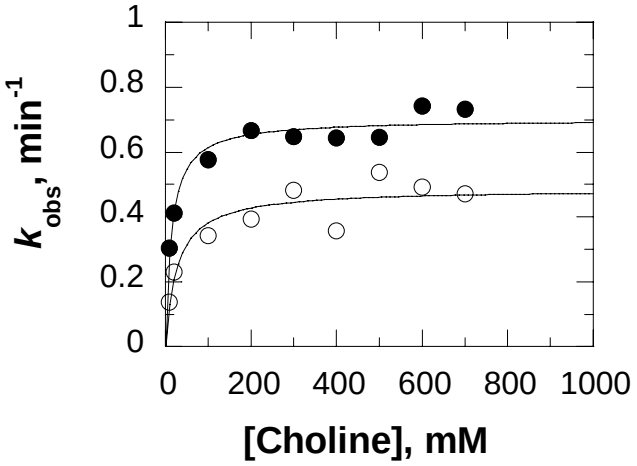

Figure 4.2. The observed rates of anaerobic flavin reduction (k_{obs}) of His351Gln/His466Ala as a function of the concentrations of choline (●) and 1,2-[$^2H_4$]-choline (○). Data were fit to eq. 1.

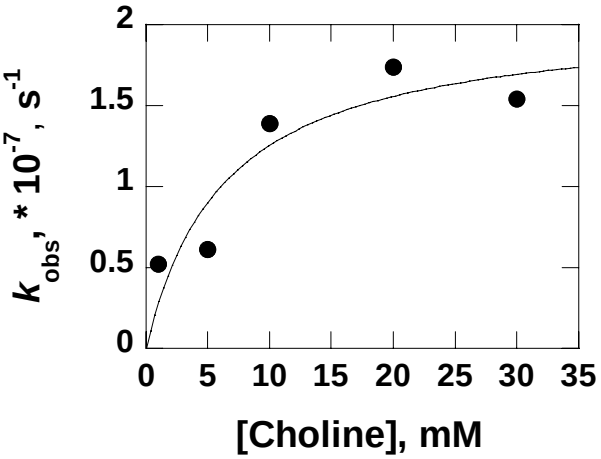

Figure 4.3. The observed rates of anaerobic flavin reduction (k_{obs}) of His466Gln as a function of the concentrations of choline. Data were fit to eq. 1.

4.5 Discussion

As depicted in Figure 4.1, the structure of choline oxidase has shown that there are two histidine residues in the active site, conserved His466 and His351. These two histidine residues are good candidates to act as a catalytic base in choline oxidase since they are properly position to abstract the hydroxyl proton from substrate. Therefore, the single mutants, His351Gln and His466Gln and double mutants, His351Gln/His466Ala and His351/His466Gln, were prepared. The effects of the mutations are consistent with these residues being important in the reaction catalyzed by choline oxidase and will be discussed here.

Histidine residues at position 351 and 466 are important for the oxidation of choline in choline oxidase. The evidence for this conclusion comes from the kinetic parameters of the mutants. The apparent k_{cat} value of His351Gln was 50-fold lower compared to wild-type enzyme (Table 4.1). The enzymatic activity of His466Gln, His351Gln/His466Ala, and His351/His466Gln mutants were too low to obtain meaningful data from the oxygen electrode instrument. The k_{red} values decrease by 9 orders of magnitude in His466Gln mutant and 8000-fold in His351Gln/His466Ala mutant, indicating the impairment in the hydride transfer reaction with choline as substrate. These results are consistent with previous studies on His351Ala and His466Ala mutants (*26, 27*). In those studies, it was found that both mutants showed effect on the reductive half-reaction, but not in the oxidation of the reduced flavin.

The conserved His466 is likely to be the catalytic base that abstracts hydroxyl proton of the substrate in the reductive half-reaction in which the choline is oxidized to betaine aldehyde. The 10^9-fold lower activity compared to wild-type on the rate of flavin reduction in His466Gln supports this conclusion. Similar results have been reported in lactate monooxygenase (*19*) and flavocytochrome b_2 (*21*). The enzymatic activity of His290Gln mutant in lactate monooxygenase

was five orders of magnitude lower than wild-type. In flavocytochrome b_2, the mutation of His373Gln resulted in an inactive enzyme (*19, 20*). In contrast, the results from previous study on His466Ala in choline oxidase suggested that this residue may not be a base due to pH dependence study showing the requirement of an unprotonated group for catalysis and an imidazole rescuing experiment (*26*). These results can be reinterpreted based on the hypothesis that His351 could act as a base when His466 is not presence in the active site. This proposal is similar to previous study in cholesterol oxidase (*5, 28*). His447Gln mutant still showed ability to catalyze the oxidation of the 3-hydroxyl to a ketone and the His477Gln structure reveals that Glu361 is hydrogen bonded to H_2O541, suggesting that Glu361 could act as the general base for oxidation reaction via a hydrogen bond network through Asn485 and H_2O541(*5, 28*). This idea could not be applied for His466Gln and His351Gln/His466Ala mutants because the His351 might change position in which it is no longer be a base in these mutants. Addition exogenous imidazole was effective in restoring the ability of His466Ala at pH 6.0 and 5.5, probably because the positive charge of imidazolium stabilizes the negative charge on the intermediate and modulates the flavin for the hydride transfer reaction. The crystal structure of His351/466Gln is the essential evidence to support this hypothesis and is currently under investigation.

His351 and 466 residues provide stabilization of the transition state that is formed after removal of the hydroxyl proton in the choline substrate as indicated by the kinetic isotope effect results on the double mutant His351Gln/His466Ala. Substitution of both histidine residues resulted in the change on the relative timing for bond cleavages in which the CH and OH bond cleavages are in the same transition state indicating the concerted mechanism (Table 4.2). In contrast, the cleavages of OH and CH bond in wild-type choline oxidase occur in a step-wise

mechanism. This result is consistent with previous studies from His466Ala and His351Ala in which the mutation showed the loss of stabilization of alkoxide species (*26, 27*).

In summary, the postulated active site base in choline oxidase, His466, was mutagenized to glutamine and double mutants, His351Gln/His466Ala and His351/466Gln including His351Gln were created. The ability of the mutant enzymes, His466Gln and His351Gln/His466Ala, to be reduced by choline substrate is decreased dramatically whereas His351/466Gln is catalytically not active. This is correlated with the absence of proton removal from the hydroxyl group of the substrate, the first step in the oxidation of choline by choline oxidase followed by the hydride transfer to the N(5) atom of flavin. This result provides strong support to the hypothesis that histidine466 plays an essential role in catalysis, being a catalytic base, in choline oxidase. However, the crystal structure of the mutant form is required to further support this proposal and this process is under investigation.

Table 4.1. Apparent Steady State Kinetic Parameters for Choline Oxidase Variants[a]

	$^{app}k_{cat}$, s^{-1}	$^{app}K_{choline}$, mM	$^{app}(k_{cat}/K_{choline})$, $M^{-1}s^{-1}$
wild-type[b]	13.4 ± 0.5	0.6 ± 0.1	22,000 ± 3760
His351Ala[c]	0.51 ± 0.02	15 ± 1	34 ± 2
His466Ala[c]	0.53 ± 0.01	13 ± 1	41 ± 3
His351Gln	0.26 ± 0.02	105 ± 11	2.5 ± 0.3
His466Gln	Nd[d]	nd	nd
His351Gln/His466Ala	nd	nd	nd
His351/His466Ala	nd	nd	nd

[a] Initial rates determined as oxygen consumption with choline as substrate at fixed atmospheric [oxygen] in 50 mM potassium phosphate, pH 7.0 and 25 °C. [b] From ref (*29*) . [c] This work. [d] Not determined.

Table 4.2. Substrate and Solvent Kinetic Isotope Effects with Choline as Substrate[a]

Parameter	wild-type[b]	His351Gln/His466Ala
$^{D}k_{red}$	8.9 ± 0.2	9.6 ± 0.2
$^{D}(k_{red})_{D_2O}$	8.7 ± 0.2	10.3 ± 0.13
$^{D_2O}k_{red}$	0.99 ± 0.02	1.21 ± 0.02
$^{D_2O}(k_{red})_{D}$	0.94 ± 0.03	1.29 ± 0.07
$^{D,D_2O}k_{red}$	8.4 ± 0.2	12.3 ± 0.74

[a] Conditions: 50 mM sodium pyrophosphate, pH or pD 10, at 25 °C. [b] From ref. (*2*).

4.6 References

1. Fan, F., Ghanem, M., and Gadda, G. (2004) Cloning, sequence analysis, and purification of choline oxidase from Arthrobacter globiformis: A bacterial enzyme involved in osmotic stress tolerance, *Arch. Biochem. Biophys. 421*, 149-158.
2. Fan, F., and Gadda, G. (2005) On the catalytic mechanism of choline oxidase, *J. Am. Chem. Soc*. *127*, 2067-2074.
3. Gadda, G. (2003) pH and deuterium kinetic isotope effects studies on the oxidation of choline to betaine-aldehyde catalyzed by choline oxidase, *Biochim. Biophys. Acta. 1650*, 4-9.
4. Ghanem, M., Fan, F., Francis, K., and Gadda, G. (2003) Spectroscopic and kinetic properties of recombinant choline oxidase from *Arthrobacter globiformis*, *Biochemistry 42*, 15179-15188.
5. Kass, I. J., and Sampson, N. S. (1998) Evaluation of the role of His447 in the reaction catalyzed by cholesterol oxidase, *Biochemistry 37*, 17990-18000.
6. Roth, J. P., and Klinman, J. P. (2003) Catalysis of electron transfer during activation of O_2 by the flavoprotein glucose oxidase, *Proc. Natl. Acad. Sci. U S A 100*, 62-67.
7. Rotsaert, F. A., Renganathan, V., and Gold, M. H. (2003) Role of the flavin domain residues, His689 and Asn732, in the catalytic mechanism of cellobiose dehydrogenase from *phanerochaete chrysosporium*, *Biochemistry 42*, 4049-4056.
8. Su, Q., and Klinman, J. P. (1999) Nature of oxygen activation in glucose oxidase from Aspergillus niger: The importance of electrostatic stabilization in superoxide formation, *Biochemistry 38*, 8572-8581.

9. Wohlfahrt, G., Witt, S., Hendle, J., Schomburg, D., Kalisz, H. M., and Hecht, H. J. (1999) 1.8 and 1.9 Å resolution structures of the *Penicillium amagasakiense* and *Aspergillus niger* glucose oxidases as a basis for modelling substrate complexes, *Acta. Crystallogr. D. Biol. Crystallogr*. *55*, 969-977.

10. Yin, Y., Liu, P., Anderson, R. G., and Sampson, N. S. (2002) Construction of a catalytically inactive cholesterol oxidase mutant: Investigation of the interplay between active site-residues glutamate 361 and histidine 447, *Arch. Biochem. Biophys*. *402*, 235-242.

11. Hecht, H. J., Kalisz, H. M., Hendle, J., Schmid, R. D., and Schomburg, D. (1993) Crystal structure of glucose oxidase from *Aspergillus niger* refined at 2.3 Å resolution, *J. Mol.Biol. 229*, 153-172.

12. Hecht, H. J., Schomburg, D., Kalisz, H., and Schmid, R. D. (1993) The 3D structure of glucose oxidase from *Aspergillus niger*. Implications for the use of GOD as a biosensor enzyme., *Biosens. Bioelectron. 8*, 197-203.

13. Kiess, M., Hecht, H. J., and Kalisz, H. M. (1998) Glucose oxidase from *Penicillium amagasakiense*. Primary structure and comparison with other glucose-methanol-choline (GMC) oxidoreductases, *Eur. J. Biochem*. *252*, 90-99.

14. Bannwarth, M., Bastian, S., Heckmann-Pohl, D., Giffhorn, F., and Schulz, G. E. (2004) Crystal structure of pyranose 2-oxidase from the white-rot fungus *Peniophora sp*, *Biochemistry 43*, 11683-11690.

15. Bannwarth, M., Heckmann-Pohl, D., Bastian, S., Giffhorn, F., and Schulz, G. E. (2006) Reaction geometry and thermostable variant of pyranose 2-oxidase from the white-rot fungus *Peniophora sp*, *Biochemistry 45*, 6587-6595.

16. Hallberg, B. M., Leitner, C., Haltrich, D., and Divne, C. (2004) Crystal structure of the 270 kDa homotetrameric lignin-degrading enzyme pyranose 2-oxidase, *J.Mol. Biol. 341*, 781-796.

17. Kujawa, M., Ebner, H., Leitner, C., Hallberg, B. M., Prongjit, M., Sucharitakul, J., Ludwig, R., Rudsander, U., Peterbauer, C., Chaiyen, P., Haltrich, D., and Divne, C. (2006) Structural basis for substrate binding and regioselective oxidation of monosaccharides at C3 by pyranose 2-oxidase, *J Biol Chem 281*, 35104-35115.

18. Murray, M. S., Holmes, R. P., and Lowther, W. T. (2008) Active site and loop 4 movements within human glycolate oxidase: Implications for substrate specificity and drug design, *Biochemistry 47*, 2439-2449.

19. Muh, U., Williams, C. H., Jr., and Massey, V. (1994) Lactate monooxygenase. II. Site-directed mutagenesis of the postulated active site base histidine 290, *J Biol Chem 269*, 7989-7993.

20. Gaume, B., Sharp, R. E., Manson, F. D., Chapman, S. K., Reid, G. A., and Lederer, F. (1995) Mutation to glutamine of histidine 373, the catalytic base of flavocytochrome b2 (L-lactate dehydrogenase), *Biochimie 77*, 621-630.

21. Rao, K. S., and Lederer, F. (1998) About the p*K*a of the active-site histidine in flavocytochrome b_2 (yeast L-lactate dehydrogenase), *Protein Sci 7*, 1531-1537.

22. Tsai, C. T., Gokulan, K., Sobrado, P., Sacchettini, J. C., and Fitzpatrick, P. F. (2007) Mechanistic and structural studies of H373Q flavocytochrome b_2: effects of mutating the active site base, *Biochemistry 46*, 7844-7851.

23. Gadda, G. (2008) Hydride transfer made easy in the reaction of alcohol oxidation catalyzed by flavin-dependent oxidases, *Biochemistry 47*, 13745-13753.

24. Schowen, K. B., and Schowen, R. L. (1982) Solvent isotope effects on enzyme systems, in Methods in Enzymology, Purich, D. L., ed., Academic Press, New York.

25. Raibekas, A. A., and Massey, V. (1997) Glycerol-assisted restorative adjustment of flavoenzyme conformation perturbed by site-directed mutagenesis, *J. Biol. Chem. 272*, 22248-22252.

26. Ghanem, M., and Gadda, G. (2005) On the catalytic role of the conserved active site residue His466 of choline oxidase, *Biochemistry 44*, 893-904.

27. Rungsrisuriyachai, K., and Gadda, G. (2008) On the role of histidine 351 in the reaction of alcohol oxidation catalyzed by choline oxidase, *Biochemistry 47*, 6762-6769.

28. Yue, Q. K., Kass, I. J., Sampson, N. S., and Vrielink, A. (1999) Crystal structure determination of cholesterol oxidase from *Streptomyces* and structural characterization of key active site mutants, *Biochemistry 38*, 4277-4286.

29. Quaye, O., Lountos, G. T., Fan, F., Orville, A. M., and Gadda, G. (2008) Role of Glu312 in binding and positioning of the substrate for the hydride transfer reaction in choline oxidase, *Biochemistry 47*, 243-256.

30. D.R. Allison, D.L. Purich, in: D.L. Purich (Ed.), Methods Enzymology, vol 63, Acadamic press, New York, 1979, pp. 3-19.

CHAPTER 5

A pH switch affects the steady-state kinetic mechanism of pyranose 2-oxidase from *Trametes ochracea*

(This chapter has been published verbatim in Rungsrisuriyachai, K. and Gadda, G., (2009), *Arch Biochem Biophys. 483:* 10-15)

5.1. Abstract

The flavin-dependent pyranose 2-oxidase catalyzes the oxidation of D-glucose and other pyranoses at the C2 atom to yield 2-keto-sugars and hydrogen peroxide. Here, the steady-state kinetic mechanism of the enzyme from *Trametes ochracea* was investigated as a function of pH. Our findings show that the enzyme follows a bi-bi ping-pong kinetic mechanism at pH values <7.0, and a bi-bi ordered mechanism at pH values >7.0. Thus, at low pH the reactivity of the reduced enzyme with oxygen is controlled a by a conformational change of the enzyme that is associated with the release of the 2-keto-sugar from the active site of the enzyme. In contrast, at high pH the reduced enzyme-product complex permits the reaction of oxygen with the flavin. The study also illustrates that caution should be exerted in extrapolating the conclusions drawn on steady-state kinetic mechanisms established at a single pH value to other pH's in flavoprotein oxidases.

5.2. Introduction

Pyranose 2-oxidase (E.C. 1.1.3.10; pyranose:oxygen 2-oxidoreductase; glucose 2-oxidase) catalyzes the flavin-mediated oxidation of D-glucose and other pyranoses at the C2 position to yield 2-keto-sugars and hydrogen peroxide (Scheme 5.1) (*1*). The enzyme has been isolated from several wood-degrading basidiomycetes (*2*), where it is proposed to participate in lignin degradation by producing hydrogen peroxide for the reactions catalyzed by manganese and lignin peroxidase (*1*). The enzyme from the white-rod fungus *Trametes ochracea* has been investigated in its biochemical, kinetic, and structural properties (*1, 3, 4*). Pyranose 2-oxidase shows broad substrate specificity with reasonably good activity on D-glucose, D-xylose, L-sorbose (*1, 3*), where D-glucose is the best substrate based on the second-order rate constant k_{cat}/K_m (*1*). In recent years, significant interest has been generated for the use of pyranose 2-oxidase as a catalyst in biotechnological applications where common sugars and their derivatives are converted into rare sugars or drugs (*5*). From a mechanistic standpoint, a detailed characterization of the reaction catalyzed by pyranose 2-oxidase, along with a comparison with the well-characterized glucose 1-oxidase from *Aspergillus niger* (*6-8*), offers the opportunity to elucidate the structural features that allow for the stereoselective oxidation of these sugars at different positions.

A wealth of structural information is available on pyranose 2-oxidase from different microorganisms, allowing to group the enzyme within the Glucose-Methanol-Choline oxidoreductase enzyme superfamily (*3, 9-13*). The *T. ochracea* enzyme is a tetramer of identical subunits with a total mass of 270 kDa, with each subunit being covalently associated to an FAD moiety through a linkage between the N(3) atom of histidine 167 and the C(8) methyl group of the flavin (*11*). The active site cavity where the flavin cofactor is located is completely secluded

from the bulk solvent by the presence of a long loop that forms a lid preventing access and exit of organic molecules (*11*). However, in the structure of pyranose 2-oxidase with 2-fluoro-D-glucose bound to the protein the loop is in an open conformation, suggesting that a significant rearrangement is required to open and close the access to the active site (*3*). An open conformation of the loop is also observed in pyranose 2-oxidase from another cellular source, *Peniosphora sp.,* in complex with the 2-keto-D-glucose product of the oxidation reaction. From a biochemical standpoint, several studies have suggested that the reaction mechanism follows a bi-bi ping-pong kinetic pattern at pH 6.5 (*3, 14, 15*), with oxidation of the reduced flavin occurring after the release of the 2-keto-D-glucose produced in the oxidation of D-glucose. Interestingly, in a recent investigation of the reduced enzyme-bound flavin reacting with oxygen using a stopped-flow spectrophotometer it was shown for the first time with a wild-type flavoprotein oxidase that a C(4a)-hydroperoxyflavin intermediate is transiently formed in the flavin oxidation reaction (*4*).

In the present study, we set out to investigate the steady-state kinetic mechanism of pyranose 2-oxidase with D-glucose as substrate in the pH range from 5.5 to 8.5, in order to establish a framework for future mechanistic investigations of the enzyme. Our findings show that pyranose 2-oxidase displays a ping-pong kinetic mechanism at pH values < 7.0 and an ordered mechanism at pH > 7.0. These observations are discussed in relation to the structural information that is available on the enzyme from other studies. The study also illustrates that caution should be exerted in extrapolating *a priori* a steady-state kinetic mechanism determined at a single pH value to other pH values when the pH profile of the kinetic parameters of a flavoprotein oxidase are investigated.

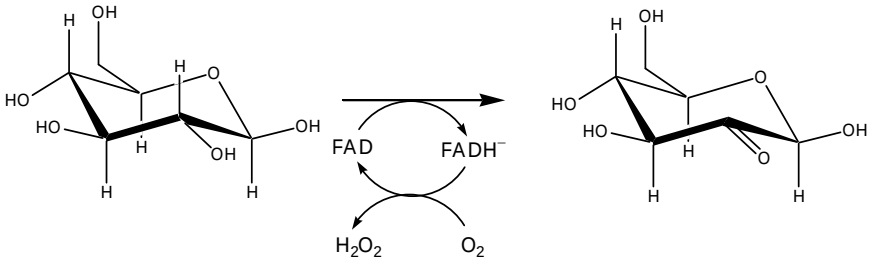

Scheme 5.1. Reaction Catalyzed by Pyranose 2-Oxidase.

5.3. Experimental Procedures

Materials. The plasmid pSE33 containing the gene encoding for pyranose 2-oxidase from *T. ochracea* was a kind gift of Dr. Peter Kyslik, Academy of Sciences of the Czech Republic, Prague. *Escherichia coli* strain Rosetta(DE3)pLysS was from Novagen (Madison, WI). Oligonucleotides used for sequencing of the gene were custom synthesized by Sigma Genosys (Woodland, TX). Isopropyl-β-D-thiogalactopyranoside (IPTG), phenylmethylsulfonyl fluoride (PMSF), lysozyme, D-glucose, Luria-Bertani agar and broth were from Sigma (St. Louis, MO). All other reagents were of the highest purity commercially available.

Expression and purification of pyranose 2-oxidase. Permanent frozen stocks of *E. coli* cells Rosetta(DE3)pLysS harboring the plasmid pSE33 were used to inoculate 50 mL of Luria-Bertani broth medium containing 50 μg/mL ampicillin and 34 μg/mL chloramphenicol. After 10 h at 37 °C, 1 mL of the overnight culture was used to inoculate 6 x 1 liter flasks of the same liquid culture medium, which were incubated at 37 °C. When the culture reached an optical density at 600 nm of 0.6 to 0.8, IPTG was added to a final concentration of 200 μM and the

temperature was lowered to 20 °C. Cells were harvested by centrifugation at 20,000*g* for 20 min at 4 °C and stored at –20 °C. All purification steps were carried out at 4 °C. Approximately 40 g of stored, wet, cell paste were suspended in 150 mL of 0.1 mM PMSF, 0.2 mg/mL lysozyme, 1 mM EDTA, and 50 mM potassium phosphate, pH 6.5. The cell suspension was then allowed to incubate with stirring for 30 min on ice with 20 μg/mL RNase and 50 μg/mL DNase in the presence of 10 mM $MgCl_2$. The resulting slurry was sonicated eight times for 5 min, with 2 min intervals, before removing the cell debris by centrifugation at 20,000*g* for 20 min. Ammonium sulfate was slowly added to a final saturation of 35% to the supernatant collected from the centrifuge. After centrifugation, the resulting supernatant was brought to 65% saturation with ammonium sulfate before centrifugation as described above. The resulting pellet was suspended in 50 mM potassium phosphate buffer, pH 6.5, and dialyzed over 20 h. After dialysis, the precipitated proteins were removed by centrifugation at 20,000*g* for 20 min and the supernatant was loaded directly onto a DEAE Sepharose Fast Flow column (3 × 28 cm) that had been pre-equilibrated with the same buffer used for dialysis. The column was eluted with a flow rate of 5 mL/min by using a linear gradient from 0 to 0.5 M NaCl over 1 L. Fractions displaying oxidase activity with glucose as substrate were pooled and dialyzed overnight against 50 mM potassium phosphate buffer, pH 6.5. Ammonium sulfate was slowly added to 35% saturation to the clear supernatant obtained by centrifugation and the resulting protein solution was directly applied to a Phenyl Sepharose Fast Flow column (3 × 15 cm) that had been pre-equilibrated with the same buffer. The column was eluted with a flow rate of 3 mL/min over 1 L with a linear gradient from 35% to 0% of ammonium sulfate. Chromatographic fractions with the highest purity as judged by enzymatic activity, UV-visible absorbance spectroscopy, and SDS-PAGE were pooled together, concentrated by 65% ammonium sulfate saturation and centrifuged as described above.

The resulting pellet was suspended in 15 mL of 50 mM potassium phosphate, pH 6.5, containing 0.1 M NaCl, and dialyzed against five 1-L changes of the same buffer over 24 h. After removal of the precipitated proteins by centrifugation, the enzyme was stored at - 20 °C.

Enzyme assays. The enzymatic activity of pyranose 2-oxidase was measured with the method of the initial rates (*16*), by monitoring the rate of oxygen consumption with a computer-interfaced Oxy-32 oxygen-monitoring system (Hansatech Instrument) at 30 °C. The steady-state kinetic parameters of pyranose 2-oxidase were determined by varying the concentration of both oxygen and D-glucose in the range from 0.05 to 15 mM for glucose and from 0.02 mM to 0.75 mM for oxygen. The assay mixtures were equilibrated at the desired oxygen concentration by bubbling with a O_2/N_2 gas mixture for at least 15 min before the reaction was started with the addition of the enzyme. The effect of pH on the kinetic parameters was investigated with assay mixtures buffered to the desired pH value with 50 mM sodium pyrophosphate, with the exception of pH 7 where 50 mM sodium phosphate was used. Enzyme concentration was expressed per enzyme-bound FAD content, using a molar extinction coefficient at 460 nm of 11.3 $mM^{-1}cm^{-1}$ (*1*).

Data analysis. Kinetic data were fit with the KaleidaGraph software (Synergy Software, Reading, PA) and the Enzfitter software (Biosoft, Cambridge, UK). The steady-state kinetic parameters at varying concentrations of both D-glucose and oxygen were determined by fitting the initial rates of reaction to Eqs. (1) and (2), which describe steady-state kinetic mechanisms without and with the formation of a ternary complex. K_a and K_b are the Michaelis constants for D-glucose (*A*) and oxygen (*B*), respectively, and k_{cat} is the turnover number of the enzyme (*e*) saturated with both substrates. When the ratio of the concentrations of D-glucose to oxygen was kept equal to a constant value α (i.e., A/B=α), Eqs. (3) and (4) were used instead of Eqs. (1) and

(2), respectively. Here, a steady-state kinetic mechanism with formation of a ternary complex yields a polynomial curve, whereas that without formation of a ternary complex yields a straight line (*17*). The pH profiles of the k_{cat}/K_m values for D-glucose and oxygen were determined by fitting initial rates data to Eqs. (5) and (6), respectively, which describe curves with a slope of +1 for glucose and -1 for oxygen with a plateau region at low pH. C is the pH independent value of the kinetic parameter of interest.

$$\frac{v}{e}=\frac{k_{cat}AB}{K_aB+K_bA+AB} \tag{1}$$

$$\frac{v}{e}=\frac{k_{cat}AB}{K_aB+K_bA+AB+K_{ia}K_b} \tag{2}$$

$$\frac{1}{v}=\left[\left(K_a+\alpha K_b\right)\frac{1}{A}+1\right]\left(\frac{1}{V}\right) \tag{3}$$

$$\frac{1}{v}=\left[\alpha K_{ia}K_b\frac{1}{A^2}+\left(K_a+\alpha K_b\right)\frac{1}{A}+1\right]\left(\frac{1}{V}\right) \tag{4}$$

$$\log Y=\log\left[C\left(1+10^{-pK_a+pH}\right)\right] \tag{5}$$

$$\log Y=\log\frac{C}{1+\frac{10^{-pK_a}}{10^{pH}}} \tag{6}$$

5.4. Results

Purification of pyranose 2-oxidase. Recombinant pyranose 2-oxidase was expressed in *E. coli* strain Rosetta(DE3)pLysS and purified using a two-step purification protocol involving hydrophobic and anionic-exchange chromatography at pH 6.5. The UV-visible absorbance spectrum of the purified enzyme showed bands at 360 nm and 460 nm consistent with the presence of oxidized FAD (Figure. 5.1). A 460/360 ratio of 0.8 was calculated from the absorbance spectrum of the purified enzyme stored in 20 mM Tris-Cl, pH 8.0, in agreement with earlier data by Leitner *et al.* (*1*). The 460/360 ratio increased to 1.06 upon replacing the buffer solution with 0.1 M NaCl, 10% glycerol, and 50 mM Tris-Cl, pH 8.0, in keeping with data reported in the literature for other flavin-dependent enzymes (*18*). A ~30% increase in the specific activity of the enzyme with 10 mM glucose as substrate was observed in the enzyme stored with NaCl and glycerol with respect to that devoid of additives (5.8 μM O_2 mg E^{-1} min^{-1} compared to 4.0 μM O_2 mg E^{-1} min^{-1}). Further studies showed that the increase in both the 460/360 ratio of the absorbance maxima and the enzymatic activity of purified pyranose 2-oxidase is attributable to NaCl, but not glycerol (data not shown). Consequently, 0.1 M NaCl was added to the last step of purification entailing the overnight dialysis of the enzyme in 50 mM potassium phosphate, pH 6.5.

Steady-state kinetic mechanism as a function of pH. The steady-state kinetic parameters of pyranose 2-oxidase with D-glucose as substrate were determined with the method of the initial rates (*16*) by monitoring the rate of oxygen consumption at varying concentrations of both D-glucose (from 0.05 mM to 15 mM) and oxygen (in the range from 0.02 mM to 0.75) at 30 ^{o}C in the pH range from 5.5 to 8.5. As illustrated in the example of Figure. 5.2A-B, at pH 5.5 sets of parallel lines were obtained in double reciprocal plots of the observed initial rates of

reaction as a function of the concentration of either D-glucose or oxygen. In agreement with this observation the kinetic data were fit best with Eq. (1), consistent with a bi-bi ping-pong steady-state kinetic mechanism. A similar kinetic pattern with parallel lines was observed at pH 6.5 (data not shown), where the kinetic data were also fit best with Eq. 1 (Table 1). Interestingly, at pH 8.5 the double reciprocal plots of the initial rates of reaction as a function of the concentration of glucose or oxygen clearly showed intersecting rather than parallel lines (Figure 5.2C-D), with the best fit of the kinetic data being obtained with Eq. (2) (Table 5.1). A similar kinetic behavior was also seen at pH 7.5 (data not shown), where the best fit of the data was achieved by using eq. (2) (Table 5.1). All the relevant steady-state kinetic parameters determined between pH 5.5 and 8.5 are summarized in Table 5.1.

As an independent approach to determine whether the steady-state kinetic mechanism of the enzyme depends on pH, initial rates of reaction were measured as a function of the concentration of D-glucose while keeping the ratio of the concentration of D-glucose to that of oxygen at a constant value. This method, which was originally employed by Tsopanakis and Herries on lactose synthetase (*17*) and recently reviewed by Cook and Cleland (*19*), allows for the simplification of the classical kinetic equations for two-substrate steady-state kinetic mechanisms in double reciprocal form to a straight line for a ping-pong mechanism (Eq. (3)) and a polynomial curve for an ordered mechanism (Eq. (4)). As illustrated in the examples of Figure 5. 3, the best fit of the data at pH 5.5 and 6.5 was attained with Eq. 3, consistent with a ping-pong steady-state kinetic mechanism; in contrast, at pH 7.5 and 8.5 a polynomial pattern was observed, suggesting an ordered mechanism. All taken together, the kinetic analysis of pyranose 2-oxidase established that at pH <7.0 the steady-state kinetic mechanism is ping-pong, and that at pH >7.0 it is ordered.

pH-Dependence of the k_{cat} and k_{cat}/K_m values. The steady-state kinetic parameters determined in the pH range from 5.5 to 8.5 upon varying the concentration of both D-glucose and oxygen are shown in Figure 5.4. The turnover number of the enzyme at saturating concentrations of substrates (k_{cat}) was independent of pH in the range considered. The second-order rate constant for the reductive half-reaction ($k_{cat}/K_{glucose}$) in which the enzyme-bound flavin is reduced with concomitant oxidation of D-glucose was independent of pH between pH 5.5 and 7.5, with a limiting value of 12,500 ± 500 $M^{-1}s^{-1}$, and increased to ~190,000 $M^{-1}s^{-1}$ at pH 8.5 (Figure 5.4). The second-order rate constant for the oxidative half-reaction (k_{cat}/K_{oxygen}) in which the enzyme-bound flavin is oxidized and molecular oxygen is reduced was also independent of pH in the range from 5.5 to 7.5, with a limiting value of 0.10 ± 0.05 $\mu M^{-1}s^{-1}$, but decreased to a value of ~0.015 $\mu M^{-1}s^{-1}$ at pH 8.5 (Figure 5.4) Instability of the enzyme at pH values higher than 8.5 prevented an accurate determination of the pK_a values for ionizable groups involved in both half-reactions catalyzed by the enzyme.

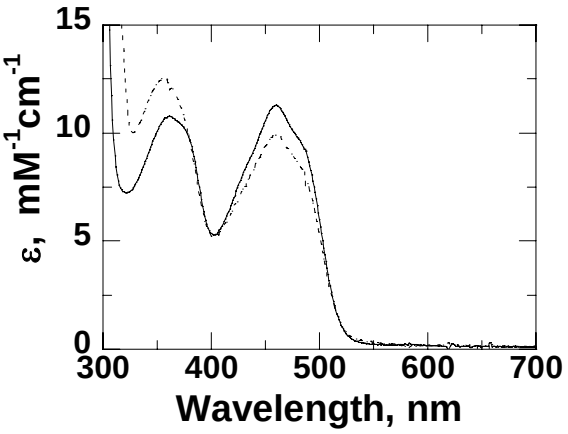

Figure 5.1. UV-visible absorbance spectra of pyranose 2-oxidase stored in 50 mM Tris-Cl, pH 8.0 (dotted curve) and 50 mM Tris-Cl, 0.1M NaCl, and 10% glycerol at pH 8.0 (solid curve).

Table 5.1. Steady-State Kinetic Parameters of Pyranose 2-Oxidase with D-glucose as substrate Between pH 5.5 and 8.5[a]

pH	Eq.	k_{cat}, s^{-1}	$K_{glucose}$, mM	$k_{cat}/K_{glucose}$, $M^{-1}s^{-1}$	K_{O_2}, mM	k_{cat}/K_{O_2}, $M^{-1}s^{-1}$	K_{ia}	R^2
5.5	1	5.9 ± 1.5	0.30 ± 0.10	19700 ± 8000	0.04 ± 0.01	147500 ± 52000	-	0.923
6.5	1	6.8 ± 0.1	0.90 ± 0.01	7550 ± 90	0.10 ± 0.01	73000 ± 850	-	0.987
7.5	2	6.5 ± 0.1	0.20 ± 0.03	22000 ± 3300	0.10 ± 0.01	70000 ± 2400	0.30 ± 0.04	0.991
8.5	2	7.5 ± 0.1	0.04 ± 0.01	190000 ± 29000	0.50 ± 0.01	15000 ± 300	0.60 ± 0.01	0.950

[a] Enzymatic activity was measured at varying concentrations of both D-glucose and oxygen at 30 °C.

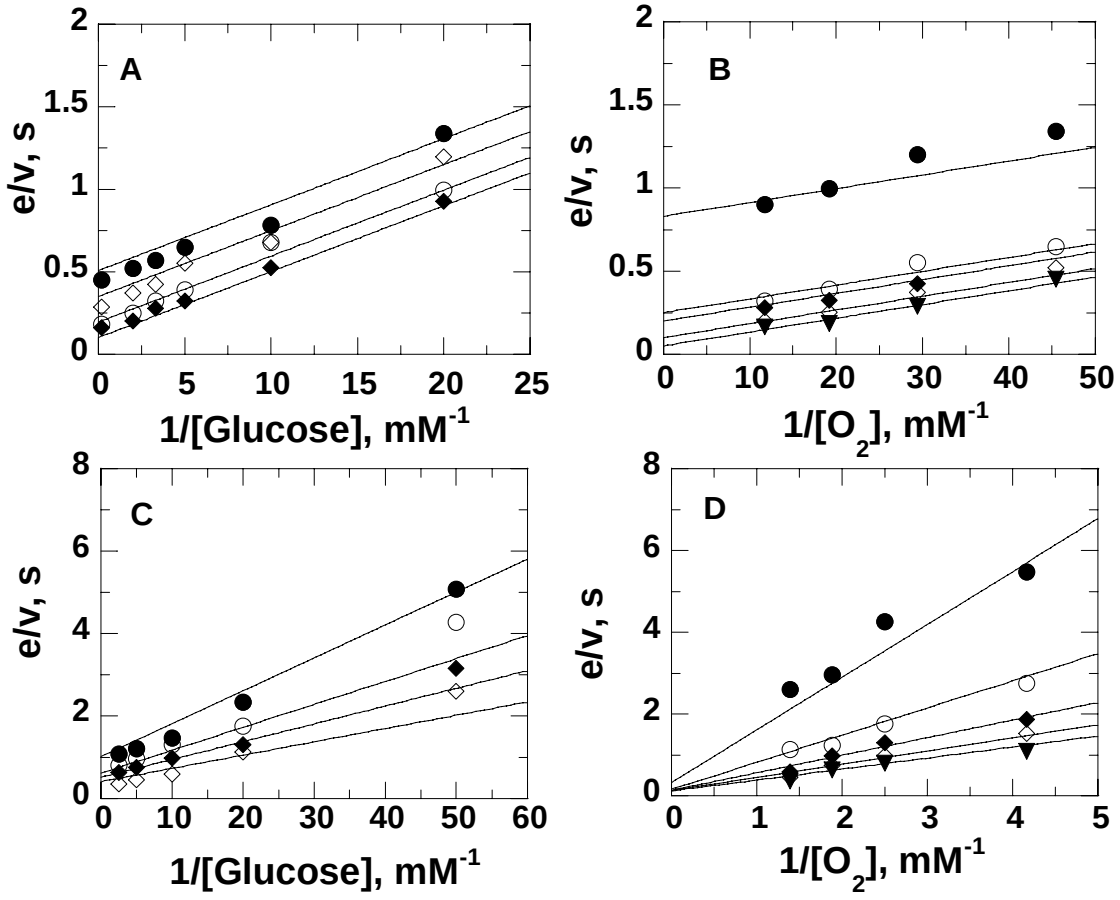

Figure 5.2. Double reciprocal plots of pyranose 2-oxidase-catalyzed oxidation of D-glucose at pH 5.5 (A and B) and 8.5 (C and D). Enzymatic activity assays were measured at varying concentration of both D-glucose and oxygen in 50 mM sodium phosphate and sodium pyrophosphate at 30 °C. Panel A, 1/*v* as a function of the inverse D-glucose concentration determined at several fixed concentrations of oxygen: (●) 0.022 mM, (○) 0.034 mM, (♦) 0.052 mM, and (◊) 0.085 mM oxygen. Panel B, 1/*v* as a function of the inverse oxygen concentration determined at several fixed concentrations of D-glucose: (●) 0.05 mM, (○) 0.2 mM, (♦) 0.3 mM, (◊) 0.5 mM and (▼) 5.0 mM D-glucose. Panel C, 1/*v* as a function of the inverse D-glucose concentration determined at several fixed concentrations of oxygen: (●) 0.24 mM, (●) 0.40 mM, (♦) 0.53 mM, and (◊) 0.72 mM oxygen. Panel D, 1/*v* as a function of the inverse oxygen concentration determined at several fixed concentrations of D-glucose: (●) 0.05 mM, (○) 0.1 mM, (♦) 0.2 mM, (◊) 0.4 mM and (▼) 1.0 mM D-glucose. The lines in panels A and B were drawn from a global fit of the data with to Eq. (1); those in panels C and D were drawn from a global fit of the data with to Eq. (2).

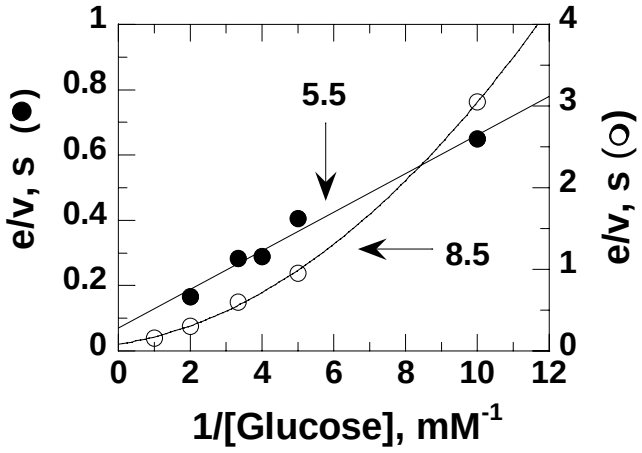

Figure 5.3. Double reciprocal plots of the initial rates of reaction as a function of the concentration of D-glucose at a fixed ratio (α) of [D-glucose]/[oxygen]. Initial rates were measured at 30 ^{o}C as described in the Methods, with α equal to 1 at all pH values tested. The line and the curve were obtained by fitting the data to Eq. (3) for pH 5.5 (R^2 =0.979) and Eq. (4) for pH 8.5 (R^2 =0.999), respectively.

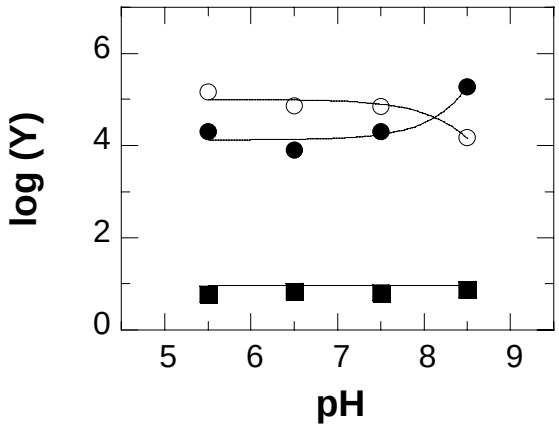

Figure 5.4. pH-Dependence of the $k_{cat}/K_{glucose}$, $M^{-1}s^{-1}$ (●), k_{cat}/K_{O2}, $M^{-1}s^{-1}$ (○) and k_{cat}, s^{-1} (■) values for pyranose 2-oxidase with D-glucose as substrate. Enzymatic activity assays were measured at varying concentration of both D-glucose and oxygen between pH 5.5 and 8.5, at 30 °C. Y represents either the $k_{cat}/K_{glucose}$, k_{cat}/K_{O2}, or k_{cat} value. The curves were obtained by fitting the kinetic data to Eqs. (5) and (6) for the $k_{cat}/K_{glucose}$ and k_{cat}/K_{O2} values, respectively. The line fitting the k_{cat} values is simply the average of the values at different pH (y = 0.65).

5.5. Discussion

The oxidation of D-glucose to 2-keto-D-glucose catalyzed by pyranose 2-oxidase consists of two mechanistically distinct half-reactions. In the first one, the enzyme-bound flavin is reduced to the hydroquinone state via the transfer of a hydride ion from the organic substrate (i.e., reductive half-reaction). In the second one, the reduced flavin is oxidized via the transfer of a hydride equivalent to molecular oxygen yielding hydrogen peroxide (i.e., oxidative half-reaction). Recent reports established that at pH 6.5 the two half-reactions of pyranose 2-oxidase are independent of one another, in that the oxidation of the reduced flavin occurs after the release of 2-keto-D-glucose from the active site of the enzyme in a ping-pong steady-state kinetic mechanism (*3, 14, 15*). Here, as a first step towards mechanistic studies aimed to further the understanding of the biochemical properties of the enzyme, we have determined the steady-state kinetic mechanism of pyranose 2-oxidase as a function of pH, showing that a pH switch affects the steady-state kinetic mechanism of the enzyme.

At pH values lower than 7.0, pyranose 2-oxidase displays a bi-bi ping-pong steady-state kinetic mechanism, with the oxidation of the reduced flavin occurring after a kinetic step of the enzyme that is associated with the release of the organic product of the reaction (Scheme 5.2). Evidence for a ping-pong kinetic mechanism comes from the patterns of parallel lines in double reciprocal plots of $1/v_o$ versus 1/[D-glucose] or 1/[oxygen] observed at pH 5.5 and 6.5 (Figure 5.2), which are consistent with product release occurring between binding of D-glucose to the enzyme and reaction of the enzyme with molecular oxygen (*19*). Independent evidence for a ping-pong kinetic mechanism is provided by the linear patterns seen at low pH values in double reciprocal plots of $1/v_o$ versus 1/[D-glucose] when the ratio of the concentrations of the two substrates D-glucose and oxygen was kept at a fixed ratio (Figure 5.3) (*17*). These data are in

agreement with recent results by other authors indicating that at pH 6.5 the enzyme follows a ping-pong kinetic mechanism (*3, 14, 15*). In the crystallographic structure of the enzyme to a resolution of 1.8 Å a loop composed of residues 452 - 461 forms a lid that has been shown to be in either an open or close conformation, governing access of the substrate and product of the reaction to and from the active site (*11*). The lid is present in the closed conformation in the crystallographic structure of pyranose 2-oxidase in complex with 2-keto-D-glucose (*20*), suggesting that it must necessarily open to allow for the release of 2-keto-D-glucose product of the oxidation reaction to the solvent. Consequently, we hypothesize that at low pH the proper assembly of the catalytic machinery for the reaction of the reduced flavin with molecular oxygen is linked to the conformational change associated with the opening of the active site lid to allow for the release of the product of the reaction. In principle, a parallel-lines pattern could also provided by a kinetic model where oxygen reacts with the reduced flavin prior to the release of the product of the reaction if the flavin reduction step was irreversible (lower loop in Scheme 5.2 with $k_4 = 0$). Although this alternate interpretation cannot be ruled out with the data at hand, it appears to be less likely. If this were the case a polynomial pattern would likely be observed at pH values < 7.0 in double reciprocal plots of the initial rates of reaction as a function of D-glucose concentration measured at a fixed ratio of the concentrations of D-glucose and oxygen, since at low concentrations of oxygen $\alpha K_{ia} K_b > 0$ in Eq. (4).

At pH values higher than 7.0, the reaction catalyzed by pyranose 2-oxidase with D-glucose occurs via a bi-bi ordered mechanism in which the reduced enzyme-bound flavin reacts with molecular oxygen prior to the release of 2-keto-D-glucose from the active site of the enzyme (lower loop in Scheme 5.2). This conclusion is supported by both the patterns with intersecting lines seen in double reciprocal plots of $1/v_o$ versus 1/[D-glucose] or 1/[oxygen] (Figure 5.2), and

the curving patterns observed in the double reciprocal plots when the ratio of the concentrations of D-glucose and oxygen was kept at a fixed value (Figure 5.3) (*19*). Thus, at high pH the reduced enzyme-product complex permits reaction of molecular oxygen with the enzyme-bound flavin. Interestingly, an oxidized form of pyranose 2-oxidase from a source that is different from that used in this study, *Peniophora* sp., was recently crystallized in the presence of 2-keto-D-glucose to a resolution of 1.41 Å (*20*). In that structure, which represents the oxidized enzyme-product complex after completion of the oxidation reaction (i.e., $E_{ox}P$ in Scheme 5.2), additional diffused density was seen between the ring oxygen atom of the pyranose product and a phenylalanine residue in the active site of the enzyme (Figure 5.5), suggesting that oxygen may locate in that region for reaction with the reduced enzyme in complex with 2-keto-D-glucose (*20*).

The pH-independence of the $k_{cat}/K_{glucose}$ values at pH values $\leq$ 7.5 suggests that the deprotonation of the hydroxyl group of D-glucose that is required for the oxidation reaction is not rate-determining for the reductive half-reaction catalyzed by the enzyme. Indeed, if that were the case the $k_{cat}/K_{glucose}$ values at low pH would decrease with a slope of +1 and approach a limiting value of zero rather than a finite value of ~12,500 $M^{-1}s^{-1}$. In this regard, pyranose 2-oxidase appears to be significantly different from the well-characterized choline oxidase, which also catalyzes a flavin-dependent oxidation of an alcohol substrate, where an active site group with a pK_a value of ~7.5 has been proposed to catalyze the deprotonation of the hydroxyl group of the alcohol substrate in catalysis (*21*).

The oxidative half-reaction in which a hydride equivalent is transferred from the enzyme-bound flavin to molecular oxygen occurs at a maximal rate at pH values comprised between 5.5 and 7.5, with a pH independent value of 10^6 $M^{-1}s^{-1}$. This value is in keeping with

values reported for other flavoprotein oxidases, such as for example choline oxidase (*21-23*), monoamine oxidase (*24*), sarcosine oxidase (*25*), nitroalkane oxidase (*26*), glycolate oxidase (*27, 28*), lactate oxidase (*29*), and is ~3-times larger than the value of 250 $M^{-1}s^{-1}$ reported for the non-enzymatic reaction of free flavins in solution (*28, 30*). Although limited to a narrow range, the pH profile of the k_{cat}/K_{oxygen} values with D-glucose as substrate for pyranose 2-oxidase is similar to that previously reported for glucose 1-oxidase from *A. niger* (*7, 31*), in that there is a decrease in the k_{cat}/K_{oxygen} values from a limiting value at low pH with increasing pH. In that case, activation of the reduced flavin and oxygen was shown to be facilitated when the conserved active site histidine 516 is protonated (*31*). A comparison of the amino acid sequences of glucose oxidase and pyranose 2-oxidase establishes that histidine 548 in the latter enzyme is equivalent to histidine 516 of glucose oxidase, thereby raising the possibility that the two enzymes may utilize similar mechanisms for the activation of the reduced flavin and oxygen in their oxidative half-reactions.

In conclusion, the study of the steady-state kinetic mechanism of pyranose 2-oxidase with D-glucose as substrate presented herein shows that the enzyme displays a ping-pong mechanism at pH < 7.0 and an ordered mechanism at pH > 7.0. A conformational change of the reduced enzyme prior to the reaction with molecular oxygen, which is associated with the release of the organic product of the reaction, has been shown to occur at low pH, but not at high pH. To our knowledge this study represents the first instance in which pH determines whether the reaction of molecular oxygen with the enzyme-bound reduced flavin in a flavoprotein oxidase occurs prior to or following the release of the organic product of the reaction. While the conclusions presented here represent a framework for future mechanistic investigations of the enzyme, they also illustrate that caution should be exerted in extrapolating *a priori* the

conclusions drawn on a steady-state kinetic mechanism determined at a single pH value to other pH values when the pH profiles of the steady-state kinetic parameters of flavin-dependent oxidases are investigated.

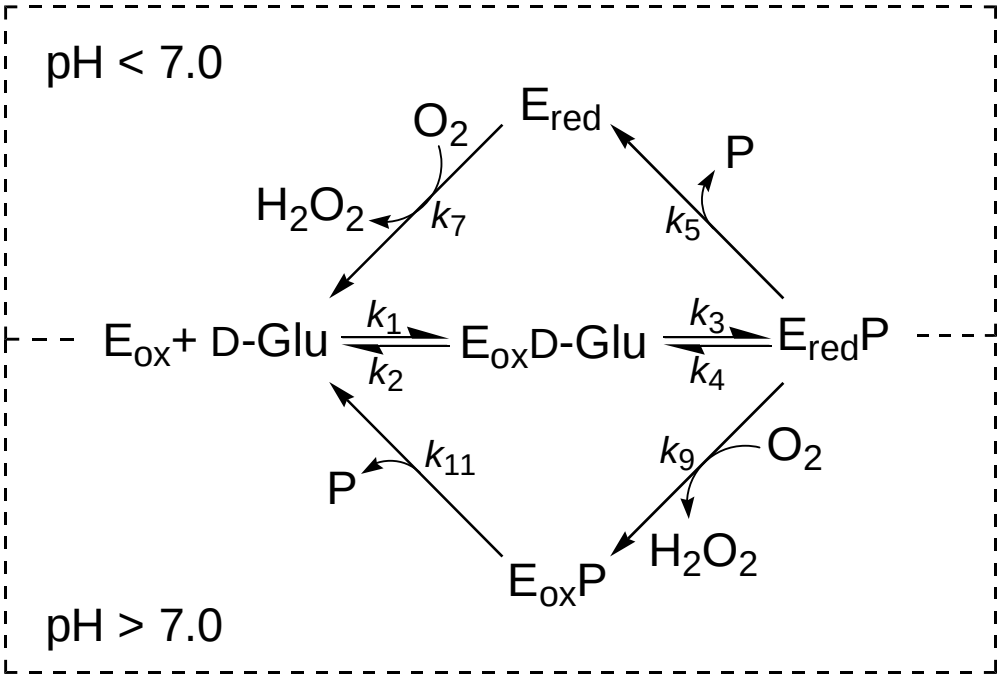

Scheme 5.2. Steady-State Kinetic Mechanism of Pyranose 2-Oxidase. E_{ox}, oxidized enzyme; E_{red}, reduced enzyme; D-Glu, D-glucose; and P, 2-keto-D-glucose.

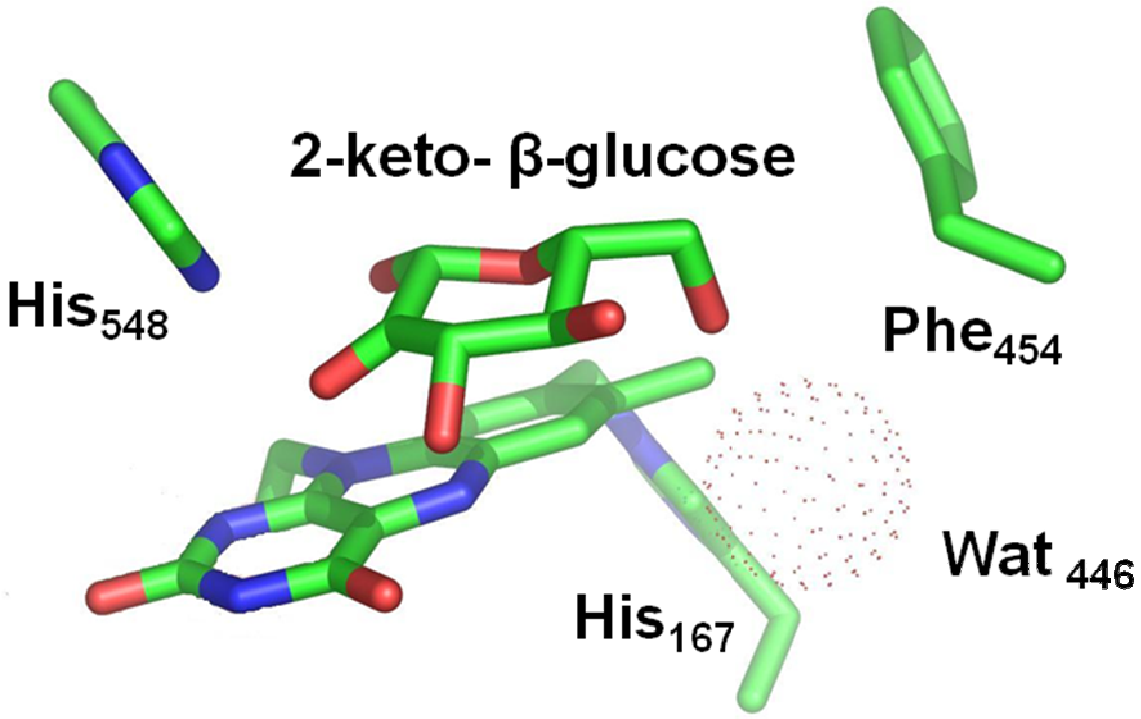

Figure 5.5. The active site of wild-type pyranose 2-oxidase from white-rot fungus *Peniophora* sp. at a resolution of 1.41 Å (PDB 2f5v). Selected amino acids are shown, together with the product of the oxidation of D-glucose, 2-keto-β-D-glucose, and a water molecule.

5.6. Acknowledgement

The authors thank Dr. Peter Kyslik at the Academy of Sciences of the Czech Republic, Prague, for the generous gift of plasmid pSE33 harboring the gene for pyranose 2-oxidase from *T. ochracea*.

5.7. References

1. Leitner, C., Volc, J., and Haltrich, D. (2001) Purification and characterization of pyranose oxidase from the white rot fungus *Trametes multicolor*, *Appl. Environ. Microbiol*. *67*, 3636-3644.
2. Leitner, C., D. Haltrich, B. Nidetzky, H. Prillinger, a., and Kulbe., K. D. (1998) Production of a novel pyranose 2-oxidase by basidiomycete *Trametes multicolor*., *Appl. Biochem. Biotechnol. 70-72*, 237-248.
3. Kujawa, M., Ebner, H., Leitner, C., Hallberg, B. M., Prongjit, M., Sucharitakul, J., Ludwig, R., Rudsander, U., Peterbauer, C., Chaiyen, P., Haltrich, D., and Divne, C. (2006) Structural basis for substrate binding and regioselective oxidation of monosaccharides at C3 by pyranose 2-oxidase, *J. Biol. Chem. 281*, 35104-35115.
4. Sucharitakul, J., Prongjit, M., Haltrich, D., and Chaiyen, P. (2008) Detection of a C4a-hydroperoxyflavin intermediate in the reaction of a flavoprotein oxidase, *Biochemistry 47*, 8485-8490.
5. Giffhorn, F. (2000) Fungal pyranose oxidases: occurrence, properties and biotechnical applications in carbohydrate chemistry, *Appl. Microbiol. Biotechnol. 54*, 727-740.
6. Leskovac, V., Trivic, S., Wohlfahrt, G., Kandrac, J., and Pericin, D. (2005) Glucose oxidase from *Aspergillus niger*: the mechanism of action with molecular oxygen, quinones, and one-electron acceptors, *Int. J. Biochem. Cell. Biol. 37*, 731-750.
7. Su, Q., and Klinman, J. P. (1999) Nature of Oxygen Activation in Glucose Oxidase from *Aspergillus niger*: The Importance of Electrostatic Stabilization in Superoxide Formation, *Biochemistry 38*, 8572-8581.

8. Weibel, M. K., and Bright, H. J. (1971) The glucose oxidase mechanism. Interpretation of the pH dependence, *J. Biol. Chem. 246*, 2734-2744.

9. Albrecht, M., and Lengauer, T. (2003) Pyranose oxidase identified as a member of the GMC oxidoreductase family, *Bioinformatics 19*, 1216-1220.

10. Bannwarth, M., Bastian, S., Heckmann-Pohl, D., Giffhorn, F., and Schulz, G. E. (2004) Crystal structure of pyranose 2-oxidase from the white-rot fungus *Peniophora* sp, *Biochemistry 43*, 11683-11690.

11. Hallberg, B. M., Leitner, C., Haltrich, D., and Divne, C. (2004) Crystal structure of the 270 kDa homotetrameric lignin-degrading enzyme pyranose 2-oxidase, *J. Mol. Biol. 341*, 781-796.

12. Schafer, A., Bieg, S., Huwig, A., Kohring, G., and Giffhorn, F. (1996) Purification by Immunoaffinity Chromatography, Characterization, and Structural Analysis of a Thermostable Pyranose Oxidase from the White Rot Fungus *Phlebiopsis gigantea*, *Appl. Environ. Microbiol. 62*, 2586-2592.

13. Takakura, Y., and Kuwata, S. (2003) Purification, characterization, and molecular cloning of a pyranose oxidase from the fruit body of the basidiomycete, *Tricholoma matsutake*, *Biosci. Biotechnol. Biochem*. *67*, 2598-2607.

14. Artolozaga, M. J., Kubatova, E., Volc, J., and Kalisz, H. M. (1997) Pyranose 2-oxidase from *Phanerochaete chrysosporium*--further biochemical characterisation, *Appl. Microbiol. Biotechnol*. *47*, 508-514.

15. Massey, V. (1991) *Flavins and Flavoproteins*, Curti, B., Rochi, S., and Zanetti, G., Eds. ed., Water DeGruyter&Co., Berlin, Germany.

16. Allison, D. R., and Purich, D. L. (1979) *Methods in Enzymology*, Vol. 63, Purich, D., L., Ed. ed., Academic Press, New York.

17. Tsopanakis, A. D., and Herries, D. G. (1975) Kinetic Discrimination between Two Types of Enzyme Mechanism. Application to Lactose Synthetase, *Eur. J. Biochem. 53*, 193-196.

18. Massey, V. (2000) The chemical and biological versatility of riboflavin, *Biochem. Soc. Trans*. *28*, 283-296.

19. Cook, P. F., and Cleland, W. W. (2007) *Enzyme Kinetics and Mechanism*, Garland Science Publishing, New York, NY.

20. Bannwarth, M., Heckmann-Pohl, D., Bastian, S., Giffhorn, F., and Schulz, G. E. (2006) Reaction geometry and thermostable variant of pyranose 2-oxidase from the white-rot fungus *Peniophora* sp, *Biochemistry 45*, 6587-6595.

21. Ghanem, M., Fan, F., Francis, K., and Gadda, G. (2003) Spectroscopic and kinetic properties of recombinant choline oxidase from *Arthrobacter globiformis*, *Biochemistry 42*, 15179-15188.

22. Fan, F., and Gadda, G. (2005) Oxygen- and temperature-dependent kinetic isotope effects in choline oxidase: correlating reversible hydride transfer with environmentally enhanced tunneling, *J. Am. Chem. Soc. 127*, 17954-17961.

23. Fan, F., and Gadda, G. (2005) On the catalytic mechanism of choline oxidase, *J. Am. Chem. Soc. 127*, 2067-2074.

24. Tan, A. K., and Ramsay, R. R. (1993) Substrate-specific enhancement of the oxidative half-reaction of monoamine oxidase, *Biochemistry 32*, 2137-2143.

25. Wagner, M. A., and Jorns, M. S. (2000) Monomeric sarcosine oxidase: 2. Kinetic studies with sarcosine, alternate substrates, and a substrate analogue, *Biochemistry 39*, 8825-8829.

26. Heasley, C. J., and Fitzpatrick, P. F. (1996) Kinetic mechanism and substrate specificity of nitroalkane oxidase, *Biochem. Biophys. Res. Commun*. *225*, 6-10.

27. Macheroux, P., Massey, V., Thiele, D. J., and Volokita, M. (1991) Expression of spinach glycolate oxidase in *Saccharomyces cerevisiae*: purification and characterization, *Biochemistry 30*, 4612-4619.

28. Mattevi, A. (2006) To be or not to be an oxidase: challenging the oxygen reactivity of flavoenzymes, *Trends. Biochem. Sci. 31*, 276-283.

29. Maeda-Yorita, K., Aki, K., Sagai, H., Misaki, H., and Massey, V. (1995) L-lactate oxidase and L-lactate monooxygenase: mechanistic variations on a common structural theme, *Biochimie 77*, 631-642.

30. Massey, V. (1994) Activation of molecular oxygen by flavins and flavoproteins, *J. Biol. Chem*. *269*, 22459-22462.

31. Roth, J. P., and Klinman, J. P. (2003) Catalysis of electron transfer during activation of O2 by the flavoprotein glucose oxidase, *Proc. Natl. Acad. Sci. U S A 100*, 62-67.

CHAPTER 6

General discussion and conclusions

The oxidation of alcohol to carbonyl compounds is catalyzed by a number of flavin-dependent enzymes. This chemical reaction is important in many biochemical pathways. The flavin dependent choline oxidase from *Arthrobacter globiformis* is well characterized since structural, mechanistic and biochemical data are available. By using choline oxidase as a model enzyme, the chemical mechanism of the alcohol oxidation catalyzed by flavoenzymes has been elucidated. This dissertation studied specifically the roles of the active site residues His351, His466 and Asn510 using biochemical, site-directed mutagenic and mechanistic approaches. In addition, the steady-state kinetic mechanism of pyranose 2-oxidase was examined and will be discussed to gain a greater understanding of the alcohol oxidation catalyzed by flavoenzymes.

Choline oxidase catalyzes the four electron oxidation of choline to glycine betaine via betaine aldehyde as an intermediate. The mechanistic, biochemical, and structural properties of the wild-type enzyme have been characterized in detail (*1-13*). Catalysis is initiated in the enzyme-substrate complex by removal of the hydroxyl proton of the alcohol substrate yielding a zwitterionic alkoxide species. The hydride ion subsequently transfers from the alkoxide α-carbon of the activated substrate to the flavin N(5) atom. The first oxidation-reduction is completed by the reaction of reduced flavin with oxygen, yielding hydrogen peroxide and oxidized flavin. To date, the active site residue that abstracts hydroxyl proton from substrate in choline oxidase is still unknown. Crystallographic and sequence alignment studies have revealed that the histidine residues at positions 351 and 466 are good candidates to serve as a catalytic base in choline oxidase. Variant forms of choline oxidase in which histidine 351 was replaced with alanine and glutamine and in which histidine 466 was exchanged with glutamine were prepared. In addition,

the double mutants His351Gln/His466Ala and His351/466Gln were also obtained in order to probe the functional roles of these residues in choline oxidase.

Histidine 466 is likely to be the active site base which initiates the oxidation of alcohol substrate in choline oxidase. This histidine residue is conserved among the GMC oxidoreductate enzyme superfamily and is proposed to be a catalytic base (*9, 13-16*). However, to our knowledge, there has been no strong evidence produced to support this proposal for this class of enzymes. The variant form of histidine 466 in choline oxidase, His466Gln, showed severe effect in enzymatic activity (nine order of magnitudes lower in k_{red} value than wild-type enzyme). In addition, the recent computational results from the Martinez group showed that among other four possible active site residues which could be the base in choline oxidase a low barrier energy profie (with a stable alkoxide intermediate) was observed for the histidine residue at position 466, indicating that this histidine is the catalytic base (personal communication). In contrast, a previous study of His466 concluded that this residue may not be the catalytic base based on the pH dependence profile and imidazole rescuing results (*9*). In that study, the authors showed that the pH dependence profile of His466Ala mutant still exhibited the requirement of an unprotonated group for catalysis; with addition of exogenous imidazole the enzymatic activity increased at lower pH, suggesting imidazolium, but not imidazole as the catalytically relevant species for the partial rescue of enzymatic activity. This conclusion could be reinterpreted, however. The activity was rescued by the positive charge on the exogenous imidazolium because this positive charge stabilized the negative charge on the intermediate of the reaction. Furthermore, when His466 was replaced with alanine, the requirement of a base was observed in the pH dependence profile. It is likely because the OH bond was cleaved with the assistance of another base (perhaps His351 or water molecule). The double mutant enzymes,

His351Gln/His466Ala and His351/466Ala were prepared in order to investigate this hypothesis. The rate of flavin reduction of His351Gln/His466Ala was dramatic decreased compared to the wild-type enzyme (k_{red} of 0.012 s^{-1} for the double mutant versus 93 s^{-1} for the wild-type enzyme). However, the crystal structure of the variant enzyme is required to support the conclusion that His466 acts as a base in choline oxidase and currently efforts have been made in our lab to obtain the crystals of His351/466Ala.

In the reaction catalyzed by choline oxidase Histidine 351 is important for the reductive half-reaction of choline oxidation but plays a minimal role in the oxidative half-reaction in which the reduced flavin reacts with oxygen. In the reductive-half reaction, His351 contributes to substrate binding and facilitates the hydride transfer reaction between the alkoxide species and the flavin N(5) atom by hydrogen bonding to the oxygen atom of the alkoxide intermediate. This conclusion is supported by the experimental results which indicate a decrease in the rate constant for flavin reduction when both choline and hydrated betaine aldehyde were used. Likewise, the kinetic isotope effect showed that the CH bond cleavage in His351Ala variant has ~ 30% lower than in the wild-type enzyme ($^{D}(k_{cat}/K_m)$ value of 7.8 as compared to 10.6). Previous mechanistic studies of the wild-type enzyme showed that the hydride transfer occurs via a quantum mechanism within a highly preorganized enzyme-substrate complex and with a small movement of the alkoxide intermediate acting as hydride donor and the N(5) atom of the flavin acting as hydride acceptor. Therefore, the decrease in the rates of hydride transfer in His351Ala may come from the disruption of preorganization in the enzyme-substrate complex in the active site. As mentioned above, His351 does not play a role in the reaction between the reduced flavin and molecular oxygen as demonstrated by the lack of pH dependence of the k_{cat}/K_m value for oxygen and the minimal decrease of 1.2-fold in the k_{cat}/K_m compared to the wild-type enzyme. This is

consistent with previous studies which established that the positive charge required to activate oxygen in choline oxidase is provided by the trimethylammonium group of the enzyme-bound substrate and not by a side chain of an amino acid in the active site of the enzyme (*6, 9, 17*). In addition, a recent study of the role of Val464 in choline oxidase has provided useful insight into the oxidation of reduced flavin by oxygen which could be used for other flavin dependent oxidases (*18*). Substitution of the valine residue at position 464 to alanine or threonine resulted in the presence of a non-polar site in proximity of the C(4a)-N(5) atoms of the flavin. This non-polar amino acyl side-chain is required since it allows oxygen to enter to the active site and subsequently the oxidative half-reaction occurs via electrostatic catalysis.

The crystal structures and sequence alignments of the GMC enzymes revealed the presence of a conserved His-Asn pair, except for glucose oxidase where the asparagine residue is replaced with histidine (*14*). In choline oxidase His466 and Asn510 represent this conserved His-Asn pair. Since previous studies have already revealed the roles of both His351 and His466 and because the crystal structure indicates that the side chain of Asn510 is positioned in proximity to His351 and His466 (3.0 and 4.0 Å, respectively), and N(1)-C(2) locus of flavin (4.7 Å), it is suggested that Asn510 may play an important role in the reaction catalyzed by choline oxidase. The results of biochemical and mechanistic studies of the mutant variants in which the asparagine at position 510 was replaced via site-directed mutagenesis by alanine, histidine, leucine, and aspartate support the assertion that Asn510 is involved in both the reductive and oxidative half-reactions of choline oxidase. This conclusion is derived from the steady-state and rapid reaction kinetic data of Asn510His and Asn510Ala mutants which demonstrate a marked decrease in the rate constants. For example, in the reductive half-reaction, the 700-and 20-fold decrease in the limiting rate constant for anaerobic flavin reduction (k_{red}) compared to the wild-

type in Asn510Ala and Asn510His, respectively, with choline as substrate. Moreover, from the steady-state kinetic data it was found that the second-order rate constants for oxygen (k_{cat}/K_{oxgyen}) decreased 50- and 15-fold in the Asn510Ala and Asn510His enzymes. In the kinetic isotope effects study, the Asn510Ala mutant showed a concerted mechanism for cleavage of the OH and CH bonds of choline. The change in the timing of the cleavages of the OH and CH bonds of choline substrate by Asn510Ala could be explained by the lack of ability to stabilize the alkoxide intermediate. In contrast, in wild-type and Asn510His enzymes, the alkoxide species are stabilized by forming a hydrogen bond interaction between the side chain at position 510 and neighboring residues such as His466 and His351 that directly interacts with a reaction intermediate in the transition state. Finally, all mutant forms of Asn510 resulted in enzymes with lower levels of FAD incorporation. Since Asn510 is in proximity to the flavin N(1)-C(2) atoms, in the Asn510Ala, Asn510His and Asn510Leu mutants there is decreased stabilization of the negative charge that is required on the flavin N(1)-C(2) locus for formation of the covalent attachment to the protein. The lack of stabilization of the negative charge on the flavin in the Asn510Asp mutant is more severe; about 75% of flavin bound to the protein is noncovalently attached. This result is in accordance with the previous study of His466 in which replacement of histidine with aspartate resulted in an enzyme devoid of enzymatic activity, with low stoichiometery of FAD: protein and ~ 75% of the enzyme-bound flavin noncovalently linked to protein (*10*). Together, the study of a conserved Asn510 in choline oxidase provided insight into the overall preorganization of the enzyme-substrate complex, stabilization of the alkoxide intermediate, and the flavinylation reaction.

Pyranose 2-oxidase (E.C. 1.1.3.10) from *Trametes multicolor* is a homotetrameric flavoprotein with a molecular mass of 270 kDa, each subunit containing one covalently bound

FAD at N(3) of His167 (*19, 20*). The enzyme catalyzes the oxidation of several aldopyranoses by molecular oxygen at the C2 position to yield the corresponding 2-keto-aldoses and hydrogen peroxide (*20*). Pyranose 2-oxidase has been studied extensively in both reductive and oxidative half-reactions. A recent study showed that the overall turnover of the reaction is limited by two steps, the flavin reduction and the decay of C4a-hydroperoxy-FAD (*21*). Pyranose 2-oxdiase is the first enzyme in the class of flavoprotein oxidases for which a C4a-hydroperoxy-flavin intermediate on the oxidative half-reaction has been detected (*22*). Similarly, a C4a-adduct intermediate in the crystal structure of choline oxidase was also reported (*23*). However, all studies in pyranose 2-oxidase have been performed only at pH 7.0 and the kinetic mechanism under these conditions was demonstrated to be a ping-pong mechanism in which the sugar product is released prior to the oxygen reaction (*21, 22*). This dissertation examined in detail the steady-state kinetic mechanism of the enzyme in the pH range from 5.5 to 8.5 with glucose as a substrate. Surprisingly, the enzyme displays a ping-pong kinetic mechanism at pH values lower than 7.0 and a ternary complex mechanism, in which the reduced enzyme-bound flavin reacts with molecular oxygen prior to the release of 2-keto-D-glucose from the active site of the enzyme, at pH values higher than 7.0. These observations can be explained with relation to the crystal structure. It was found that there is a conformational change which allows the active site lid to open and release the product before the entry of oxygen molecule at low pH but not at high pH. However, in general, if the flavin reduction step was irreversible, the parallel-line pattern for the double-reciprocal plot, instead of an intersecting-line, could be observed in the ternary complex mechanism. The reaction of D-amino acid oxidase provides such a good example (*24*). Therefore, this study illustrates that when pH profiles of the steady-state kinetic parameters of

flavoprotein oxidases are investigated, it should be cautioned that the kinetic mechanism may vary with pH.

Overall, the results presented in this dissertation have provided insight into the oxidation of alcohol substrate catalyzed by choline oxidase with respect to some of the key active site residues. The conserved histidine at position 466 serves as a catalytic base which abstracts the hydroxyl proton of the substrate and initiates catalysis. His351 provides stabilization of the alkoxide intermediate of reaction and contributes to the correct positioning of the hydride donor and acceptor in the enzyme-substrate complex. Finally, the conserved Asn510 is important for the flavinylation reaction and the stabilization of the reaction intermediate via hydrogen bonding interactions with His351 and His466 of choline oxidase. The study of the kinetic mechanism of pyranose 2-oxidase revealed the effect of pH on enzyme mechanism. Therefore, this study demonstrates how the initation of the enzyme catalysis and the stabilization of the transition state intermediate is a collective responsibility of a number of active site residues by using choline oxidase as a model. Furthermore, for the first time among flavin dependent enzymes, this study established how a pH switch affects the steady-state kinetic meachanism.

6.1. References

1. Fan, F., and Gadda, G. (2005) Oxygen- and temperature-dependent kinetic isotope effects in choline oxidase: correlating reversible hydride transfer with environmentally enhanced tunneling, *J. Am. Chem. Soc*. *127*, 17954-17961.
2. Fan, F., and Gadda, G. (2005) On the catalytic mechanism of choline oxidase, *J. Am. Chem. Soc. 127*, 2067-2074.
3. Fan, F., and Gadda, G. (2007) An internal equilibrium preorganizes the enzyme-substrate complex for hydride tunneling in choline oxidase, *Biochemistry 46*, 6402-6408.
4. Fan, F., Germann, M. W., and Gadda, G. (2006) Mechanistic studies of choline oxidase with betaine aldehyde and its isosteric analogue 3,3-dimethylbutyraldehyde, *Biochemistry 45*, 1979-1986.
5. Fan, F., Ghanem, M., and Gadda, G. (2004) Cloning, sequence analysis, and purification of choline oxidase from *Arthrobacter globiformis*: a bacterial enzyme involved in osmotic stress tolerance, *Arch. Biochem. Biophys*. *421*, 149-158.
6. Gadda, G., Fan, F., and Hoang, J. V. (2006) On the contribution of the positively charged headgroup of choline to substrate binding and catalysis in the reaction catalyzed by choline oxidase, *Arch. Biochem. Biophys*. *451*, 182-187.
7. Gadda, G., Powell, N. L., and Menon, P. (2004) The trimethylammonium headgroup of choline is a major determinant for substrate binding and specificity in choline oxidase, *Arch. Biochem. Biophys*. *430*, 264-273.

8. Ghanem, M., Fan, F., Francis, K., and Gadda, G. (2003) Spectroscopic and kinetic properties of recombinant choline oxidase from *Arthrobacter globiformis*, *Biochemistry 42*, 15179-15188.

9. Ghanem, M., and Gadda, G. (2005) On the catalytic role of the conserved active site residue His466 of choline oxidase, *Biochemistry 44*, 893-904.

10. Ghanem, M., and Gadda, G. (2006) Effects of reversing the protein positive charge in the proximity of the flavin N(1) locus of choline oxidase, *Biochemistry 45*, 3437-3447.

11. Hoang, J. V., and Gadda, G. (2007) Trapping choline oxidase in a nonfunctional conformation by freezing at low pH, *Proteins 66*, 611-620.

12. Quaye, O., Lountos, G. T., Fan, F., Orville, A. M., and Gadda, G. (2008) Role of Glu312 in binding and positioning of the substrate for the hydride transfer reaction in choline oxidase, *Biochemistry 47*, 243-256.

13. Rungsrisuriyachai, K., and Gadda, G. (2008) On the role of histidine 351 in the reaction of alcohol oxidation catalyzed by choline oxidase, *Biochemistry 47*, 6762-6769.

14. Hallberg, B. M., Leitner, C., Haltrich, D., and Divne, C. (2004) Crystal structure of the 270 kDa homotetrameric lignin-degrading enzyme pyranose 2-oxidase, *J.Mol. Biol. 341*, 781-796.

15. Kass, I. J., and Sampson, N. S. (1998) Evaluation of the role of His447 in the reaction catalyzed by cholesterol oxidase, *Biochemistry 37*, 17990-18000.

16. Rotsaert, F. A., Renganathan, V., and Gold, M. H. (2003) Role of the flavin domain residues, His689 and Asn732, in the catalytic mechanism of cellobiose dehydrogenase from *phanerochaete chrysosporium*, *Biochemistry 42*, 4049-4056.

17. Quaye, O., Cowins, S., and Gadda, G. (2009) Contribution of flavin covalent linkage with histidine 99 to the reaction catalyzed by choline oxidase, *J. Biol. Chem. 284*, 16990-16997.

18. Finnegan, S., Agniswamy, J., Weber, I. T., and Gadda, G. Role of Valine 464 in the Flavin Oxidation Reaction Catalyzed by Choline Oxidase (*in press*).

19. Halada, P., Leitner, C., Sedmera, P., Haltrich, D., and Volc, J. (2003) Identification of the covalent flavin adenine dinucleotide-binding region in pyranose 2-oxidase from Trametes multicolor, *Anal. Biochem. 314*, 235-242.

20. Leitner, C., Volc, J., and Haltrich, D. (2001) Purification and characterization of pyranose oxidase from the white rot fungus Trametes multicolor, *Appl. Environ. Microbiol. 67*, 3636-3644.

21. Prongjit, M., Sucharitakul, J., Wongnate, T., Haltrich, D., and Chaiyen, P. (2009) Kinetic mechanism of pyranose 2-oxidase from trametes multicolor, *Biochemistry 48*, 4170-4180.

22. Sucharitakul, J., Prongjit, M., Haltrich, D., and Chaiyen, P. (2008) Detection of a C4a-hydroperoxyflavin intermediate in the reaction of a flavoprotein oxidase, *Biochemistry 47*, 8485-8490.

23. Orville, A. M., Lountos, G. T., Finnegan, S., Gadda, G., and Prabhakar, R. (2009) Crystallographic, spectroscopic, and computational analysis of a flavin C4a-oxygen adduct in choline oxidase, *Biochemistry 48*, 720-728.

24. Fitzpatrick, P. F., and Massey, V. (1982) The kinetic mechanism of D-amino acid oxidase with D-alpha-aminobutyrate as substrate. Effect of enzyme concentration on the kinetics, *J. Biol. Chem*. *257*, 12916-12923.